MACHINING TITANIUM

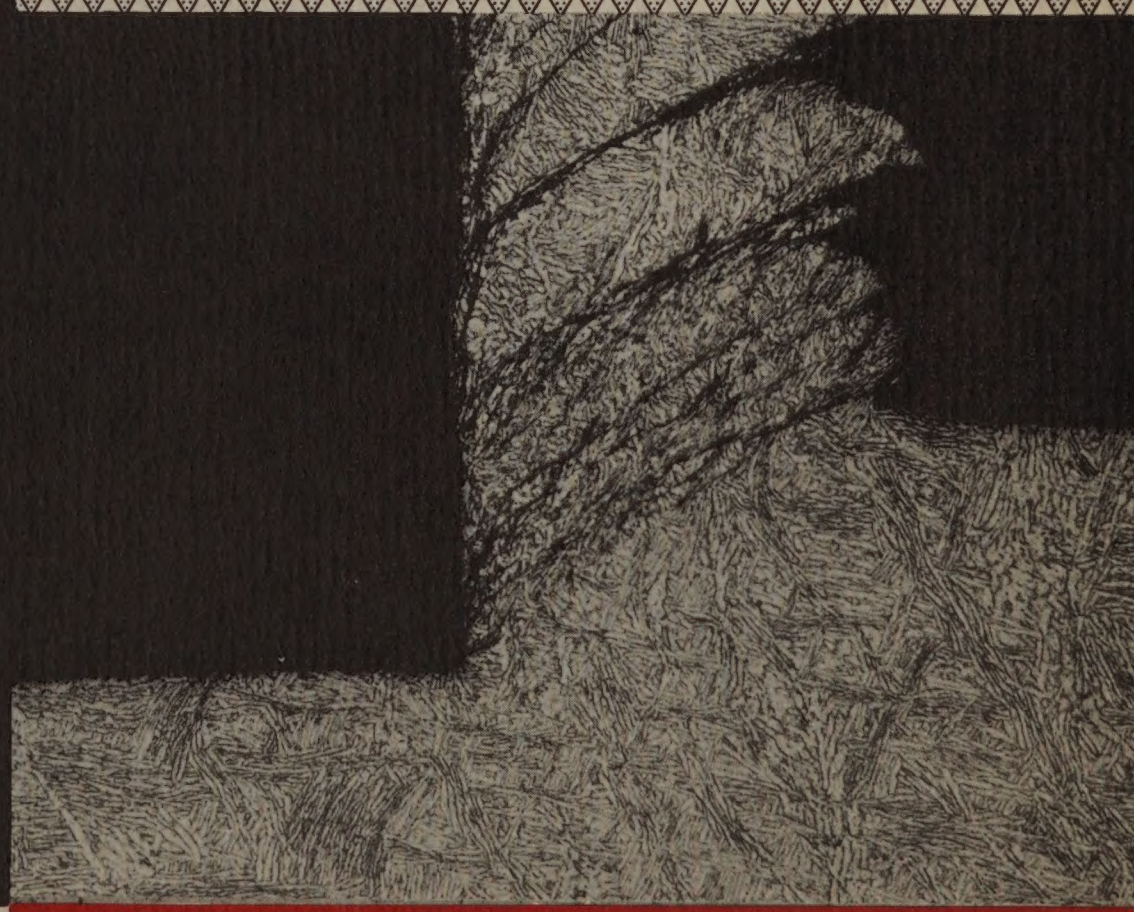

prepared by

MACHINE TOOL DIVISION

MASSACHUSETTS INSTITUTE OF TECHNOLOGY

for the

UNITED STATES AIR FORCE

1954

MACHINING TITANIUM

A Report Prepared for the United States Air Force

Wright-Patterson Air Force Base, Dayton, Ohio

Under Contract No. AF 33(600)-22674

by

M. C. Shaw
S. O. Dirke
P. A. Smith
N. H. Cook
E. G. Loewen
C. T. Yang

Machine Tool Division
Department of Mechanical Engineering
Massachusetts Institute of Technology

June 1954

Cover Photograph

Photomicrograph of Partially Formed Titanium Chip.

Work material: RC 130B; Rake angle, 0^{o}; Tool material, 18-4-1 HSS;

Cutting speed, 40 fpm.; feed, 0.0104 ipr.; cutting fluid, none.

Ent:

Massachusetts Institute of Technology

Feb. 14, 1952

Table of Contents

Table of Contents

Preface

This report has been prepared with two objectives in view:

1.) To provide a general picture of the single point machining characteristics of titanium alloys for use of practical engineers in the workshop.

2.) To provide results and discussion primarily of interest to those engaged in research.

The introductory chapter should be of interest to both groups.

The second chapter is primarily for practicing engineers and contains a summary and the conclusions of this report. The supporting data and discussion of these data are presented in the remaining chapters of the report and should be of most interest to those engaged in research into the machining characteristics of titanium alloys.

Chapter 1
INTRODUCTION

Titanium is a metal of the tin group of the periodic table that resembles iron in many of its properties. Although titanium is the fourth metal in abundance in the earth's crust, it is difficult to win from its ores due to its unusually high reactivity at elevated temperatures. Titanium dioxide or rutile (TiO_2) and iron titanate or ilmenite ($FeTiO_3$) are the chief sources of the metal. At present titanium metal is produced by chlorinating the ore in the presence of carbon at high temperature to form TiCl which is then reduced with molten magnesium to form $MgCl_2$ and titanium. The resulting sponge titanium is divided into small particles or chips by milling, and separated from the excess magnesium and magnesium chloride associated with its reduction. It is then melted in arc furnaces to make large ingots of titanium or titanium alloys.

While titanium alloys have properties that make them very attractive for certain structural applications, the high cost of these alloys in the past has precluded their use in engineering structures. Before the relatively recent interest in developing structural titanium alloys the chief uses of titanium compounds were as metallurgical deoxidizers and denitrogenizers to improve the toughness of steel alloys, as white pigments in paints and ceramics, and in dyes and mordants for paper and textiles.

The structural alloys of titanium are ductile, light in weight, and have good fatigue properties and corrosion resistance. An idea of the general properties of titanium may be obtained from Table 1 where a number of characteristics of commercially pure titanium are compared with those for SAE 1020 steel, 18-8 stainless steel and 75ST aluminum. The specific weight of titanium is but 2/3 that of steel, and only 60% greater than that of aluminum. The strength of titanium on the other hand is far greater than that for aluminum being of the same order of magnitude as that for alloy steels. These weight-strength properties of titanium alloys give them the highest strength-weight ratio of any structural material. Titanium is seen to be intermediate between steel and aluminum in tensile and shear stiffness.

Table 1 Properties of Commercially Pure Titanium and Other Structural Metals

Property	Metal			
	75A Titanium	SAE 1020 Steel	18-8 Stainless Steel	75ST Aluminum
Structure	HCP	BCC	FCC	FCC
Specific Weight ρ, lb/cu in	0.16	0.28	0.28	0.10
Ultimate tensile strength (annealed), psi	30,000	50,000	90,000	82,000
Youngs modulus, E, psi x 10^{-6}	16	30	30	10.3
Shear modulus, G. psi x 10^{-6}	6	11.5	11.5	3.9
Melting point, °F	3200	2600	2600	1035
Coefficient of linear expansion, per °F x 10^{6}	5	6.6	9	13
Thermal conductivity, k, BTU/in^2/sec/(°F/in) x 10^{4}	2.75	7.5	2.2	16
Specific heat, c BTU/lb/°F	.12	.13	.12	.21
Volume specific heat, ρc, BTU/in^3/°F	.020	.036	.034	.021
Thermal diffusivity, $K = \frac{k}{\rho c}$, in^2/sec.	.014	.021	.007	.076
$k \rho c$, (BTU/in^2°F)^2/sec x 10^{6}	5.5	27.	7.5	34

While titanium alloys have very high melting points that would suggest great temperature stability and high temperature strength these alloys are somewhat disappointing in this regard. The rapid decrease in the yield and ultimate stresses of two titanium alloys is shown in Fig. 1 together with similar data for 18-8 stainless steel. Fig. 2 shows the rapid decrease in Young's Modulus of elasticity and hardness that accompanies an increase in the temperature of a titanium alloy. The leveling off of the curves of Figs. 1 and 2 in the temperature region from 500 to 700 F is similar to that found in the blue brittle range with steel and is due to the same cause (strain aging).

The thermal properties of titanium alloys are unusually poor, and account to a large extent for the difficulties that are experienced in machining them. Before titanium alloys entered the structural picture the stainless steels were the most difficult materials machined from the point of view of adverse thermal properties. The value of $(k\rho c)$ which is the thermal combination of importance with regard to tool tip temperature was among the lowest values in the stainless steels and this made it necessary to machine these materials at reduced speeds. Titanium is seen to have a far lower value of $(k\rho c)$ than stainless steel and hence must be machined at even lower values of speed. While the thermal conductivity and specific heat for titanium are about the same as those for 18-8 stainless steel, the very low specific weight for titanium makes the value of $(k\rho c)$ much less than that for stainless steel.

The coefficient of expansion of titanium alloys is low, being even less than that for steel.

Pure titanium has a hexagonal close packed (HCP) lattice structure at room temperature, similar to that found in cadmium, zinc, and magnesium alloys. An allotropic transformation occurs at about 1625F where the low temperature HCP structure changes into a body centered cubic structure (BCC) similar to that found in iron and steel at ordinary temperatures. These allotropic forms of titanium are designated α and β respectively and the change from one to the other occurs relatively slowly.

Titanium alloys in the medium alloy range (3 to 10% alloy content) usually consist of mixtures of the α and β structure at room temperature

due to the tendency for alloying additions to make the $\beta \rightarrow \alpha$ transformation more sluggish. When the alloy content is high (i.e., 15 to 20% Cr) completely β titanium alloys can be produced that are the structural counterparts of the austenitic stainless steels in steel technology. Practically all of the present titanium alloys of commercial interest are a mixture of the HCP and BCC structures. It is difficult to differentiate from β titanium in a photomicrograph, but polarized light is helpful in this regard.

The atomic arrangements for the HCP and BCC structures are shown in Fig. 3. The chief importance of crystal structure lies in the influence upon the flow and fracture characteristics of the material. Plastic deformation results from the movement of one layer of atoms over another rather than due to the change in spacing of atoms within a plane. Any plane that can be passed through the atoms in the lattice is a potential slip plane. However, those planes that contain the greatest density of atoms (and hence those for which the spacing of adjacent planes is a maximum) will be the planes on which slip can occur most easily and the directions of easiest slip will lie in the directions of maximum atom density within the plane.

In a polycrystalline material the lattice structures of individual crystals will be oriented differently, and in order that a material deform at low stress and be ductile it is necessary that there be a large number of planes and directions of easy slip.

The number of planes and directions of easy slip is usually less in the case of HCP materials such as zinc, cadmium, and magnesium than for those materials that have a BCC structure such as iron. In addition to slip, HCP materials frequently deform by twinning, a mode of deformation normally not as readily influenced by temperature as is slip. The HCP materials are usually less ductile than iron. Normally the basal plane ABC A'B'C' (Fig. 3) is the plane of easiest slip for HCP metals, and there are relatively few of these planes. However, in the case of titanium, the relative value of c to a is so small that the prismatic planes ABDE are actually planes of easier slip (i.e., have smaller spacing) than are the basal planes. There are many more prismatic planes than basal planes and hence HCP titanium is far more ductile than would be expected from the fact that it has a HCP

structure. As the alloy content of a titanium alloy is increased distance c increases relative to a (Fig. 3). In most commercial titanium alloys we have a mixture of the HCP and BCC structures, and since the HCP material in titanium is of a more ductile variety we should expect the flow and fracture properties of titanium alloys to more closely resemble those of BCC iron than those of ordinary HCP zinc. The low alloy content titanium alloys that have an α structure are not very ductile but retain their strengths to higher temperatures than do the more ductile alloys that consist of the α and β arrangements.

The position with regard to titanium alloys might be summarized approximately as follows. In order to obtain materials of high strength and ductility for structural purposes it is necessary to make alloying additions to titanium. These slow down the $\beta \rightarrow \alpha$ transformation to such an extent that either a pure β structure or an α and β structure results. The greater the amount of the β phase the greater will be the tendency for the strength of the titanium to decrease with increased temperature. It would thus appear that high strength titanium alloys are predominantly materials that have a strong tendency to show a decrease in strength with increase in temperature. At room temperature these materials deform predominantly by slip and should be expected to exhibit flow and fracture characteristics similar to those of steel.

While commercially pure titanium undergoes an allotropic transformation, it cannot be hardened by heat treatment. It can, however, be hardened by cold work and it is found that the titanium alloys have about the same tendency to work harden as ordinary structural steels. The difficulties experienced in machining and grinding titanium alloys cannot therefore be attributed to an increased tendency to work harden.

The chemical composition of the titanium alloys of this investigation is given in Table 2. The 75A alloy is the commercially pure material while the other alloys might be characterized as alloys of low, medium, and high strength respectively. While this material has an ultimate strength of 104,000 psi, really pure titanium would be much softer and have an ultimate tensile strength of only about 50,000 psi. While Ti 75A cannot be heat treated

Table 2 Composition of Titanium Alloys Investigated

Alloy Designation	Ti	N	O	Fe	C	Mn	Al	Cr	Mo
Ti-75A	99.4	0.06	0.20	0.29	0.05	-	-	-	-
Ti-100A	99.7	0.11	-	0.15	0.04	-	-	-	-
RC-130B	93.3	0.05	-	-	0.11	3.5	3.00	-	-
Ti-140A	94.3	0.14	-	2.04	0.04	-	-	1.80	1.70

it can be work hardened, and the effects of work hardening can in turn be removed by annealing at about 1250F. Another nonheat-treatable alloy is Ti 100A.

Titanium that has been highly worked by rolling, drawing or other means will develop a pronounced texture or preferred crystal orientation as will other metals having a HCP structure. In the case of rolled α titanium, the prismatic planes of slip (ABDE in Fig. 3) tend to become aligned with the direction of rolling and this results in a greater strength in the direction of rolling than in the transverse direction.

The effects of cold working titanium can be removed by a full strain recrystallization treatment. This can be accomplished by heating the material to 1100 to 1300 F for up to one hour. A strain relieving treatment without recrystallization can be given a titanium part by holding it at a temperature between 650 to 1000 F for up to one hour.

Alloys that contain relatively large quantities of chromium, molybdenum, aluminum, manganese, or iron in solution can be quenched and age hardened. In this case the chromium and iron tend to stabilize the β (BCC) form of titanium at room temperature. For example, the Ti 140A used in this investigation is seen in Table 2 to contain 1.80% Cr, 1.70% Mo and 2.04% Fe. These additions make it possible to harden the alloy by adjusting the cooling rate in the range from 1700 to 1400°F where the $\beta - \alpha$ phase transformation normally occurs. The RC 130B alloy is seen in Table 2 to contain manganese and aluminum as the principal alloy additions.

Amounts of carbon up to 0.15% will remain in solution and will increase the strength of the alloy without loss of ductility. The small carbides that form with carbon contents between 0.15 and 0.20% are reported to have a

grain refining tendency and hence may be beneficial. A carbon content in excess of 0.2% is generally conceded to be objectionable due to the high abrasive wear associated with the titanium carbides that precipitate throughout the matrix.

Titanium has some interesting chemical properties. Its normal valence is four and the metal is characterized by a strong tendency to react with compounds containing nitrogen, oxygen, carbon and halogens, particularly at elevated temperatures. This makes it difficult to refine titanium since it has a strong tendency to react with the usual refractory materials.

At elevated temperatures nitrogen and oxygen diffuse readily into titanium. Hydrogen will also diffuse into titanium alloys and cause embrittlement. For this reason it is important that hydrogen not be used in furnaces as an inert or reducing atmosphere.

The titanium alloys have excellent corrosion resistance toward most chemical reagents and are completely immune to attack in sea water. Hydrofluoric acid is about the only material to attack titanium alloys at ambient temperature and this acid is used in metallographic etches for titanium alloy surfaces. Titanium alloys are attacked by sulfuric and hydrochloric acids at elevated temperatures but are completely safe from attack in nitric and other oxidizing acids. Titanium probably owes its good corrosion resistance to the presence of a close-knit oxide film that forms immediately upon a fresh titanium surface.

The mechanical properties of the titanium alloys of this investigation are summarized in Table 3. Standard laboratory test procedures were used in collecting all of these data.

True stress-strain tensile curves are shown in Fig. 4. The slope of such a curve in the region of plastic strain is the best measure available of the tendency for a material to strain harden. Here it is evident that titanium alloys have only slightly greater tendency to strain harden than ordinary steel. Normally a neck forms on a tensile specimen for a ductile material at a strain of about 0.2 in/in. In the case of all titanium specimens the strain at rupture was close to 0.2 in/in and there was essentially no neck formed. The titanium alloys tested were significantly less ductile than steel specimens of comparable hardness.

Table 3. Physical Properties of Titanium Alloys

Material	Yield Point [1] psi	Ultimate [2] psi	Young's Modulus x10^{-6} psi	% Elongation	% Area Reduction	Brinell Hardness
Ti-75A	72,000	104,000	16.3	23.5	30	240
Ti-100A	74,500	90,000	16.7	28.5	30	214
RC-130B	139,000	148,000	17.0	16.5	35	319
Ti-140A	142,000	140,000	16.6	18.0	21	320

1. Yield = stress at 0.2% offset
2. Engineering ultimate stress = maximum load divided by initial area.

Torsion data are shown plotted in Fig. 5 and these results are in general agreement with the tensile curves of Fig. 4. The Ti 100A material is seen to have a lower flow stress in torsion as well as in tension. The fact that the hardness of the Ti 100A specimen is lower than that of the Ti 75A specimen is in agreement with both of these observations. From Figures 4 and 5 it is possible to rate the particular materials tested in this investigation in order of increasing flow stress for large plastic strain approximately as follows:

Ti-100A
Ti-75A
Ti-140A
RC-130B

The cutting forces should be expected to lie in this same order, and we shall later note that this is the case.

Notched bar impact data obtained at different test temperatures are shown in Fig. 6. These data were obtained on standard Charpy impact specimens. The impact strength of Ti-140A is seen to be unusually good and similar to steel. This could be due to the high Cr and Mo content of this alloy which will tend to provide a mixed α - β structure and hence one that contains less of the HCP material which is not as ductile as the β structure of ordinary steel. The other titanium alloys have relatively poor impact strength at ordinary temperatures.

Meyer hardness data are given in Fig. 7 for the titanium alloys as well as for other materials. This test is believed to tell little regarding the strain hardening tendency of a material. These results are presented only to illustrate the misleading nature of the Meyer exponent. The slopes of the curves of Fig. 4 give the true modulus of strain hardening by definition. The lack of agreement between the slopes of the curves of Fig. 4 and the Meyer exponents of Fig. 7 can only mean that the latter are a poor measure of strain hardening. Stainless steel (18-10) which is known to have an unusually high modulus of strain hardening is seen to have a Meyer exponent about equal to that for 4140 steel which in turn is known to have a much smaller tendency to strain harden.

While thermal conductivity and specific heat are properties of titanium of major interest particularly with regard to cutting tool temperatures there are surprisingly few values available in the literature, particularly for high values of temperature. It was therefore decided to determine the temperature variation of these thermal properties for a number of alloys. This was done in a specially constructed apparatus. Determinations were made to temperatures of 1000F for thermal conductivity and 1500°F for specific heat. The resulting curves of thermal conductivity vs. temperature were approximately straight lines, and results are given in Table 4a for titanium alloys and other metals. The thermal conductivities of the titanium alloys were found to be slightly less than that for commercially pure titanium, but the values for all titanium alloys are relatively small. Values of specific heat are given in table 4b.

Table 4a Variation of Thermal Conductivity (k) in BTU/in^2/sec/(°F/in) with Specimen Temperature (t) in °F.

Material	Thermal Conductivity x 10^4
Titanium Alloys	
RC 55	$k = 3.05 - .0015\,t + 76\times10^{-8}t^2$
Ti 75A (specimen 1)	$k = 3.1 - .00017t$
Ti 75A (specimen 2)	$k = 2.75 - .00018t$
Ti 130A	$k = 1.88 + .00035t$
Ti 150A (specimen 1)	$k = 2.25$
Ti 150A (specimen 2)	$k = 2.0$
Ti 140A	$k = 2.22$
Armco Iron	$k = 10.3 - .0049t$
SAE 1045	$k = 6.75 - .0015t$
Carbides	
CA-2 (steel type)	$k = 7.25 - .001t$
CA-4 (C.I. type)	$k = 16.5 - .01t + 4.5\times10^{-6}t^2$
High Speed Steels	
T-1	$k = 5.05 - .0005t$
M-1	$k = 4.90 - .5\times10^{-6}t^2$
M-2	$k = 4.50 - .0002t$
M-10	$k = 4.50 + .00025t$

Table 4b Variation of Specific Heat and Volume Specific Heat With Specimen Temperature (t) in °F. (From measurements made in range from 70 to 1500F).

Material	Specific Heat (c), BTU/16/°F
Ti 75A	$0.122 + 4 \times 10^{-5} (t-70) + 6 \times 10^{-9} (t-70)^2$
Ti 150A	$0.116 + 5.8 \times 10^{-5} (t-70) + 4.5 \times 10^{-9}) t-70)^2$
	Volume Specific Heat, (SC), BTU/in ^{3}/°F
Ti 75A	$0.0198 + 6 \times 10^{-6} (t-70) + 10^{-9} (t-70)^2$
Ti 150A	$0.0192 + 9.3 \times 10^{-6} (t-70) + 0.7 \times 10^{-9} (t-70)^2$

Chapter 2

Recommended Turning Practice

In this chapter, recommendations for the efficient turning of titanium alloys are given based upon the experiments and reasoning presented in subsequent chapters.

In chapter one the physical and chemical characteristics of titanium alloys were reviewed. Those properties of titanium that are significant with regard to its machining characteristics follow:

1. Low value of the product of thermal conductivity and volume specific heat ($k\rho c$) which gives rise to high tool temperatures when titanium is machined.

2. The tendency for the strength of titanium alloys to decrease with increase in temperature beginning at relatively low temperatures.

3. The tendency for titanium to form strong bonds with other metals.

4. The tendency for titanium to react with nitrogen, oxygen and carbon at elevated temperatures to form very hard and abrasive surface products.

5. The low stiffness of titanium alloys as reflected by low values of Young's Modulus of Elasticity.

6. The relatively low ductility of titanium alloys.

The procedures to be followed in machining titanium alloys differ from those commonly in use for steels of the same hardness and strength in but one important respect. The optimum speed for a titanium alloy will usually be but about 1/3 that for the comparable steel due to the very poor thermal properties of titanium. The types of tool wear found in titanium machining are similar to those for steel. For example when machining titanium alloys, tools are found to crater excessively when the speed is too high (particularly for the stronger alloys) and to chip excessively at the cutting edge when the speed is too low (particularly for the softer, weaker alloys). Tools used to machine steels are found to behave in the same way. The Taylor tool life equation is found to hold for titanium alloys in the practical range of speeds, just as it holds for steel. The relative machinability of the titanium alloys of this investigation are as follows, with the machinability of 1045 steel taken as 100%:

Ti 100A	70%
Ti 75A	65%
Ti 140A	35%
RC 130B	30%
1045 steel	100%

This means that the tool life of Ti 140A will be the same as that of 1045 steel if the speed used to machine the titanium alloy is 35% that used to machine the steel. As a good first approximation of titanium alloy may be successfully machined if all variables are fixed at values to give good results for 1045 steel with the exception of speed which should be in proportion to the foregoing machinability ratings.

In order to be more specific concerning the conditions under which a titanium alloy should be machined we will consider each of the important variables in turn and recommend good average values. It should be recognized, however, that hard and fast rules cannot be cited and that the quantities recommended represent only a good point of departure. For a specific application values on either side of the recommended values should be tried and tested for improved performance based not on improved tool life or increased productivity but upon minimum cost per part. The items of cost to be considered in deciding when a change results in more efficient machining with regard to cost include:

1. Cost of machine and operator during time required to make cut.
2. Cost of machine and operator while changing tools prorated over number of parts produced per grind.
3. Cost of reconditioning the tool prorated over the number of parts produced per grind.

Analytical expressions for use in determining optimum speeds and feeds based upon minimum cost are presented in the later chapters.

Tool Geometry - The following tool geometry should give good results with a carbide tool under average machining conditions:

Back rake angle = 0°
Side rake angle = 10°
Clearance and relief angles = 5°
Side cutting edge angle (SCEA) = 10°
Nose radius = 0.02 in.

For very heavy roughing cuts (large feed) or interrupted cuts, the side rake angle should be reduced to zero or -5° while at the same time the SCEA is increased to from 30 to 45°. For light finishing cuts the side rake angle might be increased to 15° and the nose radius increased to .03 inch. For HSS tools, the average side rake angle should be from 15 to 20°, and the SCEA about equal to the side rake angle. Otherwise, the tool geometry should be the same as for a carbide tool. For very rigid conditions, rake angles as high as 25° and SCEA's as high as 30° may be beneficial with HSS tools.

Tool Material - In general carbide tools are preferable to HSS tools in machining titanium. Only at speeds below 10 or 20 fpm should HSS tools be considered. Under normal conditions, when rough machining at the feed and speed corresponding to minimum cost, the steel cutting grade carbides will give best results. These include the following manufacturers designations: 78C, K2S, T04, CA5, etc., all of which are supposed to be equivalent. When finishing or otherwise machining at high speeds, (speeds >150 fpm for titanium alloys) the cast iron grade carbides will give better results. Carbides of this type include K-6, 883, HA, CA4, etc. If cast iron grade carbides are used at cost optimum speeds they give poorer results than steel cutting grade carbides due to excessive chipping, while if steel cutting grade carbides are used at higher speeds they give poorer results than the cast iron grade carbides due to excessive wear. When HSS tools are indicated, tools of the T-15 type give far better results then either the M-2 or T-1 varieties.

Maximum Wear Land - An important criterion with regard to the use of any tools has to do with the maximum wear land that may be used without danger of sudden tool failure and attendant increase in scrap loss and tool reconditioning cost. Ordinarily HSS tools of normal clearance can be used to a .060 inch wear without danger of sudden failure, while carbide tools are taken out of service and reground when the wear land reaches 0.030 inch. In the case of titanium it is advisable to revise these values downward, regrinding carbide tools after a 0.015 inch wear land has appeared and HSS tools after a .030 inch wear land is present. If these values prove satisfactory the wear land should be cautiously increased until it

becomes apparent that a further increase will give danger of an occasional catastrophic tool failure.

Cutting Speeds and Feeds - With carbide tools cost optimum speeds will correspond approximately to the following representative values:

Ti 75A and Ti 100A	180 to 200 fpm.
Ti 140A	100 fpm.
RC 130B	85 fpm.
1045 steel	275 fpm.

Corresponding speeds for HSS tools follow:

Ti 75A and Ti 100A	50 fpm.
Ti 140A	30 fpm.
RC 130B	25 fpm.
1045 steel	90 fpm.

These values represent good speeds to start with in roughing operations where cost optimum feeds are of the order of 0.010 to 0.015 ipr. For finishing operations, where best feeds are of the order of 0.005 to .008 ipr, higher speeds should be used.

Cutting Fluids - While commercial cutting fluids fail to reveal a significant effect upon the rate of tool wear, water base cutting fluids tend to increase the wear land that can be used without danger of sudden tool failure. It is recommended that a copious supply of a water base cutting fluid be used when machining titanium alloys with either a carbide or HSS tool.

Chip Control - Chip disposal is normally not a problem in machining titanium alloys due to the low ductility of these materials. Ordinary chip breaking arrangements are adequate but in many cases unnecessary for satisfactory chip control.

Finish - The finish produced on machined titanium surfaces is in general superior to that obtained on steel of the same hardness. The high speeds required with steel to produce good finish are not necessary with titanium due to the fact that titanium does not tend to form a large built-up edge even at low speeds.

Vibration - Titanium has a tendency to excite chatter in cutting tools

due to the tendency to form either discontinuous or inhomogeneous chips. The latter type of chip while appearing as a continuous ribbon to the naked eye is made up of segments separated by regions of large strain. Inhomogeneous or discontinuous chips will give rise to higher maximum tool temperatures and provide an increased opportunity for welding between chip and tool. Accelerated tool wear will result. Chips suspected of being discontinuous or inhomogeneous should be observed under the microscope and if this is the case, speed, feed or tool rigidity should be altered to provide a continuous and homogeneous chip. The low stiffness of titanium makes it difficult to machine thin sections that are unsupported without chatter.

Hard skin - Workpieces that have been forged or worked at temperatures above 1000 to 1200 F are apt to have a hard skin of titanium dioxide or titanium nitride due to the tendency for these products to form when titanium is heated in air. Excessive tool wear will result unless certain precautions are taken. The depth of cut should be sufficient to penetrate the skin. The feed should be as large as the strength of the tool will allow. This provides a minimum length of tool travel per unit axial length of bar. A low speed will usually be necessary to limit the temperature to a reasonable value (since temperature varies with both feed and speed). Feeds in excess of 0.05 ipr may be used at speeds of the order of 10 fpm. Under such conditions HSS tool life is comparable with that for steel grade carbides (which are superior to the cast iron grades under such conditions). While HSS tools wear more rapidly than carbide, the allowable wearland is greater, and the net result is that tool life is about the same. The lower cost of HSS tools makes it advisable to use them under such conditions.

Titanium containing oxygen and carbon - An increase in the oxygen concentration of a few tenths of a percent has a detrimental effect on tool life. This is true regardless of alloy content. In the stronger alloys poor tool life is also obtained when the carbon content is greater than about 0.2%. If an alloy containing large amounts of oxygen and carbon must be machined it is advisable to adopt a large feed, and correspondingly reduced speed in order to minimize abrasive wear.

Low speed machining - When for any reason it is advisable to machine at low speeds, (1 to 10 fpm), either carbide or HSS tools may be used with titanium alloys. While greatly accelerated wear rates result when steel is machined at low speeds with carbide tools, such is not the case for titanium alloys machined with carbides.

Chapter 3
Theoretical Background

In this chapter a number of the fundamental quantities of interest in connection with any metal cutting investigation are presented and briefly discussed. These concepts will be applied in the discussion of specific titanium and steel data in subsequent chapters.

In machining any work material we are interested in knowing the relative magnitudes of each of the following quantities and why they may be relatively high or low.

1. Life of cutting tool
2. Surface finish produced
3. Accuracy of finished part
4. Forces and power involved in making a cut.

The overall performance of a work material with regard to these quantities is vaguely referred to as its machinability and some sort of machinability index is frequently assigned to the material, the one most frequently used being the cutting speed to give a certain tool life, as for example the 60 minute tool life $(V)_{60}$ Such a rating ignores items 2, 3 and 4 and gives only an approximate picture of item one.

In the absence of a good machinability index it is best to study the fundamental quantities that control the cutting process and compare the individual magnitudes of each item for any new material with the corresponding quantity for a well known material such as steel. In this way a feeling for differences and similarities can be quickly obtained and a rather thorough familiarity with the new material established.

Some of the fundamental items of interest in understanding the cutting performance of a given work material include.

1. The physical and chemical properties of the material.
2. The physical manner in which chips are produced and the geometry of chip formation.
3. The forces and energy involved in making a cut and the resulting stresses.
4. The friction characteristics on the tool face.

5. The tendency for metal to transfer and remain on the tool.
6. The nature and characteristics of tool wear.
7. The temperature on the shear plane and along the tool face.

Item 1 is obviously of importance in all four aspects of machinability and a rather complete picture of the physical and chemical properties of titanium alloys have been given in Chapter 1. Items 2 to 7 have to do with tool life in one way or another, while items 2 and 5 have to do with the surface finish produced. (Item 2 is of importance to finish inasmuch as it may give rise to tool vibration.) The accuracy of the finished part will of course depend on tool vibration (items 2 and 4), the extent of the built-up-edge (item 5), the amount of tool wear that is allowed before the tool is reground, (item 6), elastic deflection of the tool (item 3), and the thermal expansion of the workpiece and machine tool resulting from the heat generated in cutting (item 7).

It is thus seen that machinability is a very complex concept that means different things to different people. There need be little wonder why machinability cannot be expressed in terms of a single index.

Chip Formation - In machining steel and other ordinary structural materials the chips produced are in the form of a continuous ribbon, individual segments, or some combination of these extremes where cracks extend part way across the chip. In continuous chip formation the material is deformed in simple shear and the process can be analyzed analytically for stresses, strains, etc. In the case of purely discontinuous chip formation the chip is produced by a complex process resembling extrusion and this process cannot be treated analytically (3). The intermediate type of chip can be treated analytically to a degree of approximation that depends upon the extent of crack formation in the chip. Normally ductile materials yield continuous chips while normally brittle materials such as cast iron and beta brass yield discontinuous chips.

Since titanium and its alloys are not particularly ductile at room temperature (Fig. 4) it is not surprising to find discontinuous chips at low cutting speeds (i.e., for low temperatures). At higher cutting speeds the material becomes sufficiently ductile, due to the rise in temperature, to produce chips in the form of continuous ribbons. However, these chips

are normally quite different in appearance from ordinary continuous chips in that the strain in them is not uniformly distributed but is largely confined in certain bands (4).

When cutting at high speeds, the material adjacent to a potential fracture plane (i.e., at a weak point) becomes very hot in the case of titanium alloys due to the rapid rate of energy input. The strength of titanium and its alloys falls off quite rapidly at elevated temperatures as illustrated in Chapter 1. (Figs. 1 and 2). Thus, at high speeds, "thermal softening" may overcome strain hardening" to the extent that the process becomes unstable. That is, when strain in any given zone reaches a certain value, the material within this zone becomes so hot that further strain makes the material behave softer, and if the load is maintained, strain will continue in that zone. Fig. 8 shows a chip which was formed in this manner, and plastic strain is seem to be distributed in an inhomogeneous manner. Chips of this type seem to be peculiar to titanium and its alloys and the inhomogeneous chip represents a third basic type distinctly different from the purely continuous and discontinuous types of chips.

The discontinuous type of chip that is obtained when titanium is cut at low speeds is shown in Fig. 9. While this chip is composed of discrete segments, it is mechanically in one piece since the segments have rewelded together following fracture. The distinct difference between the chips of Figs. 8 and 9 should be noted.

At certain intermediate speeds a continuous chip, such as that of Fig. 10, can be obtained. However, the exact conditions for obtaining and maintaining continuous cutting are difficult to find when cutting titanium alloys.

Whenever either a discontinuous or a non-homogeneous chip is obtained, the peak forces will be larger than the mean; peak temperatures will be very high; and there will be a period of zero relative motion between chip and tool. These conditions favor the formation of strong welds and will therefore lead to excessive tool wear.

Tool Vibration - Whenever we observe discontinuous or non-homogeneous cutting, we also observe tool vibration. The question immediately arises,

if the tool and workpiece were perfectly rigid, could these types of chips obtain. Unfortunately, present theory will lead to either a yes or no answer, depending upon particular conditions; also an infinitely rigid experimental set-up is obviously not available for test. However, several indirect observations definitely show that tool rigidity does influence chip formation.

The spacing of the regions of large strain in an inhomogeneous chip is about equal to the feed, and the cutting force is found to vary significantly over each cycle. The frequency of this force variation is found to be approximately

$$f = \frac{V}{5t}, \text{ cps} \qquad (1)$$

where V is the cutting speed in fpm and t is the feed in ipr. For a lathe cut at 200 fpm and 0.004 ipr feed, the frequency is found to be about 10,000 cps. Such high frequency force fluctuations can excite natural modes of vibration in the machine tool and cause poor finish. Or, they can lead to surface fatigue of the tool face and high rates of wear.

If the equation of motion governing tool vibration in the direction of cutting velocity is written, it is found that the slope of the F_p vs V curve appears as a damping coefficient, where F_p is the power force component and V is the cutting speed. However, since the slope of this curve is generally negative, when machining titanium, we have a case of negative damping and a self-excited vibration may result. Fig. 11 shows F_p vs V curves for a series of feeds when machining Ti 140A. Note that in general the curve has a steep negative slope, then tends to level out and then again exhibits a steep negative slope. If the curve should have a zero or positive slope over a wide enough speed range, the tool would tend to be stable. Thus the tendency for stability is seen to increase with decreased feed and will vary with cutting speed.

The similarity between the shape of the curves of Fig. 11 and the curves of Figs. 1 and 2 showing the variation of yield stress or hardness with temperature is striking. In general there is a region of low slope in the central portion of the plot for each of the two types of curves. The region of low slope for the yield stress and hardness vs temperature curves

occurs in the region from 500 to 700 F and is due to strain aging.

As a vibrating tool cuts, the cutting speed varies. It has been shown by Salje (5) that tool life is a direct function of the maximum cutting velocity, i.e., the mean velocity plus the vibrational velocity. It is important then that we cut with a minimum of tool vibration regardless of the type of chip that is produced.

For a given set of cutting conditions, a more rigid tool-workpiece set-up will always give lower vibrational velocities. In the zero slope region of the F_p vs V curve, the greater the rigidity the less will be the variation in velocity, and the less chance for reaching the negative slope portions of the curve. Thus, high rigidity will limit vibration and can in certain circumstances eliminate it.

In summary it may be observed that it is most desirable to have a continuous chip. In general this will not be obtained in machining titanium alloys. The tendency toward chip continuity can be increased through metallurgical changes that reduce the degree of thermal softening (for case of inhomogeneous chips) or by effecting an increase in the shear-strain required for fracture (for case of discontinuous chips). If discontinuous chips are obtained it is important to limit tool vibration as much as is possible. This is best done by maintaining high tool and workpiece rigidity, and if possible, by operating near the zero slope portion of the F_p vs V curve by properly selecting the speed-feed combination. It is more important to have a rigid set-up when machining titanium alloys than when machining other metals due to the unusually steep nature of the strength vs temperature curve.

Cutting Forces and Energies - The forces involved in cutting may be measured by means of a sort of spring balance or dynamometer that is introduced between tool and machine in order to measure the components of force to which the tool is subjected. A lathe dynamometer is shown in Fig. 12. Here, a 5/8 inch square tool bit is shown projecting from the end of a heavy circular member. When the tool is subjected to a vertical or horizontal force the circular member bends very slightly. This elastic deflection causes a resistance change in strain gages mounted on the circular

member and connected in the form of a bridge circuit. The output from the bridge circuit when amplified is recorded directly in pounds upon a moving chart. The vertical component of force which is oriented tangentically to the workpiece is termed the power force F_p since it is responsible for all of the power consumed in making a cut. The axial force component in the direction of feed is at right angles to F_p and is designated F_Q. The geometrical relationship between the components of force F_p and F_Q and the shear plane and tool face is shown in Fig. 13.

When the cutting force components F_p and F_Q are known, together with the shear angle (ϕ) and rake angle (α) it is possible to compute several quantities of interest by application of the simplest principles of geometry and static mechanics (6). Some of the more important of these quantities follow.

1. The mean shear (τ) and normal (σ) stresses on the shear plane are obtained by dividing the tangential and normal components of the resultant cutting force on the shear plane respectively by the area of the shear plane.

$$\tau = (F_p \cos\phi - F_Q \sin\phi) \left(\frac{\sin\phi}{bt}\right), \text{ psi} \qquad (2)$$

$$\sigma = (F_p \sin\phi + F_Q \cos\phi) \left(\frac{\sin\phi}{bt}\right), \text{ psi} \qquad (3)$$

2. The shear strain in the chip (γ) is

$$\gamma = \cot\phi + \tan(\phi - \alpha) \qquad (4)$$

3. The coefficient of friction between chip and tool (μ) is

$$\mu = \frac{F_Q + F_p \tan\alpha}{F_p - F_Q \tan\alpha} \qquad (5)$$

4. The amount of energy consumed in the shear process per unit volume of metal cut (u_s) is

$$u_s = \tau\gamma, \text{ in lb/cu in} \qquad (6)$$

5. The amount of energy consumed in overcoming friction on the tool face (u_f) is

$$u_f = \left(\frac{F_Q \cos\alpha + F_p \sin\alpha}{bt}\right)\left(\frac{V_c}{V}\right), \text{ in lb/cu in} \qquad (7)$$

where V_c is the velocity of the chip relative to the tool face.

6. The total energy per unit volume consumed in cutting (u) is

$$u = u_s + u_f = \frac{F_p}{bt}, \text{ in lb/cu in} \qquad (8)$$

The derivations leading to these quantities are well known (6) and need not be given here.

Friction of Titanium Alloys - The modern view of friction recognizes that all surfaces are rough on a microscale and that mating surfaces touch only on their high points. The points of contact are plastically deformed under load to produce a real area of contact (A_R) that is distinguished from the apparent area of contact (A). The relation between the applied load (N) and the real area (A_R) follows

$$N = \sigma_y A_R \qquad (9)$$

where σ_y is the flow stress of the material constituting a high point on the surface. Welding or adhesion occurs at mating high points and the force required to rupture such welds is the friction force (F). For clean surfaces

$$F = \tau A_R \qquad (10)$$

where τ is the shear stress required to break the weld. The coefficient of friction for clean surfaces will be

$$\mu = \frac{F}{N} = \frac{\tau A_R}{\sigma_y A_R} = \frac{\tau}{\sigma_y} \qquad (11)$$

An effective lubricant will contaminate some of the real area (A_R) and decrease the shear stress to a lower value τ_L. If α is the fraction of the real area that is contaminated then

$$F = \tau_L \alpha A_R + \tau (1-\alpha) A_R \qquad (12)$$

and

$$u = \alpha \frac{\tau_L}{\sigma_y} + (1-\alpha)\frac{\tau}{\sigma_y} \qquad (13)$$

To be effective the lubricant must adhere strongly to the surface. Most monomolecular films of long chain polar compounds are effective lubricants for moderate loads. For the heaviest loads such as those on the face of a tool a very strong bond is required and probably a layer of considerable thickness. In such cases the low shear strength layer is usually achieved by having the fluid react chemically with the metal at the points of contact to form solid reaction products of low shear strength such as metal chlorides or sulfides.

The friction characteristics of titanium alloys have been extensively studied by Dr. E. Rabinowicz in the Lubrication Laboratory at M.I.T., and certain important differences have noted between the characteristics of titanium sliders and those of other metals.

When two like metals (other than titanium) are slid together in dry air the coefficient of friction is usually about one. The coefficient of dry friction of unlike metals is usually much less and of the order of 0.2. When a steel rider is caused to slide over a titanium surface the initial coefficient of friction is found to be about 0.2 but very quickly this value increases to about 0.45. The value of the coefficient of friction of titanium on titanium is also 0.45 and it is evident that a layer of titanium has quickly formed on the steel surface and completely covers it. From this point on we have titanium sliding on titanium. As a particle of titanium is plucked from the steel surface another takes its place. The layer of titanium that is built up is not only found to be quite complete but also very thin.

All metals give the same coefficient against titanium as steel after a short time, as long as their hardness is above a certain value. For very soft metals such as lead the particles of titanium that transfer become embedded in the softer metal and a thin layer of lead spreads over the harder particles to provide a greatly decreased shear strength (τ), but increased flow stress (σ_y) and hence a low value of coefficient of friction. When the junctions giving rise to friction are broken they break in the weaker lead layer for the most part.

The polar lubricants that absorb on most metals and give lower friction are completely ineffective on titanium as are the extreme pressure types of fluids that react chemically to produce a low shear strength layer. The failure of the usually effective polar compounds is believed to be due to the strong tendency for titanium to react with oxygen to produce a TiO_2 layer on the surface. The oxide which carried the opposite electrostatic charge from a clean metal surface will not produce strong polar bonds with the fluid molecules. The chemical type, extreme pressure lubricants are probably ineffective for the same reason titanium alloys are so corrosion resistant, which is also believed due to the speed and compactness of the oxide layer that is formed on titanium. Graphite bonded to a titanium surface with a resin and certain fluorocarbons have been successful in lowering the friction when steel slides on titanium. Certain fluids of very high viscosity that would not be expected to react with titanium have also been somewhat successful in lowering friction. This may be due to the reduction in the rate of diffusion of oxygen through the very visions fluid in the vicinity of a sliding titanium surface.

In summary, the dry friction of titanium on titanium is found to be considerably less than for most pairs of similar metals. This, however, is not due to any tendency for titanium to refrain from bonding to other metals. On the contrary, another metal surface is very quickly coated with a titanium layer. This layer is quickly oxidized and then we have a pair of titanium oxide surfaces sliding one over the other. The presence of a strong compact oxide film prevents the usually effective boundary and extreme boundary lubricants from being effective.

Wear and Metal Transfer - When one metal slides over another the surfaces contact each other only at the highest points and the junctions that are formed give rise to a friction force as already described. As the junctions are broken material is transferred from one surface to the other since the junctions do not always rupture at the exact points where they went together. For each junction that is made there is a probability that the breaking of this junction will result in a wear particle. This probability will depend upon the metals in contact and the lubricant that is present. If one surface is harder and stronger than the other then the

probability of a particle being plucked from the harder surface when a junction is broken will be less than the probability that a wear particle will be pulled from the softer surface.

It is found experimentally that when wear occurs in an orderly fashion the particles are quite small and of fairly uniform size (volume). The volume worn away on either surface (W) should be expected to be equal to the product of the total number of encounters and the probability of an encounter resulting in a wear particle, thus

$$W = K A_R L \qquad (14)$$

where L is the actual sliding distance A_R is the real area of contact and k is a constant (proportional to the probability mentioned above and a function of the metals in contact and the lubricant present). The quantity $A_R L$ will be proportional to the total number of contacts that correspond to a sliding distance L. From equation (9) we may eliminate A_R and obtain

$$W = k \frac{N}{\sigma_y} L \qquad (15)$$

Burwell and Strang (7) have shown that the quantity (k/σ_y) is a constant for a given material combination regardless of the distance of sliding (L), the sliding speed, the hardness of the metal surface, and the applied load (N), as long as the applied load is below a certain critical value (N_c), where

$$\frac{N_c}{A} = \sigma_{y_b} \qquad (16)$$

Here, A is the apparent area of contact and σ_{y_b} is the bulk yield stress of the softer of the pair of metals in sliding contact.

The nature of the experimental results obtained is shown in Fig. 14. Here it is seen that equation (15) holds very well until N/A exceeds σ_{y_b}, which for steel is about 1/3 the Brinell hardness but for softer metals may be 1/4 to 1/6 the Brinell hardness. At this point the wear becomes catastrophic since the high points on the softer surface are pushed into the underlying surface and there is a sudden increase in the real area of contact (A_R).

It is interesting to note that the coefficient of friction was the same for all values of W/A in Fig. 14 including those in the catastrophic

wear region. Since from equation (11) the coefficient of friction is the ratio of the shear stress to hardness (τ/σ_y) it follows that in general when τ changes, σ_y also changes by approximately the same amount. It is because of this fact that the coefficient of friction is independent of the rate of wear and hence cannot be used to infer anything with regard to the wear characteristics of a system.

Tool Wear - In the case of a cutting tool, wear occurs on either the clearance face or chip face, and must involve the uniform non-catastrophic type of wear corresponding to equation (15) for a reasonable tool life. From this well established relationship we should expect the volume of tool lost to vary directly as the load between the work material (or chip) and tool and the length of surface that passes over the tool surface (L).

In addition to the transfer type of wear described above, metal may also be lost from a tool due to:

1. A plowing action of hard particles of built-up edge or in the matrix. This is most pronounced at low cutting speeds when the built-up edge is likely to be large.
2. A chipping action in which particles that are larger than those in transfer wear (although still small) are broken from the tool from time to time as welds are broken.
3. Corrosion of the tool due to the action of sulfur or chlorine containing additives upon the tool. This is most common in the case of carbide tools where over-active additives sometimes attack and etch away the cobalt binder in the carbide.

In addition to these gradual methods of tool breakdown, tools may fail suddenly as a result of overheating or softening (particularly carbon and HSS tools) or due to actual breakage. If a tool fails due to overheating a reduction in cutting speed is most effective in reducing the amount of heat generated per unit time. The feed may also be reduced but is not quite as effective in reducing the temperature as is the speed. The tool temperature is rather insensitive to changes in depth of cut as we shall see in the following section. A water base cutting fluid may sometimes lower the tool temperature.

If a tool fails by rupture this indicates either a force on the tool point that is too high or an included tool angle that is too small. A decrease in rake angle or feed will usually tend to reduce tool breakage. Instead of decreasing rake angle over the entire tool face it is sometimes sufficient to stone a small secondary rake surface of decreased angles on the tool face near the cutting edge, thus leaving the main portion of the tool with the larger original rake angle. Also, an increase in side cutting edge angle may be necessary in order to prevent breakage at the end of a heavy-cut as the tool breaks through the surface. Sometimes a crater will form on the tool face, starting not at the tool point but at a position removed from the tool point at which the temperature is a maximum (Fig. 15). As the crater it extends to the cutting edge and has the effect of weakening the tool by reducing the included angle. When a large crater develops on the tool surface, failure by rupture across the point from a region of stress concentration in the base of the crater is frequently observed. The tendency for a tool to crater can usually be reduced by an increase in rake angle (to lessen the stress on the tool face), or by causing a decrease in tool face friction. Although the friction force usually decreases with speed, the ratio between the wear rate on the chip and clearance faces of the tool is found to increase with increasing cutting speed, and hence most tools crater significantly at high speeds. The remedy to be applied to tools that fail prematurely due to overheating, large scale breakage or excessive cratering is usually evident. It is the gradual type of tool wear on the clearance face that is not persistent and difficult to combat.

The wear land that develops on the clearance surface of the tool (w in Fig. 15) is a convenient measure of the amount of gradual tool wear on that surface. Tools are frequently reground when the value of w equals some definite value such as .015, 0.030 or 0.060 in, the lower values generally being used when the hardest materials are cut with carbide and the highest values being used when soft metals are cut with HSS tools. If the tolerance on the part cut is severe a low value of w will generally be used. It is of course important that the limiting value of w be reached in any case before the crater becomes sufficiently large to allow tool

breakage to occur.

If the length of work material passing the tool point (L) is plotted against the size of the wear land (w) curves of the type shown in Fig. 16 may be obtained for different values of cutting speed (V). At speed V_3 after an initially rapid breakdown of the cutting point, a gradual wear of the clearance surface occurs in accordance with equation (15). The volume worn from the clearance face of the tool (W) is related to the wear land (w) as follows:

$$W = \frac{1}{2} b w^2 \tan \} \qquad (17)$$

where b is the depth of cut (distance perpendicular to the paper in Fig. 15) and $\}$ is the clearance angle of the tool.

For constant values of b and $\}$ equation (17) becomes

$$W = \text{const.}\ w^2 \qquad (18)$$

If this is substituted in equation (15), then for values of normal load on the clearance land less than N_c:

$$L = \text{const.}\ \frac{W^2}{N} \qquad (19)$$

If the normal force on the clearance land is proportional to w then we obtain the linear relationship

$$L = \text{const.}\ w \qquad (20)$$

If on the other hand the normal force on the wear land is independent of w then

$$L = \text{const.}\ w^2 \qquad (21)$$

Curves such as those shown in Fig. 16 are often linear (eq. 20) but are sometimes found to be parabolic (eq. 19) as in the case of titanium alloys. Curves such as those of Fig. 16 are sometimes not exactly smooth, but show frequent non-periodic vertical jogs resulting from chipping (i.e., the formation of unusually large wear (particles) from time to time. It is important to note that in general the L vs W curve is not a straight line but is intermediate between the straight line of eq. (20) and the parabola of eq. (19).

As the wear land develops, the cutting forces increase. Should the

value of the normal force on the wear land satisfy eq. (16), due for example to N increasing linearly with w while the workpiece hardness decreases with rise in temperature, the wear rate will increase suddenly as at point A in Fig. 16. The value of L corresponding to point A is practically the same for complete failure of the tool and tool life has frequently been defined as the value of L (or the cutting time or cubic inches of metal removed or other equivalent measures of the basic quantity L) for complete tool breakdown. This tool life definition has been most widely used for HSS tools. For carbide tools the value of L corresponding to a certain value of w has been more widely adopted. When such a definition is used it is important that tests be run all the way to w_{max} in order to be sure that point A is not reached before w_{max} is obtained. The fallacy of running a short time test to point B on the curve marked V_4 in Fig. 16 and extrapolating these results to w to obtain L_4^* is evident. (L^* corresponds to the value of L when w_{max} is obtained.) In this case catastrophic wear sets in almost immediately beyond point B.

When values of life (L^*) defined either in terms of complete failure or a given wear land w_{max} are plotted against cutting speed on log-log coordinates an approximately straight line is obtained (Fig. 17) at elevated cutting speeds, i.e.

$$VL^{*A} + B \qquad (22)$$

where A and B are constants.

This curve fails to hold at very low speeds due to the increased tendency to form built-up-edge and the chipping that results when the BUE is removed. It is more common to express tool life in terms of the cutting time (T) in minutes corresponding to a given length of travel (L^*) in feet. Since

$$L^* = VT$$

then from eq. (22) we have

$$V(VT)^A = B \qquad (23)$$

or

$$VT^{A/A + 1} = B^{1/A + 1} \qquad (24)$$

This is seen to be equivalent to the familiar Taylor equation.

$$VT^n = C \qquad (25)$$

which also plots as a straight line on log-log coordinates where n and C are other constants. In the discussions of this report to follow we shall use equations (22) and (25) interchangeable.

In studying the development of a wear land the question of just what value to use arises whenever the wear is not uniform along the cutting edge. Frequently the wear land will have the appearance of Fig. 18 which is a plan view of the clearance surface. Here the wear land develops more rapidly in the vicinity of A than elsewhere. We have found the maximum wear land to give a more consistent picture of tool performance than the mean wear land, and consequently have adopted the maximum wear land as the criterion of tool life. Also, from a weakest link point of view it should be expected that the maximum wear land would be most significant.

When a tool wear curve is plotted for a titanium alloy cut with a hard carbide a plot such as that shown schematically in Fig. 19 may be obtained. In the case of a normal steel test the curve will usually be more linear and the vertical jogs in the curve will not be nearly so pronounced. These exaggerated jogs have been observed to be due to non-periodic chipping that occurs in a rather random manner, the tendency of chipping being a function of the material machined and the tool material and geometry. The resultant wear curve up to point A is made up of three parts.

1. A rapid initial breakdown
2. Gradual uniform wear
3. The chipping out of particles larger than those produced in uniform wear.

At point A the catastrophic wear rate sets in and the tool fails rapidly.

It has been found convenient to separate the three types of wear and to study them independently. In this way a better view of the life that can be achieved in the absence of chipping and initial breakdown can be obtained. The dotted curve represents the wear curve that would be obtained in the absence of initial breakdown and chipping. The portion of the curve extending from B to C is seen to correspond to a portion of the dotted curve displaced.

In order to illustrate the type of curve that Fig.19 is meant to represent a specific example will be considered for a Ti 140A specimen machined with a very hard carbide tool at 150 fpm (Fig. 20). An unusually large jog occured at point A due to chipping, but the equivalent portion of the wear curve from B to C (Fig. 20) was immediately resumed. At a value of w of about 0.015 in. catastrophic failure began.

From the observations of a large number of wear plots it has been found that the gradual wear curve when machining titanium is parabolic corresponding to eq. (21) displaced an amount equivalent to the initial breakdown. The gradual wear curve that has been found applicable when machining titanium is

$$L = \text{const}\,(w^2 - w_o^2) \qquad (26)$$

where w_o is the value of w corresponding to initial breakdown. The specific equation of this type for the data of Fig. 20 is

$$L = 16.7 \times 10^6\,(W^2 - 19\times10^6) \qquad (26a)$$

and is shown by the dotted curve in Fig. (20). For this example the following values obtain:

$$L_o = -317$$

$$L^* = 1600$$

$$L^{**} = 3750$$

This means that the 0.015" wear land life would be 3750 ft if no chipping or initial breakdown occurred. Comparing this with the actual life it is seen that initial breakdown and chipping are responsible for an unusually large reduction in the life of the tool. This, however, is to be expected for such a hard tool with zero degrees side cutting edge angle. The foregoing method of analysis is far more revealing than the conventional tool life analysis. In the example considered chipping is responsible for a 49% reduction in life from that potentially available while initial breakdown is responsible for an 8% reduction in the potential life.

Wear Tests on Titanium Alloys - In order to study the wear characteristics of different tool material - titanium alloy combinations, a special test apparatus was devised in the hope that it would speed the testing. A piece of titanium about 3" diameter was mounted in the lathe between centers and a light cut taken from the surface with a clean carbide tool in order to clean the surface. The apparatus shown in Fig. 21 was then swung into place and a wear test made.

The wear apparatus consisted of a rigid arm pivoted on bearings, (A) mounted on a bracket, (B) attached to the cross slide. A dynamometer (C) capable of measuring vertical (N) and tangential (F) components of force was mounted on the arm, and a specimen holder (D) which held a 1/4 inch diameter specimen (F) of tool material, with its axis at right angles to the work-piece axis, was attached to the dynamometer. Normal load was applied by placing weights (F) at any point of the arm. The wires shown connect the dynamometer bridge circuits to the strain recorder used to automatically plot forces F and N as the test proceeded. The 1/4 inch diameter specimen was fed along the axis of the workpiece at such a rate that new material was continuously traversed. The temperature at the work - tool interface was measured by the thermoelectric technique used in cutting to be presently discussed.

The nature of the wear scar left on the tool specimen after a test is shown in Fig. 22. The volume of material removed (W) is related to the major axis of the elliptical wear scar (2a), and the diameters of the two specimens (d) and (D) as follows:

$$W = \frac{(2a)^4}{13.46D\sqrt{\frac{D}{d}}} \qquad (27)$$

or since d was always 1/4 inch

$$W = \frac{(2a)^4}{26.92D^{3/2}} \qquad (28)$$

Representative wear data obtained from this apparatus are shown in Figs. 23 to 25. In Fig. 23 test results using K-6 carbide against Ti 140A are shown. The rate of wear is seen to have a general linear trend, but

to deviate from this general trend significantly for short periods of time. The vertical jogs in the wear curve are believed to result from chipping or the loss of relatively large particles of tool material from time to time, while the horizontal jogs are the results of the development of a built-up protective layer. It was generally found that a period of zero or slight wear was followed by a sudden loss of material as the protective layer became so large as to be unstable. In Fig. 24 the results of tests at three speeds are plotted together to show that unlike the wear in cutting this wear is approximately independent of sliding speed. The data of Fig. 25 show results for different tool materials where it is evident that HSS exhibits less rapid wear than the carbides, and particularly the very hard carbides.

The results of Figs. 23 to 25 resemble those obtained in cutting at very low speeds. Under such conditions

1. Carbides will wear more rapidly than HSS
2. Wear rate will be independent of speed since surface temperature are so low that temperature is not the quantity of paramount importance
3. Wear is very erratic alternating between a slow rate when a built-up protective layer is being formed by a smearing action and a more rapid rate when this layer leaves the surface and chipping occurs.

The basic difficulty with this sort of wear test lies in the fact that the same temperatures are not reached as in cutting when the speeds are the same. For example, in one that operated at a normal load of 9 pounds and a speed of 160 fpm, the coefficient of friction was observed to be 0.62, while the mean contact temperature was but 465F. In a cutting test at this speed the temperature on the face of the tool would have been several times this value (see representative values in Chapter 5). The intensity of shear stress on the wear surface is of a much lower order than in cutting and as a result there is a greater tendency for the softer metal to smear onto the harder surface and to build up a protective layer which upon leaving causes a chipping type of wear. In cutting, the surfaces are cleaner and the greater mean shear stress causes the protective layer to be largely swept from the surface as fast as it is built up. The appearance of the wear area resembles

that found on a cutting tool at very low cutting speeds. Thus, for several reasons the wear characteristics in the wear test at speeds in the normal cutting range resembles those for a cutting tool operated at a very much lower speed.

The gradual rate of wear (dotted curve) of Fig. 20 may be compared with that of Fig. 23 since these tests were run under comparable conditions except for the method of test. From equations (17) and (26a) we have

$$L = 16.7 \times 10^{6} \frac{W}{1/2(.06)\tan(5)}$$

if the initial breakdown of the tool is ignored. From this equation the volummetric wear per foot (W/L) is found to be 0.16×10^{-9} cu in/ft. From Fig. 23 the value of (W/L) is found to be 0.64×10^{-9} cu in/ft. Thus the rate of wear in the wear test is seen to be greater than that found in a cutting test at the same speed. This may be explained by the fact that the rate of wear of cutting tools is normally greater at very low speeds than at moderate speeds. The tool life - speed curve will normally be as shown in Fig. 26. While the wear rate for the cutting test corresponds to point A (low wear rate) the value for the wear test might be at point B (high wear rate) due to the equivalent speed being so much less for the wear test. The fact that very hard tool materials yield higher rates of wear in the wear test (See Fig. 25) is in keeping with the concept of a low relative speed, since very hard carbide tools frequently give poorer life than softer tools when operated at very low cutting speeds.

In view of the major differences that exist between a friction-slider and the surface of a cutting tool further tests on the wear apparatus were not made. It was considered preferable to study the wear characteristics of the actual cutting process instead.

Tool temperature - The temperature at the tip of a cutting tool is extremely important with regard to tool life. The cutting speed is the single most important operating variable having an influence on tool life, and the chief effect of cutting speed in turn resides in its influence upon the temperature of the cutting tool.

A relationship connecting tool temperature with other quantities of

greatest importance may be obtained by a simple application of dimensional analysis which is a useful analytical tool in certain engineering subjects notably fluid mechanics. We begin by listing all variables influencing the temperature together with their dimensions in terms of the fundamental set: temperature (Θ), length (L), force (F), and time (T):

Table 5. Dimensional Analysis for Tool Temperature

Symbol	Quantity	Dimensions
$\bar{\Theta}_t$	Mean tool face temperature	Θ
u	Total energy per unit volume	FL^{-2}
V	Cutting speed	LT^{-1}
t	feed	L
k	thermal conductivity of work	$FT^{-1}\Theta^{-1}$
ρc	volume specific heat of work	$FL^{-2}\Theta^{-1}$

Careful study will reveal that this is the total list of variables of primary importance for a tool of fixed geometry. For example it should not be difficult to see that the depth of cut (b) is relatively unimportant. Upon performing the dimensional analysis following the usual technique (8) we obtain

$$\frac{\bar{\Theta}_t \rho c}{u} = \psi \left(\frac{V \rho c t}{k} \right) \tag{29}$$

where ψ is some function that cannot be determined by dimensional analysis.

It is found experimentally that to a good approximation when $\frac{\bar{\Theta}_t \rho c}{u}$ is plotted against $\left(\frac{V \rho c t}{k} \right)$ on log-log coordinates a straight line is obtained having a slope of -0.5 and hence

$$\left(\bar{\Theta}_t \frac{\rho c}{u} \right) \left(\frac{V \rho c t}{k} \right)^{-0.5} = \text{constant} \tag{30}$$

or

$$\bar{\Theta}_t = \text{const } u \sqrt{\frac{Vt}{k \rho c}} \tag{31}$$

If we had been a little more astute we should have noted that in heat transfer problems involvinga moving heat source, k and ρc are always associated as the product ($k \rho$ c) just as the quantities E (young's modulus) and I (moment of inertia) come into all elastic

deflection problems as the product (EI) but in no other way. If then the dimensional analysis were repeated using ($k\rho c$) in place of (k) and (ρc) we end up with but one dimensional group and hence

$$\frac{\theta_t}{u}\sqrt{\frac{k\rho c}{vt}} = \text{const.} \qquad (32)$$

which is identical with equation (31) and obtained without recourse to direct experiment.

Equation (31) is useful in understanding the influence of workpiece hardness and strength (u), workpiece thermal properties ($k\rho c$) and of speed (V) and feed (t), upon the mean tool temperature. The thermal group ($k\rho c$) of the workpiece is seen to be the important quantity with regard to tool temperature. It is revealing to consider the relative tool temperatures to be expected for the materials listed below.

Table 6. Values of u and ($k\rho c$) for several metals

Metal	u. in lb/cu in x 10^{-6}	$(k\rho c)$, $(BTU/in^2{}^oF)^2/sec \times 10^6$
1020 steel	0.3	27
75-ST Aluminum	0.1	34
140A Titanium	0.3	6.4

If each of these metals are cut with the same feed, at a speed to give the same tool temperature, the corresponding speeds will stand in the ratios:

$$\frac{V_{Al}}{V_{St}} = \left(\frac{k\rho c_{Al}}{k\rho c_{St}}\right)\left(\frac{u_{St}}{u_{Al}}\right) = 11.3$$

$$\frac{V_{Ti}}{V_{St}} = \left(\frac{k\rho c_{Ti}}{k\rho c_{St}}\right)\left(\frac{u_{St}}{u_{Ti}}\right)^2 = .24$$

Thus, if a speed of 500 fpm gives a tool temperature of 1000 F when cutting steel, the corresponding speeds to give the same temperature for aluminum and Ti 140A would be

$V_{Al} = 5650$ fpm.

$V_{Ti} = 120$ fpm.

It is seen that whereas aluminum may be machined at a very high speed relative to steel, titanium must be machined at a relatively low speed compared with steel. The reason that titanium alloys must be machined at such low speed is seen to lie in their unusually low values of ($k\rho c$).

While the foregoing treatment represents a useful first approximation a more elaborate analysis can be performed that introduces several other secondary factors influencing tool temperature. Such an analysis has been given in a recent publication (9) but only a qualitative picture of what is involved will be given here. In the more elaborate analysis it is recognized that heat is dissipated at two important regions in the vicinity of the tool point, 1) along the shear plane and 2) along the tool face (see Fig. 27). The assumption that all of the shear energy is converted into a quantity of heat (Q_1) on the shear plane while all of the frictional energy ends up as heat (Q_2) on the tool face is a good one. If R_1 is the fraction of the shear plane heat going into the chip, the remainder $(1-R_1)\ Q_1$ flows into the workpiece. By equating the mean temperatures along the shear plane computed as points in the chip and in the workpiece respectively, expressions for R_1 and the mean temperature on the shear plane ($\bar{\theta}_s$) may be found. Similarly, by equating the temperature rise at the tool face computed first as a point in the chip and then as a point in the tool, the quantity R_2 may be found together with the temperature rise at the tool face. The mean tool face temperature ($\bar{\theta}_t$) is then the sum of the mean shear plane temperature ($\bar{\theta}_s$) and the mean temperature rise at the tool face. Four important quantities result from the more elaborate calculation:

1. Fraction of shear energy going to chip (R_1)
2. Mean shear plane temperature ($\bar{\theta}_s$)
3. Fraction of tool face energy going to chip (R_2)
4. Mean tool face temperature ($\bar{\theta}_t$)

From the more elaborate analysis it is found that the depth of cut (b) has a very small effect. The mean tool temperature also decreases slightly as tool conductivity increases.

The mean tool temperature ($\bar{\theta}_t$) can be measured experimentally by measuring the thermoelectric emf generated at the interface between a tool and dissimilar work material. The usual arrangement for making such measurements is shown diagramatically in Fig. (28) where the hot junction

of the thermoelectric circuit is at h while cold junctions are at a and c with intermediate junctions at b, d, and e. As long as the temperatures at a, b, c, d, e remain constant the emf measured with the recording potentiometer (P) will be a measure of the temperature at h. The amalgamated copper disc which rotates in the mercury cup provides a means for completing the circuit without the use of a slip ring or brush system of possibly variable contact resistance.

With most carbide tools the emf developed at the brazed junction with the shank becomes noticeable as soon as heat reaches this point. However, this spurious voltage can be compensated by making the wire of (a) of alumel and attaching it directly to the carbide. Since alumel happens to have very nearly the same thermoelectric properties as most carbides the effect of temperature changes at the brazed joint are reduced. Furthermore, temperature equilibrium is reached at the tip of a cutting tool in a fraction of a second, and usually the temperature reading can be obtained long before the brazed interface has an opportunity to become heated.

There are two fundamental difficulties associated with the use of thermoelectric data. One lies in the fact that the chip-tool interface actually consists of a large number of junctions each of which generates its own thermoelectric emf. These miniature thermocouples are connected in parallel and the value measured is some sort of average value, the particular average obtaining depending upon the nature and extent of the stray currents that flow between adjacent thermoelectric junctions.

The second difficulty is associated with the presence of a transferred layer of built-up material upon the tool face. Such a layer when present removes the corresponding junctions from the measurement since there is no longer a dissimilar pair of metals at the interface. However, the dissimilar metal interface is not removed entirely but is merely transferred to a point where the temperature is lower due to the steep temperature gradient that always obtains near the surface of a cutting tool. The result of a built-up layer is to yield mean temperatures that are too low.

Despite the two objections discussed above the thermoelectric measurements appear to agree quite well with computed temperature values provided the speed is sufficiently high so that no large amount of built-up edge is present.

In order to convert measured values of emf to temperature values, each tool-work combination must be calibrated. This is readily accomplished by use of the apparatus shown in Fig. (29). A long piece of work material in the form of a chip is placed in a bath of molten metal near the tip of a long piece of tool material (direct contact need not be made). A standard chromel-alumel junction is placed close to the chip and tool and the metal bath heated by means of an electric heater. One recording potentiometer measures the emf from the standard couple while the other measures the emf from the chip-tool couple to the nearest 0.1 mv. The cold end of the tool must be kept at constant temperature. This is most easily accomplished by brazing several pieces of tool material together to provide a long "lead". The cold end is further kept cool by means of a damp cloth. It is usually convenient to use a long enough length of chip so that the cold junction correction at the cold end of the chip offers no problem. The sign of the thermoelectric emf of HSS against steel (or Ti) is opposite that for carbide against steel (or Ti). Calibration curves for several tool-workpiece combinations are given in Fig. 30.

Since calibration curves are inconvenient to obtain attempts have been made to decrease the number of curves required. One of these is the two-tool thermocouple technique of Gottwein and Reichel. By this method two tools of widely different composition are used simultaneously. Then, if the temperature at both tools is the same the potentiometer reading will be independent of the work material and will depend only on the tool materials. A single calibration of one tool material against the other will then suffice for all work materials.

Unfortunately, the basic assumption on which this method is based, namely, that the temperatures at both tools will be the same, is false. Chip-tool interface temperatures are dependent upon the tool materials due

To the different friction and thermal properties pertaining to each tool material. The set-up is not only complicated but the useful speed is limited by the weaker of the two tool materials which is usually HSS. While the two tool method has been used in Germany as an acceptance test to check the uniformity of material to be machined it is not a useful research method and will not be used in this investigation. The single tool thermocouple method already described will be used instead.

Representative values of cutting temperatures and their interpretation will be presented in Chapter 5.

Temperature and the Tool Life Equation - The Taylor equation (eq. 25) expresses the relation between tool life in minutes (T) and cutting speed in feet per minute (V). If we differentiate this equation we obtain

$$\frac{dT}{T} = -\frac{1}{n} \quad \frac{dV}{V} \tag{33}$$

This says that the percent change in tool life is proportional to the percent change in cutting speed, the factor of portionality being $(\frac{1}{n})$. In most cases the value of n is of the order of 0.1 which then means that the percent change in tool life is about 10 times the corresponding percent change in speed.

In the speed range where the Taylor equation holds (i.e. for speeds above say 100 fpm) the temperature plays a very important role in determining tool life and it is for this reason that small changes in velocity have such a large effect on changes in tool life. From equation (31) it is evident that tool temperature varies as $V^{1/2}$ and hence from equation (25)

$$\text{Tool life } (T) \sim \frac{1}{V^{1/n}} \sim \frac{1}{\bar{\theta}_t{}^{2/n}} \tag{34}$$

If n is equal to 0.1, then tool life is seen to vary inversely as V to the tenth power (another way of saying what was said above in terms of a percentage change) but inversely as $\bar{\theta}_t$ to the twentieth power. Small

changes in tool temperature thus normally give rise to very important changes in tool life. This effect is seen to be the more pronounced as the value of n decreases.

Actually the value of the exponent n in the Taylor equation (eq. 25) may be considered a measure of the degree of importance of temperature relative to tool life. At low cutting speeds tool life is independent of cutting speed. In this range of cutting speeds the exponent in the Taylor equation (n) will be one. This may be seen as follows. Since the tool life (L*) in feet is related to tool life in minutes (T) as follows:

$$T = \frac{L^*}{V} \qquad (35)$$

then upon substituting for T in the Taylor equation (25) we have

$$V \left(\frac{L^*}{V}\right)^n = C \qquad (36)$$

The only way L* can be independent of V is for n to be one. Thus, the Taylor equation for slow speed cutting reduces to

$$L^* = \text{constant}. \qquad (37).$$

As the role of temperature becomes more important the value of (n) in the Taylor equation decreases. In most cases values of n are found to range from 0.05 to 0.2. The magnitude of n does not depend on the absolute tool temperature alone but really reflects the importance of temperature upon wear relative to other causes such as general affinity of the metals, abrasiveness, or cleanliness of the surfaces. On the other hand, the constant C in the Taylor equation depends directly on tool temperature. (C is the value of speed corresponding to a one minute tool life). Thus, we normally find that values of n for HSS tools are slightly less than corresponding values for carbide tools, while the values of C for these two materials differ by a factor of about 3. The following are representative values for n and C for HSS and carbide tools respectively when mild steel is machined.

Table 7. Representative values of n and C in Taylor Equation

Tool Material	n.	C
HSS	.10	200
Carbide	.15	600

Inasmuch as we have found that titanium gives unusually high tool temperature we might expect to find unusually low values for n and C in the Taylor equation. While C is found to be about 1/3 that for steel, the values of n are nearly the same as those for steel. This is due to the fact that although C depends directly on the influence of temperature, n reflects the influence of temperature on wear relative to other causes. Since titanium has a very strong tendency to bond to steel as well as to yield high cutting temperatures the resulting values of n turn out to be very close to those for steel when either a HSS or carbide tool is used.

Machining Economics - In choosing the operating variables to be used in any machining operation we are usually not interested in obtaining the longest possible tool life or in operating at the shortest possible cycle time. However, we are interested in producing a piece with satisfactory surface finish at the lowest possible cost. In roughing operations the question of finish usually does not arise and we will consider a roughing operation first. Gilbert (10) has presented an equation for the tool life corresponding to minimum cost and this is derived below.

In computing the maching cost per part, four items should be considered:

1. Cost of machine and operator including overhead for time to make cut (Tc). If x is cost of machine in ¢/min, then cutting cost per part is (x Tc).

2. Cost of machine and operator during time required to change work-pieces. If idle time to change work is (Ti) then work changing cost per part is (x Ti).

3. Cost of machine and operator during down time (Td) necessary to replace worn tools. The cost of tool replacing time per part will be

$x\ Td\ \frac{Tc}{T}$ where T is the tool life, Tc is the time to cut one part and

hence T/Tc is the number of parts produced per tool.

4. Average cost to regrind work tools (Yϕ). Tool reconditioning cost per part will then be Y (tc/T).

The total cost per part (ϕ) is the sum of the four foregoing items or

$$\phi = xTc + xTi + xTd\,\frac{Tc}{T} + Y\,\frac{Tc}{T} \qquad (37)$$

The cutting time per part will be

$$T_c = \frac{\pi D\,\ell}{Vt12} \qquad (38)$$

where D is work diameter, in

ℓ is axial length of work, in

t is feed, ipr

Substituting into equation (37) we obtain:

$$\phi = xTi + \left(\frac{\pi D\,\ell}{12}\right)\left(\frac{x}{Vt}\right) + \left(\frac{\pi D\,\ell}{12}\right)\left(\frac{xTd+Y}{Vt\,T}\right) \qquad (39)$$

After eliminating (V) from equation (39) by use of the Taylor equation (25) we may differentiate the cost (ϕ) with respect to T and equate the result to zero to find the tool life for <u>minimum cost</u> (T_m). When this is done holding the feed (t) constant we find the usual value for the cost of optimum tool life (T_m):

$$T_m = \left(\frac{x\,Td + Y}{X}\right)\left(\frac{1}{n} - 1\right) \qquad (40)$$

Where n is the exponent in the Taylor equation (25). From the Taylor equation, the speed corresponding to (T_m) is

$$V_m = \frac{C}{T_m^n} \qquad (41)$$

The tool life in minutes for minimum cost (T_m) is seen to depend only on a combination of the machine cost, tool regrinding cost and down time $\left(\frac{x\,Td + Y}{x}\right)$, and a function of the exponent in the Taylor equation (n). Thus, since it has been observed that (n) will have about the same value when machining titanium as when machining steel we should expect to find about the same economic tool life for titanium and steel when using a tool,

machine and operator of the same value. However, in equation (41) the speed to give minimum cost (V_m) is seen to depend on the constant C in the Taylor equation and hence V_m for steel should be expected to be 3 or 4 times that for titanium.

When speed (V) is held constant and the feed (t) is varied, a sort of Taylor equation is found to hold for tool life (T) <u>for large values of feed</u>

$$t\, T^{n_1} = C_1 \qquad (42)$$

where n_1 and C_1 are constants.

In a roughing operation the feed may be chosen (with speed held constant) to give minimum cost in the same way the speed was chosen for minimum cost when the feed was held constant. It can be similarly shown that the tool life for minimum cost in the case of variable feed is

$$T_{m1} = \left(\frac{x\, Td + Y}{x}\right)\left(\frac{1}{n_1} - 1\right) \qquad (43)$$

while the corresponding value of optimum feed (t_m) is

$$t_m = \frac{C_1}{T_{m1}}\, n1 \qquad (44)$$

In a finishing operation the maximum allowable feed will usually be fixed by considerations of roughness. As the feed is reduced the speed for minimum cost per part (V_m) will increase. The value of (n) in the Taylor equation is approximately independent of feed and hence (T_m) should not change appreciably with feed. However, C in the Taylor equation increases as feed is reduced and consequently (V_m) increases with decrease in feed. A better finish will then be produced by reducing the feed for two important reasons.

1. A direct reduction in feed roughness.

2. The resulting increase in V_m will usually give rise to less built-up edge.

Finishing operations can be carried out most economically if the following rules are applied.

1. In those cases where a high speed is not needed to give good finish, the feed should be as large as possible.

2. In those cases where (V_m) corresponding to the feed of first choice cannot be used due to machine limitations, an attempt should be made to use a larger feed which will yield a lower value of V_{m1}. In each of the above cases an increase in nose radius may make it possible to operate with increased feed and still produce the finish desired. While the general rule of the workshop calls for light feeds and high speeds in finishing operation, it should be appreciated that the most economical finishing operation corresponds to the one utilizing the largest feed permissible.

While it might be expected that difficulty due to built-up edge roughness might be experienced in finishing operations on titanium due to the low cutting speeds used, this is not true due to the inherent tendency for titanium to form a small built-up edge.

In equations (40) and (42) the cost ratio $R = \left(\frac{x\,Td + Y}{x}\right)$ appears. This quantity has the following range of values for most practical applications where the higher values of the range correspond to cases where the tooling cost is relatively large compared with machine and operator cost.

Table 8. Representative values of machining cost ratio (R).

Tool Material	Range of $R = \left(\frac{x\,Td + Y}{x}\right)$, min.
HSS	5 to 15
Carbide	25 to 75

Chapter 4
Low Speed Cutting Tests

A series of tests has been conducted to determine the cutting characteristics of titanium at very low cutting speeds. Ti 140A was cut at speeds of .4 fpm and 12 fpm. For purposes of comparison, similar tests were also made on C1112 steel. The apparatus used is shown in Figs. 31 and 32. The tool was fastened to the column of a milling machine while the workpiece was held in a dynamometer and fed past the tool by means of a table feed. The exact depth of cut was determined by indicating the cut surface relative to the dynamometer before and after each cut. The difference between the two readings is obviously the depth removed (t) which corresponds to the feed in a turning operation.

The standard test conditions were as follows:

Speed (V), .4 and 12 fpm
Depth (t), .002, .004, and .008 in.
Rake angle (α), 15°, 30°, 45°.
Fluid: dry, CCl_4.

Experience shows that when tool life is of major interest, the stresses and temperatures existing at the chip-tool interface are of considerable importance. A quantity which reflects both stress and temperature is the total cutting energy per unit volume (u), which energy is found to be a function of the following variables:

Material cut
Cutting speed (in the low speed range)
Depth of layer removed (feed in turning)
Width of cut (depth of cut in turning)
Effective rake angle
Friction condition on the tool face (cutting fluid, etc.)
Tool sharpness

In the tests considered here, material, width of cut and tool sharpness were held constant.

Fig. (33) shows energy per unit volume (u) plotted against depth of cut (t) for different conditions of speed, rake angle and fluid. The conclusions that may be drawn from these data include:

1. At $\alpha = 15°$, and at large depths of cut, the energy required to remove a unit volume of titanium is actually less than that required for a soft, free-machining steel (C1112).

2. As the rake angle is increased from 15° to 30° the decrease in energy for steel is quite large (35%-45%) while for titanium, the decrease is hardly noticeable (0%-10%). The major reason for this apparently lies in the difference in chip formation between steel and titanium. When cutting C1112 steel, a continuous chip is formed. Increasing the rake angle will increase the shear angle, thus decreasing both the shear stress and the area over which this stress acts, the net result being a decrease of specific energy (u). On the other hand, at low speeds, titanium gives a discontinuous chip. It has been observed that the angle of fracture varies very little with rake angle. Because of this, the fracture stress and fractured area will remain essentially constant.

3. Over the range of depths investigated, the decrease of energy as depth increases is much greater with titanium than with steel. It is generally accepted that materials exhibit a greater strength when very small specimens are tested than when large specimens are tested. Metal cutting provides a means of "testing" very small specimens because when a continuous chip is formed, the plastic deformation is largely limited to a very small zone along the shear plane. A direct result of this size effect is an increase of energy at low depths of cut. However, this is usually not appreciable until depths of about .001 inches are reached. In the case of titanium the size effects appears to be quite pronounced even in the range from .005 - .008 inches depth of cut. Perhaps this is due to the fact that a large portion of the energy is consumed in a small region surrounding the fracture surface between two discontinuous chips. If this is so, and it seems quite probable, a large portion of the energy will vary with the amount of fracture surface produced. As the depth of cut is decreased,

the discontinuities tend to remain geometrically similar. Thus, the fracture area increases inversely with the depth. This would explain why the size effect in titanium persists to such large depths of cut.

Cutting Fluids - It is quite apparent in Fig. 33 that the effect of a cutting fluid on titanium is greater at small rake angles and at low speeds. The speed effect is consistent with the usual observation that as the speed is increased, there is less time for fluid penetration and for chemical reaction of whatever fluid is able to penetrate.

Table 9 shows the effect of a series of cutting fluids on both titanium and C1112. The numbers listed represent the percentage decrease in energy per unit volume (u) when cutting with a fluid compared to cutting dry.

Table 0. Effect of Cutting Fluids at Low Speeds

$\alpha = 15°$; t = .005 inches

	Decrease of Energy per Unit Volume (u) %			
Fluid	C1112		Ti140A	
	0.4 fpm	12 fpm	0.4 fpm	12 fpm
Carbontetrachloride	45	2	36	7
Lauryl Alcohol	34	3	6	0
Aerosol (0.1% in water)	29	9	-3	0
Lauryl Mercaptan	28	7	6	0
STH - 3% in water	28	5	3	0
Oleic Acid	23	9	9	0
Lauryl Chloride	22	0	6	0
Distilled Water	17	-1	0	0
Benzene	-10	-27	3	0
Mercury	-	-	3	-

This table speaks for itself. Of the normally active cutting fluids, only carbontetrachloride has any noticeable effect at 12 fpm. At higher speeds, these fluids can act as coolants, but their effect upon the friction and cutting processes will be negligible. These cutting results are found to be in agreement with the slider friction test results reported in Chapter 3.

Inasmuch as the titanium chips produced at low speeds were discontinuous, the coefficient of friction, stresses in the chip and other values that are normally computed in a metal cutting study would have no meaning and hence have not been presented. The only quantity that appears to have meaning in such a case is the energy per unit volume.

In summary it has been found from the low speed tests that the energy per unit volume (u) is not excessively large when machining titanium, and does not decrease with increased rake angle nearly as much as in the case of steel. However, (u) does increase with decreased depth of cut much more rapidly for titanium than for steel. This would indicate use of small rake angles and large depths of cut (0.010 inch or larger). It appears that most cutting fluids will have little effect other than cooling at speeds above 10 fpm.

Chapter 5

Comparison Between Titanium and Steel in Turning

In the foregoing chapter a comparison was made between the low speed machining characteristics of titanium and steel. This study was restricted by the fact that the titanium chips were discontinuous. In order to obtain continuous chips or inhomogeneous continuous chips it is necessary to cut titanium at appreciable speed. In this chapter turning results obtained under good machining conditions for a representative titanium alloy (Ti 140A) are compared with similar results for 1045 steel.

In each case carbide tools were used since such tools give the best performance. However, the carbides chosen were not the same in each case but rather represented the best choice for each material. For the steel, a steel cutting grade carbide was used while for Ti 140A a cast iron grade carbide was used.

The general arrangement of the apparatus is shown in Fig. 34, and the manner in which the chip and clearance faces of the tool were examined microscopically in wear studies is shown in Fig. 35. The microscope is shown in position to observe the face of the tool across which the chip flows. The microscope is turned through 90 degrees to measure the wear land on the clearance surface.

Representative observed data for Ti 140A and 1045 steel are given in Table 10, while calculated data are given in Table 11. The values from individual tests are given in Table 10 in order to illustrate the nature of the variation between repeat runs. The average values from this table were then used to obtain the calculated values given in Table II.

The values labeled a_1 and a_2 in Table 10 are the minimum and maximum estimates of the extent of chip contact along the tool face measured from the cutting edge. These values were obtained by measuring the distance from the cutting edge to the upper-most scratches on the polished tool face with a toolmakers microscope. The quantity (e) is the chip-tool thermocouple emf in mv., and forces F_P and F_Q are the tangenial or power force and nonpower or axial force components respectively as measured with the lathe dynamometer shown in Figs. (34) and (35).

Table 10. Observed Cutting Data for Ti 140A and 1045 Steel

Tool material, k-6 carbide (Ti-140A) and k2s (SAE 1045); depth of cut, 0.06 in; cutting fluid, none; tool geometry; 0, 0, 5, 5, 5, 0, 0.015[1]

Work material	Test No.	Tool No.	V fpm	t ipr	e mv.	F_p lb.	F_Q lb.	a_1 in.	a_2 in.	r
Ti 140A		1A	150	0.0104	15.6	180	82	.012	.020	1.22
		1A	↓	↓	15.7	177	84	.012	.025	1.22
		2A			15.8	168	76	.010	.023	1.22
	1	2A			16.1	171	81	.010	.025	0.90
		1B			15.7	167	77	.012	.025	1.04
		1B	↓	↓	16.1	170	78	.013	.025	1.02
		Av.	150	0.0104	15.85	172	80	.012	.024	1.11
		2B	100	.0052	12.8	112	60	.010	.020	.74
	2	2B	↓	↓	13.0	110	61	.013	.020	.80
		1C			12.9	110	57	.010	.017	.74
		1C	↓	↓	13.1	109	56	.012	.020	.87
		Av.	100	.0052	12.95	110	58.5	.011	.019	.79
SAE 1045		4A	100	.0052	8.0	94	40	.012	.023	.40
		4A	↓	↓	8.2	97	41	.015	.025	.43
	3	5A			8.4	93	41	.012	.023	.43
		5A	↓	↓	8.4	95	42	.015	.028	.40
		Av.	100	.0052	8.30	95	41	.014	.025	.42
		4B	150	.0104	11.4	193	83	.015	.030	.494
	4	5B	↓	↓	11.4	192	83	.019	.032	.415
		5B			11.6	192	89	.015	.032	.472
		5B	↓	↓	11.6	184	84	.020	.038	.452
		Av.	150	.0104	11.50	192	85	.017	.033	.46
		6A	400	.0104	13.0	204	97	.016	.040	.443
	5	6A	↓	↓	12.9	207	109	.020	.040	.473
		4C			12.8	202	105	.020	.045	.473
		4C	↓	↓	12.8	202	105	.023	.045	.488
		Av.	400	.0104	12.9	204	104	.020	.043	.470
		6B	535	.0104	-	206	102	.020	.038	.474
		6B	↓	↓	13.8	201	102	.020	.040	.485
	6	6B			13.8	213	111	.022	.045	.490
		6B	↓	↓	13.8	221	118	.020	.045	.465
		Av.	535	.0104	13.8	210	108	.020	.043	.480

1. In accordance with the ASA system of tool angle specification.

Table 11. Calculated Cutting Data for Ti 140A and SAE 1045 Steel

Tool material, k-6 carbide (Ti-140A) and k2s, (SAE 1045); depth of cut, 0.06 in; cutting fluid, none;
tool geometry: 0, 0, 5, 5, 5, 0, 0.015

Test No.	Work Material	V fpm		Ø deg.	u_f psi	u psi	u_f/u	σ psi	τ psi	γ	$/^u$	OBS $\bar{\theta}_t$ ^oF	Calc $\bar{\theta}_s$ R_1	Calc $\bar{\theta}_s$ ^oF	Calc for a_1 $\bar{\theta}_t$ R_2	Calc for a_1 $\bar{\theta}_t$ ^oF	Cal for a_2 $\bar{\theta}_t$ R_2	Cal for a_2 $\bar{\theta}_t$ ^oF
1	Ti-140A	150	.0104	48	142000	275000	.52	216000	66000	2.02	.47	1665	.74	535	.78	2075	.77	1647
2	↓	100	.0052	38	148000	350000	.42	224000	100000	2.06	.53	1365	.62	690	.62	1332	.59	1163
3	SAE 1045	100	.0052	23	55000	304000	.18	93800	89500	2.78	.43	780	.51	473	.60	646	.55	591
4	↓	150	.0104	25	62500	307000	.20	107000	93300	2.60	.44	1095	.66	583	.77	1075	.75	943
5	↓	400	.0104	25	78400	327000	.24	122000	95500	2.60	.51	1230	.76	652	.89	1564	.88	1274
6	↓	535	.0104	26	83000	336000	.25	130000	99000	2.56	.52	1320	.79	683	.92	1743	.90	1458

Notes: In the thermal calculations the following values were used:

1. Thermal conductivity of tool (k_3) = 9.55×10^{-4} BTU/in^2/sec/(^{o}F/in) for k-6
and 7.63×10^{-4} BTU/in^2/sec/(^{o}F/in) for k-2s
2. Volume specific heat of Ti-140A (ρC):

t, ^{o}F	500	1000	1500	2000
ρC, BTU/in^3/^{o}F	.023	.028	.033	.039

3. Volume specific heat of SAE 1045 (ρC):

t, ^{o}F	0	400	800	1000	1200
ρC, BTU/in^3/^{o}F	.030	.035	.041	.047	.056

4. Values of thermal conductivity for the work material were obtained from Table 4a for the appropriate temperatures obtaining.
5. Room temperature was taken to be 75^{o}F.

The chip length ratios (r) were determined from chip weight. The value for the titanium specimen cut at 150 fpm is seen to be greater than one; a very unusual observation. Upon examining the chips microscopically they look quite ordinary as shown in Fig. (36a). The chips of test 1 appear to be continuous. However, when these same chips are observed microscopically we see that they are of the inhomogeneous type. The unusually large chip length ratio (greater than one) results from the inhomogeneous nature of titanium chip formation. When it was observed that the chips of test 1 were highly inhomogeneous it was decided to make a second test under conditions to give a continuous chip. By consulting Fig. 11 it was decided to try cutting conditions corresponding to point B (point A in Fig. 11 corresponds to the conditions of test one) and when this was done continuous chips were in fact obtained. This is evident in Fig. (37b). Similar steel chips are included in Figs. (36) and (37) for comparison. By comparing the chip thicknesses of Fig. 37b and c) it is evident that continuous titanium chips are considerably thinner than corresponding steel chips. This is also evident in the mean chip length ratio values for tests 2 and 3. (0.79 for Ti 140A and 0.42 for 1045 steel) From the foregoing experience it would appear that a note of caution is in order. Just because titanium chips appear to be continuous when observed microscopically is no assurance that they are so in fact. Analysis of results obtained under inhomogeneous cutting conditions are very difficult to analyze and can be misleading if it is not recognized that inhomogeneous strain is involved in the chip formation.

The data of Table 11 were computed in the manner outlined in Chapter 3. In interpreting these data it should be kept in mind that while the chips for test 1 were inhomogeneous all others were continuous. Study of the data presented in Table 11 allows several interesting observations to be made.

1. The shear angle (ϕ) is unusually large for titanium. This is associated with the unusually large chip length ratios obtained with titanium and results in smaller values of strain and higher chip velocities than

normally experienced in cutting steel.

2. The total energy per unit volume (u) associated with the machining of titanium alloys is about what might be expected for a steel of the same hardness.

3. The shear energy per unit volume (u_s) for titanium is lower than for steel (due to the smaller strains obtaining for titanium alloys) while the friction energy per unit volume (u_f) is unusually high for titanium. This is reflected in the ratio (u_f/u) which for steel normally runs between 20 and 25% but for titanium alloys is between 40 and 50%.

4. The shear stress on the shear plane (τ) is about the same for titanium and steel.

5. The normal stress on the shear plane (σ) is unusually high for titanium alloys. This makes it possible for the normally semi-brittle titanium alloys (which break before necking in a tensile test - see Fig. 4) to produce continuous chips even when the strain in the chips exceeds 2. Were it not for the unusually high normal stress on the shear plane in the case of titanium, all titanium chips would be discontinuous.

6. The coefficient of friction on the tool face is about the same when cutting titanium and steel.

7. The observed tool temperatures are very much higher when machining titanium than when machining steel. (For example, the temperatures for titanium and steel under identical conditions (tests 2 and 3) were observed to be 1365F and 780F respectively. This is due primarily to the low values of ($k\rho c$) for titanium alloys.

8. The agreement between observed and calculated cutting temperatures is poor when the chip is highly inhomogeneous (see test 1). The calculated value for test 1 is unusually large and is believed to be closer to the actual maximum temperature than the observed value. In inhomogeneous cutting the chip is starting and stopping periodically. When moving, the chip will travel above average speed and exceedingly high values of temperature will obtain. This is one of the reasons that cutting under conditions to give an inhomogeneous chip should be avoided.

The surface finish produced when machining titanium alloys is usually

much better than when steel is machined under comparable conditions. This is illustrated by the reproductions of plastic surface replicas shown in Fig. (38). These replicas were produced by moistening the clean machined surface with acetone and pressing a thin piece of clear plastic into the surface. The solvent softened plastic takes the form of the underlying steel surface.

The tool life characteristics of Ti 140A and 1045 steel were also compared. Plots of the distance the tool travels over the work (L) against the extent of the wear land (w) are given in Fig. 39 for both materials. All of the curves are seen to be distinctly parabolic in shape. The tool life in this study was taken as a 0.015 inch wear land, and the corresponding value of L is designated L^*. The values of L^* obtained at the several speeds are shown plotted in Fig. 40a against speed. The curves for both materials are seen to have the same general shape. In each case a maximum tool life is obtained as speed is reduced.

The same data of Fig. 40a are shown replotted in Fig. 40b in the form of the more familiar Taylor plot where tool life expressed in time (T) is plotted against cutting speed (V) on log-log coordinates. The curves are linear and correspond to the Taylor equation (25) only at higher cutting speeds (above 100 fpm for Ti 140A and above about 200 fpm for 1045 steel).

These plots are representative of the sort of tool life curves usually observed. Such curves have three distinct regions as illustrated diagramatically in Fig. (41).

1. In the first region (1) corresponding to the highest speeds, temperature is the predominant variable and the wear rate is a strong function of the cutting speed. This is the region where Taylor's equation ($VT^n = c$) holds and n is usually between .1 and .2.

2. In the second region (2) we have the type of wear that is experienced in most sliding contacts other than tools. The wear particles are very small and the wear rate is <u>independent of speed</u>. For this type of wear the exponent (n) of the Taylor equation equals one.

3. In the third region (3) we have the type of wear that is characteristic of sliding under very high load and low speed. There is ample time for large

welds or junctions to form and when these come apart large particles are pulled from the sliding surfaces. This action has been previously described in this report as chipping. This is the type of wear that predominates when cutting with large built-up edge. In this region the rate of wear usually decreases with increased cutting speed since the change in speed results in a decrease in the amount of built-up edge. Brittle materials such as carbides give poorer results than ductile tool materials such as HSS in this region of operation.

The curves of Fig.(40b) are seen to correspond to the diagramatic plot of Fig. (41). In the case of steel, region (2) is very small and the wear may be characterized as being either of the chipping (low speed) or Taylor (high speed) varieties. In the case of Ti 140A, chipping is not nearly as pronounced and all three types of wear are distinctly present. The fact that titanium does not tend to form a large built-up edge even at low speeds was mentioned in connection with the good finish obtained when machining titanium.

While it is impractical to use carbide to machine steel at low speeds, good results are obtained when titanium is machined with carbide at low speeds. This point is illustrated by the data of Fig. 42. Here, tool life results are given for HSS and carbide when machining Ti 140A and 1045 steel at the low speed of 20 fpm. From these data the following observations may be made.

1. The carbide tool gives 4 times the life of the HSS tool when machining Ti 140A but only 1/5 the life of the HSS tool when machining 1045 steel. This reflects the strong tendency for steel cutting tools to chip at low cutting speeds and thus the need for using a more ductile tool material (HSS) when machining steel at low speeds. Titanium having a much smaller tendency to form built-up edge can use carbide to advantage to much lower speeds.

2. The machinability of titanium at 20 fpm with the best tool material (carbide) is superior to that for steel with its best tool material (HSS). At 20 fpm the poor thermal properties of titanium are not important and the tendency for titanium to form less built-up edge results in a net advantage over steel.

In considering item (2) above it should be kept in mind that the comparison is on the basis of equal values of wear land. Normally HSS tools are used to a greater wear land than carbide tools. For example, under ordinary conditions of speed and work material hardness, carbide tools are taken out of service when w reaches .03 inch while HSS is kept in service until w is 0.06 inch. As the cutting conditions become more severe (higher speeds or more difficult materials) it is advisable to reduce w_{max} in order to avoid the risk of total tool breakdown resulting in increased scrap loss and greater tool reconditioning cost. We might conclude that at low cutting speeds titanium will machine about as well as steel provided the best tool materials are used in each case.

In the high speed region of operation tool life may be expressed in terms of the Taylor equation ($VT^n = C$) or its equivalent in terms of length ($VL^{*A} = B$). The constants in these equations for the Ti 140A and 1045 steel experiments of Fig. (40) are given in Table 12.

Table 12. Constants in Tool Life Equations

Material	A	B	n	C
Ti 140A	0.19	635	0.160	225
SAE 1045 steel	0.26	4200	0.206	750

The main use of the Taylor equation lies in the determination of the most economical cutting speed following the analysis given in Chapter 3. The assumption is of course made in this analysis that the cost-optimum speed lies within the range of speed for which the Taylor equation holds. An example illustrating the method to use when a straight line relationship between log T and log V is not obtained is given in Chapter 7.

Use of the economic tool life equation may be illustrated by an example. If we assume:

1. the value of a machine and operator is \$8 per hour (or 13.3 ¢/min = x).
2. the mean cost of reconditioning the carbide tool used is \$4.00 (Y = 400 ¢)
3. the time required to change tools is 3 minutes (T_d = 3 min)

then, the magnitude of the cost ratio (R) in equation (40) is

$$R = \frac{xT_d + Y}{x} = 33$$

which is seen to be within the range of values mentioned in Table 8. Substituting the appropriate values from Table 12 into equations 40 and 41 we obtain the following values for economic tool life and speed.

Table 13. Economic Tool life and Speed

Material	T_m, min	V_m, fpm
Ti 140A	173	99
SAE 1045 Steel	127	276

From Fig. (40b) these speeds are found to lie within the range for which the Taylor equation holds. The economic tool life for titanium is 35% greater than that for steel.

The ratio of economic speeds (V_m) for two materials provides a good measure of their machinability characteristics with regard to tool life. On the basis of this criterion the machinability of the 1045 steel of this example is related to that for Ti 140A as follows:

$$\frac{V_{m(\text{steel})}}{V_{m(\text{Ti})}} = \frac{276}{99} = 2.8$$

It may be said that the steel machines 2.8 times as readily as the titanium alloy when both are machined most economically, in this particular example. The ratio of the speeds to give a 60 minute tool life (V_{60}) is also frequently used as a measure of machinability, and the resulting ratios are usually in good agreement with those based on the foregoing more logical economic comparison. For example, in the present instance we have

$$\frac{V_{60(\text{steel})}}{V_{60(\text{Ti})}} = \frac{750}{\dfrac{.206}{\dfrac{\dfrac{60}{225}}{.16}}} = 2.75$$
$$60$$

which is seen in this case to be identical with the ratio ($V_{m\ \text{steel}}/V_{m\ \text{Ti}}$).

A 240 minute tool life comparison is also sometimes used and for the foregoing example we have

$$V_{240(\text{steel})} = \frac{750}{\dfrac{.206}{\dfrac{\dfrac{240}{225}}{240}^{.16}}} = 2.58$$

This is likewise seen to be in good agreement with the economic tool life comparison and shows that when machinability is based on the ratio of speeds corresponding to a given tool life in minutes the particular time that is chosen in the comparison is relatively unimportant.

Photographs of representative worn tools used to cut titanium and steel are shown in Fig. 43. The greater area of contact on the chip face of the tool in the case of steel is clearly evident.

Chapter 6
General Survey

In the foregoing chapters of this report the data presented were chosen to illustrate specific points under discussion. In this chapter a number of the more important variables that influence the turning characteristics of titanium alloys will be surveyed in a more systematic way. While the number of combinations of variables that could be studied is formidable a reasonable picture can be obtained by taking some condition as standard and observing the influence of changing one variable at a time.

Unless otherwise stated the standard condition corresponds to the following:

Table 14 - Standard Machining Conditions

Tool Geometry:	0, 0, 5, 5, 5, 0, .015 in
Tool Material:	K-6 carbide
Work Material:	Ti 140A
Cutting speed:	150 fpm.
Depth of cut:	0.060 in.
Feed:	0.0104 ipr
Cutting Fluid:	None
Wear land in determining tool life:	0.015 in.

Data for HSS tools are presented in only a relatively few cases since it became evident early in the investigation that the performance of carbide tools was superior. In the tool life plots L* corresponds to the length of work material that traverses the tool in feet to give a 0.015 inch wear land. The corresponding life in minutes (T) may be found by dividing this value by the cutting speed in fpm (V).

Tool Geometry - Fig. (44) shows results obtained when cutting conditions were standard except for side rake angle, which was varied from -20 to +10 degrees. Energy per unit volume (u) friction force on the tool face (F) and temperature ($\bar{\theta}_t$) all decreases with increasing rake angle.

Tool life appears to have a maximum at zero degrees. The life would follow

the dotted curve were it not for the onset of excessive chipping at about zero degrees with this particular tool - work combination. Usually with steel, u decreases about 1% per degree increase in rake angle and this in turn gives rise to decreases in F and $\bar{\theta}_t$.

It was found that an increase in side cutting edge angle (SCEA) to 10 or 15° enabled the rake angle of carbide tools to be increased to 10 or 15° without excessive chipping. In the case of HSS tools considerably improved performance was obtained by increasing both SCEA and side rake angle to 25°. A tool life curve for such a tool is shown at A (Fig. 48) which may be compared with curve B corresponding to the standard cutting conditions with a HSS tool. The reason that an increase in SCEA enables a higher and more efficient rake angle to be used without chipping lies in the fact that the increased SCEA causes the cutting force to be distributed over a greater length of cutting edge.

In a few tests with tools of increased nose radius (0.040 in) slightly improved performance was obtained.

In summary it might be said that the desired tool geometry for carbide tools used to cut titanium alloys differed little from the tool geometry that would be used to cut a steel of the same hardness. As a point of departure a good set of tool angles to try initially might be as follows:

0, 10, 5, 5, 5, 10, .02".

Operating variables - The influence of cutting speed on tool performance is shown in Fig. (45). The energy per unit volume (u) is about constant while the coefficient of friction appears to pass through a minimum value at about 150 fpm. The tool temperature varies as $V^{1/2}$ in accordance with equation (31). The unusually high temperatures that obtain at high speeds should be noted. The tool life curve for this material (Ti 140A) has been analyzed from the economic point of view in Chapter 5 and in this example the economic speed (Vm) was found to be 99 fpm. In this analysis it was also observed that the Taylor equation fit the tool life data to a speed of about 100 fpm.

Feed is found to have similar effects on cutting performance as speed (Fig. 46). However, the effect of feed on energy per unit volume is found to be greater than that for speed. In fact in Fig. (46) the effect of feed on (u) is found to be considerably greater than that normally observed for

steel, as was also found in Chapter 4 at low speeds. The size effect evident in Fig. 46 for titanium at feeds in excess of .016 ipr, is usually nil for steel at this feed rate. The friction force increases with feed as might be expected, but not linearly.

The tool temperature increases approximately parabolicly with feed. Analysis of the temperature curves of Figs. 45 and 46 reveals that temperature increases more rapidly with speed than feed. This is really what might be expected from equation (31) where it is evident that a greater influence of V on temperature is to be expected due to the smaller inverse effect that speed has upon u than feed has upon u.

The tool life curve of Fig. (46) has the same appearance as that for speed in Fig. (45). When the life curve of Fig. (46) is expressed in terms of time and plotted on log-log coordinates a straight line results corresponding to equation (42).

$$t\,T^{.27} = 0.021$$

This equation is similar to the Taylor equation but written for feed instead of speed. In Chapter 3 economic analyses were presented whereby the speed (Vm) corresponding to minimum cost per part would be found at constant feed as well as the feed (t_m) corresponding to minimum cost at constant speed. In Chapter 5 an example was presented to illustrate the determination of Vm. We may now continue this example to find the most economic feed when machining at 150 fpm and under the cost conditions of the previous example. From equation (43) the feed optimum tool life is found to be

$$T_{m1} = 33\left(\frac{1}{.27} - 1\right) = 89 \text{ min.}$$

while the corresponding optimum feed is found from equation (44) to be

$$t_m = \frac{.021}{89^{.27}} = 0.0063 \text{ ipr.}$$

Thus, when machining at 150 fpm and under the cost conditions previously outlined, the minimum cost per part would be found to obtain at a feed of 0.0063 ipr. Actually, the speed of 150 fpm is above the economic optimum (in Chapter 5 Vm was found to be 99 fpm) and the foregoing calculation should be repeated for a speed of about 100 fpm. If this were done it would be found that the economic value of feed at 100 fpm would be higher than the .0063 value given above for 150 fpm, and probably would lie in the vicinity of 0.010 ipr.

Tests in which the depth of cut is varied show that this operating variable is almost without importance.

In summary it might be stated that speed and feed are the important operating variables, feed being only slightly less important than speed in determining cutting forces, temperatures and tool life. A good combination of speed and feed to use initially in machining a titanium alloy with a cast iron grade of carbide is 100 fpm at a feed of .010 ipr.

Tool material - Representative cutting results for three grades of carbide are given in Fig. (47). The energy and temperature results would lead us to list these materials in the following order of increasing performance: K-6, K-8, K-2s.

However, the tool life picture is more complex. The solid lines show the life L^{*} including chipping. At speeds below 140 fpm the tools should be listed: K8, K6, K-2s in order of increasing performance. This order is however reversed at speeds above 1450 fpm. The reason for this lies in the fact that the tendency to chip increases with decreased speed and with increased hardness of carbide. At the lower speeds the harder carbide (K-8) while wearing less rapidly than K-2s has a greater tendency to chip and the net result favors the K-2s carbide. At high speeds where the tendency to chip is less K-8 is superior to K-2s because of its greater resistance to wear. The dotted curves shown give the tool life results for K-8 and K-2s without chipping (L^{**}). At all speeds the K-8 curve is found to correspond to greater values of tool life as we should expect due to the greater wear resistance of the K-8 carbide.

A note of caution regarding accelerated tool life tests would appear to be in order at this point. If only short time tests had been run, as is frequently the practice, the K-8 carbide would be clearly the best. However, as we have seen the economic cutting speed is apt to be in the vicinity of 100 fpm and in this region the K-2s carbide is superior. It is suspected that recommendations of very hard carbides made by other investigators based on high speed, short length, tests may be in error for economic cutting speeds.

In the case of HSS and stellite tools only tool life results are

presented in Fig. (48). Here it may be observed that M-2 and T-1 HSS gave indistinguishable results while stellite J is a little better. The tendency for stellite to chip is greater than for HSS, particularly at the lower speeds. The previously mentioned desirability of using increased rake angles and SCEAs with HSS tools is evident in Fig. (48).

In summary we may observe that it is not safe to infer tool life from temperature or energy values alone but cutting tests should be made. In general carbide is so much better than HSS in machining titanium alloys that it should be used where possible. While the cast iron grades of carbide usually give better results with titanium than steel cutting grades at very high speeds steel cutting carbides may give better results at practical speeds. The optimum grade of carbide should be determined by trial. When HSS must be used, large side rake angles and SCEAs should be employed (about 25° in each case)

Work material - Results for different titanium alloys are given in Fig. (49). The tool life for the four alloys tested are seen to lie in order of decreasing life as follows: Ti 100A, Ti 75A, Ti 140A, RC 130B. Comparing this order with the order of increasing flow stress in the torsion test results of Fig. 5 shows good correlation, and it would appear that torsion data provides a good measure of the relative machinability of titanium alloys. The values of u in Fig. (49) are also seen to lie in the same order as the tool life values. All of the tool life results obtained at speeds above 100 fpm for carbide tools plotted as straight lines on log-log coordinates in accordance with the Taylor equation. Representative values of n and C in the Taylor equation (25) are given in Table 15, together with values for a 60 minute tool life (V_{60}).

In Table (15) results are given for Ti 140A machined with 3 different carbides. When the economic speeds are computed based on the cost values of Chapter 5 (R = cost ratio = 33) the cost optimum speeds given in table 16 are obtained.

Table 15. Representative Constants for Taylor Equation
When feed is 0.0104 ipr (for tool angles etc. see Table 14)

Tool Material	Work Material	n	C	V_{60}
K-6	Ti 100A	.215	530	221
K-6	Ti 75A	.190	445	205
K-6	Ti 140A	.160	225	117
K-6	RC 130B	.160	170	90
K-8	Ti 140A	.265	320	108
K-2s	Ti 140A	.145	220	122
T-1 or M2	Ti 140A	.090	40	28
Stellite J	Ti 140A	.075	50	37
K-2s	1045 Steel	.206	750	323

Table 16. Cost Optimum Speeds for Different Carbides

Tool Material	Work Material	Vm. fpm	Tm. min.
K-6	Ti 140A	99	173
K-8	"	97	91
K-2s	"	102	195
K-2s	1045 steel	275	127

From this table the optimum speed is seen to be about the same for all three tool materials ($\cong$100 fpm). However, the K-2s carbide is seen to have a somewhat greater optimum life than the K-6 carbide, (and hence would give lower machining costs), while the K-8 carbide is distinctly inferior to these two. This further illustrates the observation made earlier to the effect that very hard carbides do not show up well at practical machining speeds.

In chapter 5 it was pointed out that the 60 minute tool life is a good measure of the relative machinability of work materials, based on economic considerations. Using the data of Tables (15 and 16) it can be shown that this observation of a workpiece is approximately independent of the tool material used.

Table 17. Machinability of Ti 140A Relative to 1045 Steel

Tool material	$\frac{Vm\text{-}Ti}{Vm\text{-}Steel}$ [1]	$\frac{V_{60} - Ti}{V_{60} - steel}$ [2]
K-6	.360	.362
K-8	.352	.365
K-2s	.371	.378

1. Values from Table (15)
2. Values from Table (16)

From the values of Table (17) it is evident that a machinability rating of 35% based on 1045 steel as 100% is a good approximation regardless of the carbide used in the comparison or on the exact method of comparison (i.e., whether V_{60} or Vm is used).

In Fig. (50) the relative machinability rating for the four alloys of this investigation are given, with 1045 steel taken as 100%. These values are rounded off to the nearest 5% since the data from which they are obtained are not consistent with closer reporting.

Cutting Fluids - When turning tests were performed using a wide variety of fluids, including gaseous atmospheres such as nitrogen, carbondioxide and trifluoro bromomethane negligible differences in cutting force were observed. The only exception to this rule was the case of carbontetrachloride which showed a 15% decrease in power force at practical turning speeds. Unfortunately this material cannot be used commercially. These observations are consistent with those reported for slow speed tests in Chapter 4. When water base fluids were used a small decrease in the rate of tool wear of the order of 10% was observed.

From these observations it might be concluded that a cutting fluid is not worthwhile in machining titanium. However, in certain tests where the tool had a tendency to fail catastrophically before the desired wearland was reached (as at point B in Fig. 16), it was found that use of a cutting fluid extended the wear land at which rapid wear set in even though essentially the same wear curve obtained with and without a fluid. This is another

indication of the danger of accelerated tests. It would thus appear desirable to use a water base cutting fluid in machining titanium, not for its effect on the rate of wear but rather for its effect on the maximum wear land at which a tool can be operated without risk of sudden failure.

Carbon and Oxygen Content - In order to investigate the influence of variations in carbon and oxygen content upon tool life, the following special titanium alloys were obtained.

Table 18. Composition of special titanium alloys for investigation of influence of oxygen and carbon content.

Heat N°.	Ti	N	O	Fe	C
5090	99.6	.034	-	.26	.04
5091	99.5	.013	.20	.26	.01
5098	99.3	.013	.40	.27	.03
5089	99.4	.013	-	.30	.27
5099	99.4	.012	-	.27	.32

Values of tool life (L^*) are shown plotted in Fig. 51 for a speed of 345 fpm.

The basic material (Heat 5090) had a composition very similar to the Ti 100A of this investigation (see Table 2), and had a life (L^*) very similar to that for Ti 100A. The influence of oxygen on tool life is most pronounced. The specimen with .4% oxygen had a life of but 1/8 that of the base material. The major difference between alloys Ti 75A and Ti-100A is seen to lie in the larger oxygen content of Ti 75A (see Table 2) and this is believed to be the major cause for the lower life observed for Ti 75A.

The influence of added carbon in the amounts 0.27 and 0.32 is observed to be nil. While it has been reported that carbon contents in excess of about 0.2 have a serious adverse influence on machinability of titanium alloys this was not found to be the case here. The explanation for this might lie in the fact that previous workers have added carbon to titanium

already significantly alloyed (such as Ti 140A) while in this investigation the base material to which the carbon was added was essentially commercially pure titanium.

Representative pictures of worn tools are presented in Fig. 52. The first at (a) shows a tool used to cut steel where the length of contact along the tool face is seen to be much larger than for the titanium alloys. Photograph (b) is for the base titanium alloy of the carbon, oxygen series and corresponds essentially to Ti 100A. Photographs (c) and (d) correspond to the .4% added oxygen and .3% added carbon alloys respectively. The high carbon alloy is seen to have greater chip surface wear for the same amount of clearance face wear than do the other titanium alloys. This is a detail that is not reflected in ordinary wear land studies.

Chapter 7

Results from Other Investigations

The turning of titanium alloys has been discussed in references 11 to 15, and some of the more significant findings will be abstracted here as a matter of convenience.

A recent report of the U.S. Air Force (11) presents turning life data on several titanium alloys. While some of these results are for highly accelerated tests, others are carried to values of tool life that are in the practical range. In Table 19 values of n and C in the Taylor equation together with values of V_{60} are given for T-1, HSS, and K-6 carbide tools used to machine several titanium alloys.

Table 19. Taylor constants from Reference (11)[3]

Work	Brinell Hardness	T-1 HSS[1] n	C	V_{60}	K-6 Carbide[2] n	C	V_{60}
3Al, 5 Cr 0.4C	363	-	-	-	.20	245	108
130B	341	.09	39	27	.20	300	132
150A	338	.04	61	52	.25	440	158
140A	302	-	-	-	.15	330	179
75A	187	-	-	-	.21	830	350

1. Values based on 0.060 inch wear land; tool angles: 0, 15, 0, 5, 5, 0.010; feed, 0.009 ipr; fluid, 1.25 soluble oil in water.
2. Values based on 0.015 inch wear land; tool angles: 0, 6, 0, 6, 6, .040; feed, 0.010 ipr; fluid, none.
3. Taylor plots for missing points were nonlinear.

The values of n and V_{60} for carbide tools are very similar to those of this investigation (Table 15). While the HSS values of V_{60} in Table (19) are considerably higher than those of this investigation due mainly to the difference in wear land associated with tool life in each case, the exponents (n) in the two investigations are seen to be in good agreement.

In the Air Force Tests cast iron type carbides were considered to be better than steel cutting grade carbides. However, the tests upon which this conclusion was based were carried out at speeds above the practical level. As noted in Chapter 6 the harder cast iron grade carbides were found to be best only at elevated speeds. The T-15 type HSS was found to be far superior to the M-2 or T-1 varieties in the Air Force tests.

All tool life curves in the Air Force report were not found to satisfy the Taylor equation, even in the practical range of speeds. In the present investigation deviation from the Taylor equation was only observed at low cutting speeds. Since the Taylor equation may occasionally not hold in the range of interest, it is important that the procedure for finding the economic machining speed be altered to take this into account.

A nonlinear tool life curve from page 78 of the Air Force report is shown in Fig. (53). The slope of this curve (n) is not constant but may be found at each value of (V). Then, when the values of n are substituted in the optimum tool life equation (40) to obtain (T_m), different values of (T_m) will be found for each speed instead of a single value as in the usual case. In order to find the value of Tm and Vm in such an instance it is necessary to plot T vs V and Tm vs V. The required answer then lies at the point of intersection of these two curves.

For example, the data in Fig. (53) are shown replotted on rectangular coordinates in Fig. (54) (curve marked T). Then, values of Tm obtained for the variable values of n obtained by measuring slopes of Fig. (53) are plotted against V. Several of these Tm curves are shown in Fig. (54) for different values of R. If R is 30 then the optimum tool life is seen to be 23 minutes while the optimum speed is 97 fpm. The effect of changes in R on Vm is evident in Fig. (54) at a glance. This extension of the economic analysis enables problems to be readily solved when the operating point lies on the nonlinear region of the T vs V curve.

Two tool life vs feed curves are shown in Fig. 55 from page 82 of the Air Force Report. In order to understand the shape of these curves it is important to note that temperature is the most important item with regard to tool life, and that it is because of this that speed has such an important influence on life. Since feed has almost an equal affect on tool temperature

we should expect tool life to vary with feed in about the same way it does with speed. In Fig. 26 a diagramatic sketch was presented showing the general type of tool life curve obtained when feed is held constant and speed is varied. A similar curve such as that of Fig. 56 is to be expected if speed is maintained constant while feed is varied. Depending on the speed of the tests, different parts of this curve will be obtained. In Figs. (55a and b) the portions of the general curve of Fig. (56) are those marked A and B respectively.

Very frequently tool life is expressed in terms of the volume removed instead of time. If Fig. (55a) is plotted on rectangular coordinates in terms of tool life expressed in volume removed, a curve as shown in Fig. (57) is obtained. It is customary to state that the optimum tool life corresponds to the maximum value indicated at point A. Actually, we should determine the best feed from economic considerations just as we do for speed. An example of how this can be done was given in Chapter 6. However, in this case the curve of T vs t was a straight line on a log-log plot. Since the curve in Fig. 55a is nonlinear a method similar to that just used for the nonlinear speed curve must be applied.

The cost optimum must lie to the right of point A in Fig. (55a) where the exponent n_1 in the expression $t\,T^{n1} = C_1$ is just equal to one. If n_1 is determined for different values of t we may plot Tm (obtained from equation (43) vs t for different values of the cost ratio R as shown in Fig. (58). Also shown plotted in this figure is the T vs t curve from Fig. (55a). The optimum feed will correspond to the point of intersection of the T and Tm curves. For example, assume the following cost values for the operation of Fig. (55a).

x = Cost of machine and operator including overhead

= \$6 per hour or 10 ¢/min.

T_d = Down time required to change tools = 2 min.

Y = Average tool reconditioning cost = 80¢

then the value of the cost ratio (R) is

$$R = \frac{xT_d + Y}{x} = 10$$

From Fig. (58) the optimum feed is seen to correspond to .0096 ipr and this feed is indicated on Figs. (57) and (55a) by the letter B. Actually the speed corresponding to Fig. (55a) is only slightly higher than Vm which in this case is found to be about 40 fpm. It may thus be concluded that a speed of 40 fpm and a feed of 0.009 ipr will correspond very closely to the cost optimum machining conditions for this combination of tool and work material.

The influence of a change in R can be seen immediately from Fig. (58). If the tool regrinding cost (Y) were to increase to 180¢ then R would be 20 and the best machining conditions would correspond to V_m = 35 fpm and t_m = .0085 ipr.

The curve of Fig. (55b) has a slope of one at point A for which t is about .014 in. The optimum feed will lie to the right of this point just as point B was to the right of point A in Fig. (55a) and (57). The optimum feed in this case will probably be .020 ipr or greater. However, the speed for Fig. (55b) is 250 fpm which is far above the optimum. For a value of R of 30 (carbide tool) the optimum speed V_m is found to be 143 fpm when the feed is .010 ipr from the appropriate equation of Table 19. The curve of Fig. (55b) should be redetermined for a speed near 143 fpm.

In recent paper before the ASME Fersing and Smith (12) have studied the machinability of Ti 150A at high speeds and feeds. The authors prefer to plot their tool life values in terms of square inches of surface machined in order, as they put it, not to unduly concern the operator with the short tool life values in minutes that are obtained at the high speeds recommended. However, in adopting this criterion for tool life the authors make it impossible for their results to be compared with those of others on an absolute basis, since the diameter of the workpiece is not stated. Another unusual feature of their tool life studies lies in the use of the increase in the feed force (F_Q) as the item used to determine tool life. The life of a tool by the procedure is determined when the F_Q force has increased 50 to 100%. The weakness of this method lies in the fact that it fails when a tool craters

appreciably or when a large built-up edge is present on the tool face. Under such conditions the force F_Q frequently decreases rather than increases with tool wear.

Despite these limitations Fersing and Smith make some interesting observations. They observe distinctly parabolic plots of wear land vs time for 8647 steel as was found in this investigation for both 1045 steel and all titanium alloys. They state that a feed rate of .015 ipr was better than .022 ipr which in turn was better than .033 ipr. These statements are based on the total amount machined before tool replacement and as such are consistent with the foregoing discussion of the Army feed data. They indicate best results with a side rake angle of minus 5°, but it should be kept in mind that this corresponds to cutting at high power levels (high speeds and feeds). As in all machining the rake angle may be increased with a decrease in power level. In the tests of this investigation the power level was significantly lower while the best rake angle was found to be between 0° and plus 10°.

Fersing and Smith advocate either large SCEA (60°) with small nose radius (.010 to .020) or zero SCEA with very large nose radius (1/4 inch). In either case there is a large effective SCEA which distributes the load on the cutting edge over a greater distance and lessens the tendency for chipping. This observation is worthy of note but it should be observed that it is usually easier to maintain and recondition tools with large SCEA's than with large nose radaii. Fersing and Smith found K-6 carbide superior to K-8 but their tests were at unusually high speeds. Softer carbides of the steel cutting type should prove better in the practical speed range for roughing as previously mentioned. In finishing operations where light feeds and very high speeds are the rule then carbides of the K-6 or K-8 type should prove of value.

In a paper before the ASME in December 1953, representatives of the Cincinnati Milling Machine Company (13) emphasize the importance of the directional properties as produced by rolling upon the chip forming properties of titanium alloys. It was clearly demonstrated that when titanium sheet was very heavily rolled and not subsequently annealed, the chip shape was different depending on the direction of cut relative to the

direction of rolling. The bars used in turning investigations, however, will show no such drastic variation in texture since in their fabrication they are not so highly cold worked and further the small strains present will be symmetrically distributed in the bar.

It was also stated that alloying action plays a significant role in tool wear when titanium is machined. Experiments of the Dawihl (14) type, in which carbide and titanium specimens are held in contact in vacuum for a long period at high temperature and then examined for alloy formation, were cited in support of this view. Cast iron grade carbides were found to form less brittle alloy layers than the steel cutting types. In interpreting such results it must be kept in mind that the particular area of chip is in contact with the tool a fraction of a second while it is necessary to have contact for several hours at chip temperatures to obtain intermetallic diffusion and alloying action in vacuum experiments.

Considerable work has been done on the machining of titanium at the University of Michigan by Professor Colwell and his associates under an Army Ordnance contract with the Watertown Arsenal (15). The emphasis in this work has been upon HSS tools. It was found that when unusual care was taken to provide a rigid set-up rake angles as high as 30° could be successfully used. The results presented in Table 20 were obtained with a T-1, HSS tool under the following conditions:

Tool Geometry: 0, 28, 6, 6, 6, 15, .010
Feed: .006 ipr
Depth of cut: .050 in.

Table 20. HSS (T-1) Results Obtained at University of Michigan (15)

Material	Empirical Equation	For t = .01 ipr, b = .06	
		Equation	V_{60}
Ti 130B	$VT^{.075} = \frac{1.42}{t^{.6}\, b^{.1}}$	$VT^{.075} = 30$	22
Ti 150A	$VT^{.1} = \frac{1.18}{t^{.62}_{b}\ .17}$	$VT^{.10} = 33$	22
18-8 S.S.	$VT^{.085} = \frac{7.52}{6^{.43}_{b}\ .17}$	$VT^{.085} = 87.5$	62
1045 Steel	$VT^{.061} = \frac{4.25}{t^{.63}_{b}\ .10}$	$VT^{.061} = 103$	85

The values of the exponent of T are seen to be in good agreement with those of Table (15) of this investigation. The influence of b (the depth of cut) on tool life is seen to very slight. The values of V_{60} for the two titanium alloys are also seen to be very close to the HSS value of Table 15.

Improved results were obtained when the nose radius was increased to a value of approximately half the depth of cut (usually b/2 = 0.025 in). Water base cutting fluids were found useful, including a 5% solution of sodium nitrite in water. When such a solution which is very useful in grinding titanium alloys was tried in this investigation it was not found better or worse then other water base cutting fluids.

References

1. Handbook on Titanium Metal, Anon., published by Titanium Metals Corp. of America (1953)
2. Mechanical Properties of High Purity Ti-Al Alloys by H. R. Ogden, D. J. Maykuth, W. L. Finlay and R. I. Jaffee, Jour. of Metals, 5, 267 (1953).
3. Discontinuous Chip Formation by N. H. Cook, I. Finnie, and M. C. Shaw, Trans. ASME 76, 153, (1954).
4. Visual Study of the Machining of Titanium by N. H. Cook. Report WAL 401/172-6, Watertown Arsenal, Nov. 1953.
5. Ursachen und Minderung von Werkzeugschwingungen by E. Salje Industrie - Anzeiger Nr. 80, p. 1023, Oct. 6, 1953
6. a.) Mechanics of the Metal Cutting Process by M. E. Merchant, J. App. Physics, vol. 16, p. 267, (1945).
   b.) Metal Cutting Principles, Published at M.I.T., April 1954.
7. On the Empirical Law of Adhesive Wear by J. T. Burwell and C. D. Strang, J. App. Physics 23, 18, (1952).
8. Analysis and Lubrication of Bearings, Chapt. III by M. C. Shaw and E. F. Macks, McGraw Hill Book Co., New York (1949).
9. On the Analysis of Cutting Tool Temperatures by E. G. Loewen and M. C. Shaw, Trans. ASME 76, 217, (1954).
10. Economics of Machining by W. W. Gilbert, Chapter in ASM book: Machining - Theory and Practice p. 465, Published by American Society for Metals, Cleveland, Ohio (1950).
11. United States Air Force Machinability Report - 1954 by J. VanVoast, Published by Curtiss Wright Corp., Woodbridge, N.J. (1954).
12. Machinability Research with J and L. Tool Dynamometer on Titanium 150A, by L. Fersing and D. N. Smith, ASME Paper No. 53-A-207 (1953).
13. Fundamental Factors in the Machining and Grinding of Titanium by E. J. Krabacher and M. E. Merchant. Paper before ASME, December 3, 1954, N. Y. Annual Meeting, ASME.
14. Investigation of the Process in the Wear of Cemented Carbide Tools by W. Dawihl, Zeitschrift für Technische, Physik, Vol. 21, 1940, p. 337.
15. University of Michigan - Watertown Arsenal Titanium Machinability Reports by L. V. Colwell and Associates. Published by Watertown Arsenal, Watertown, Mass. (1953).

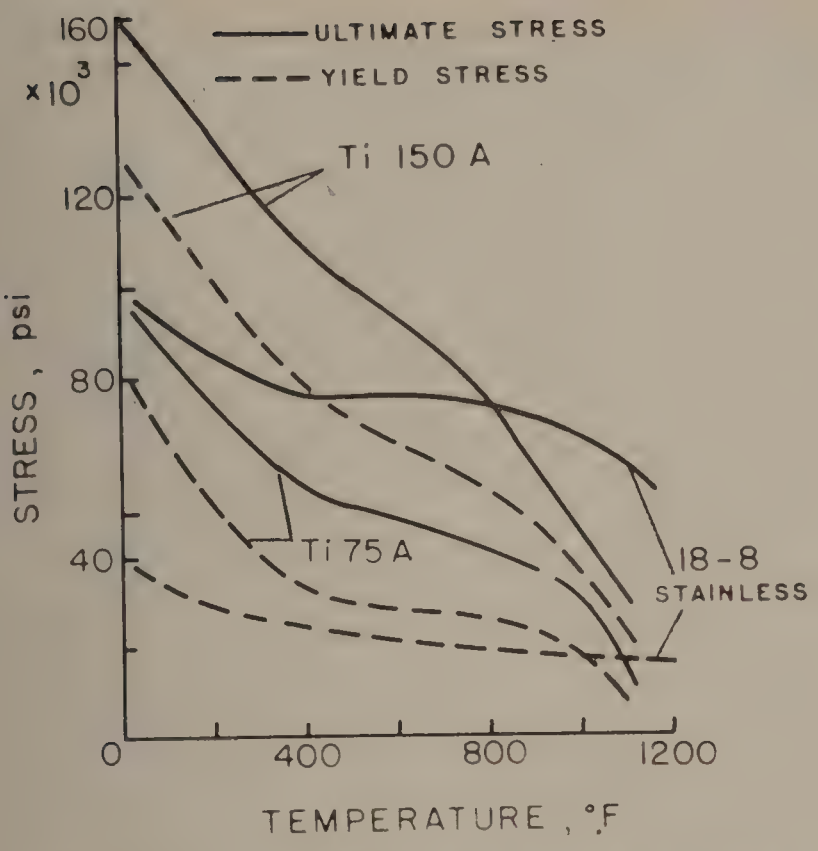

Fig. 1. Ultimate and yield stress values in tension for titanium alloys and 18-8 stainless steel tested at different temperatures (data from ref. 1).

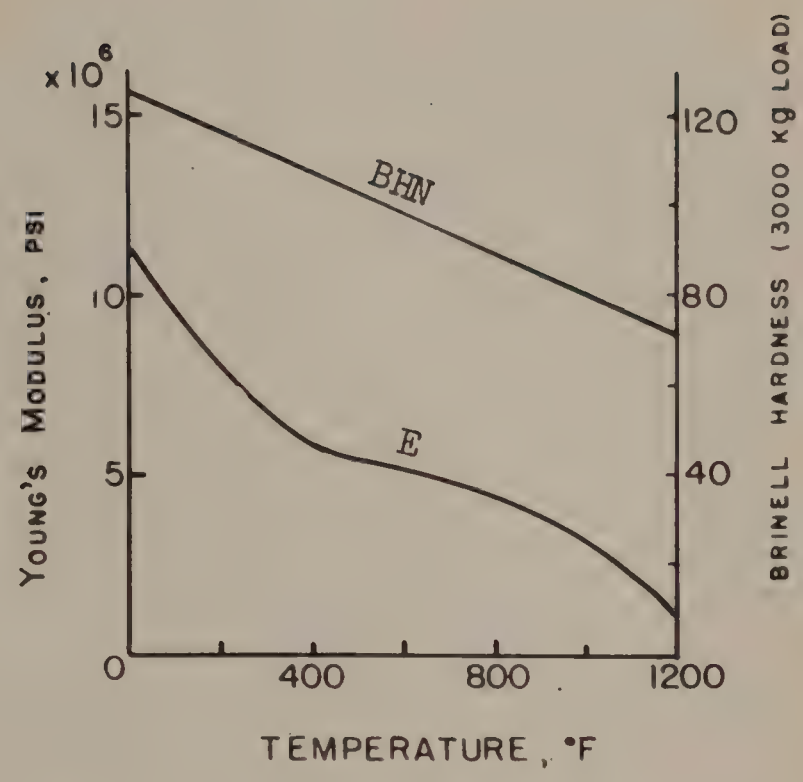

Fig. 2. Variation of Young's Modulus of Elasticity and hardness with temperature for titanium alloy Ti-100A (data from ref.2).

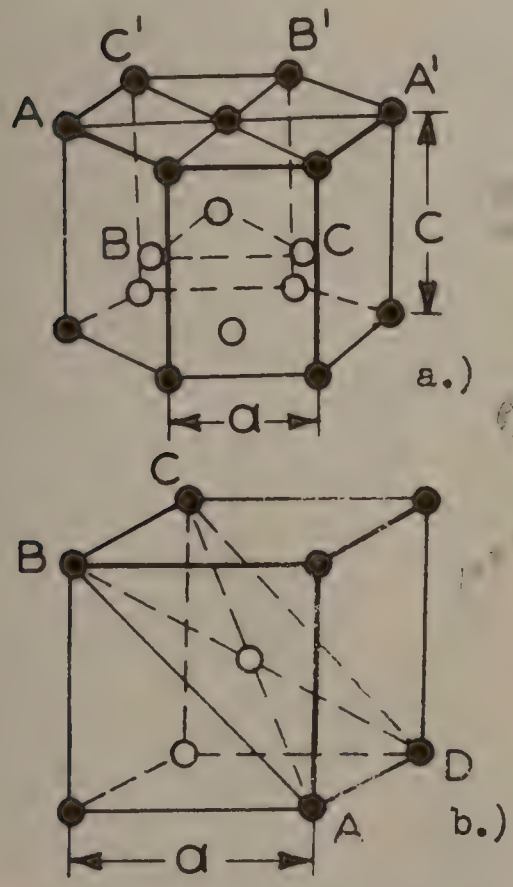

Fig. 3. Arrangement of atoms in the structural forms of titanium
a.) Hexagonal close packed structure
b.) Body centered cubic structure.

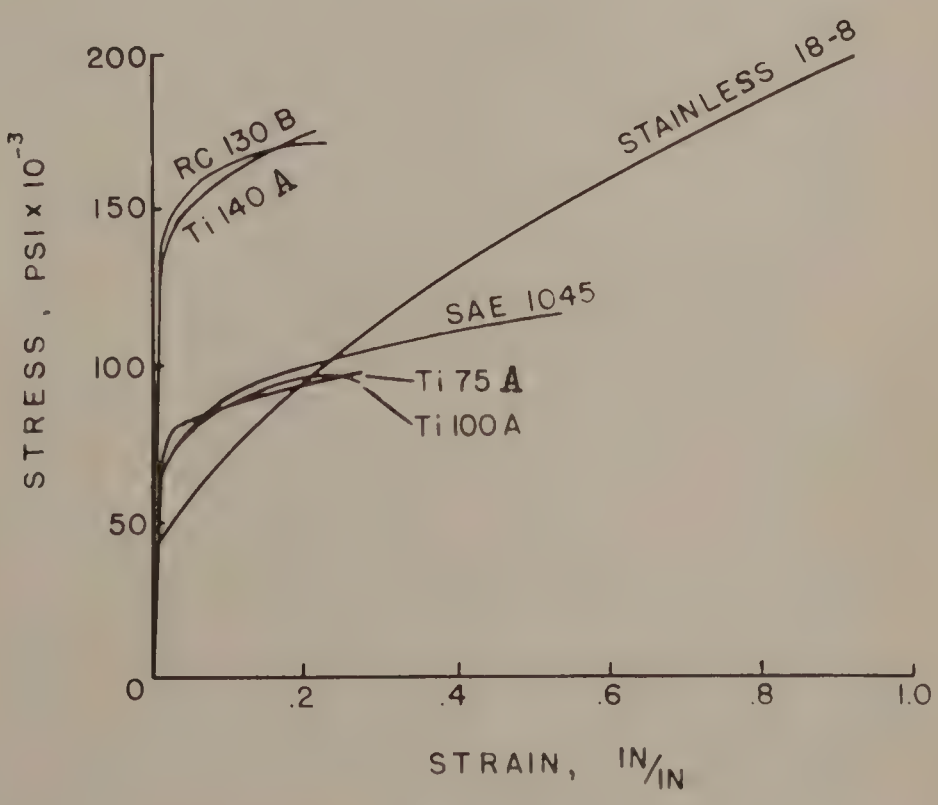

Fig. 4. True stress-true strain tensile data for titanium alloys and other metals.

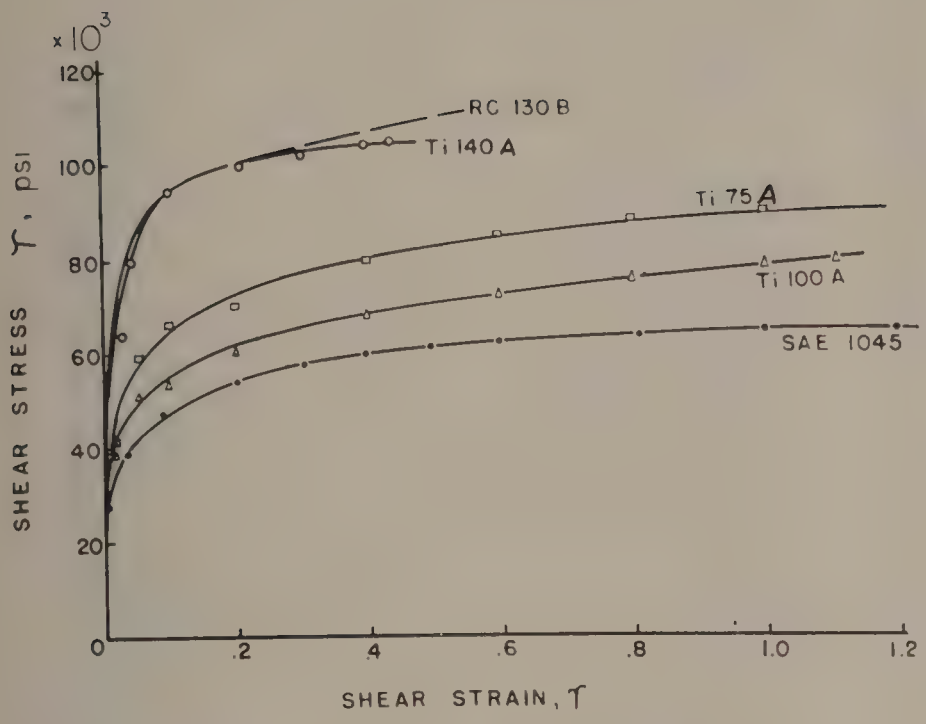

Fig. 5. Torsion test results for titanium alloys and other metals.

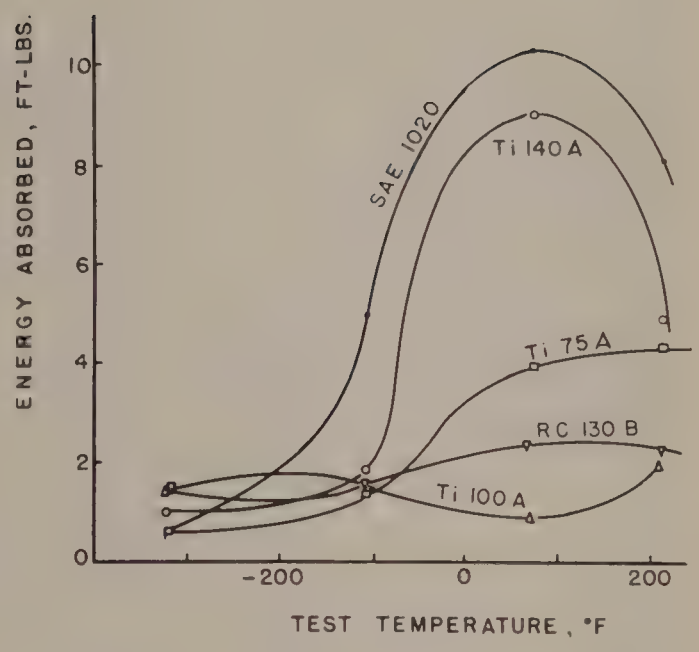

Fig. 6. Charpy impact - temperature curves for titanium alloys and 1020 steel.

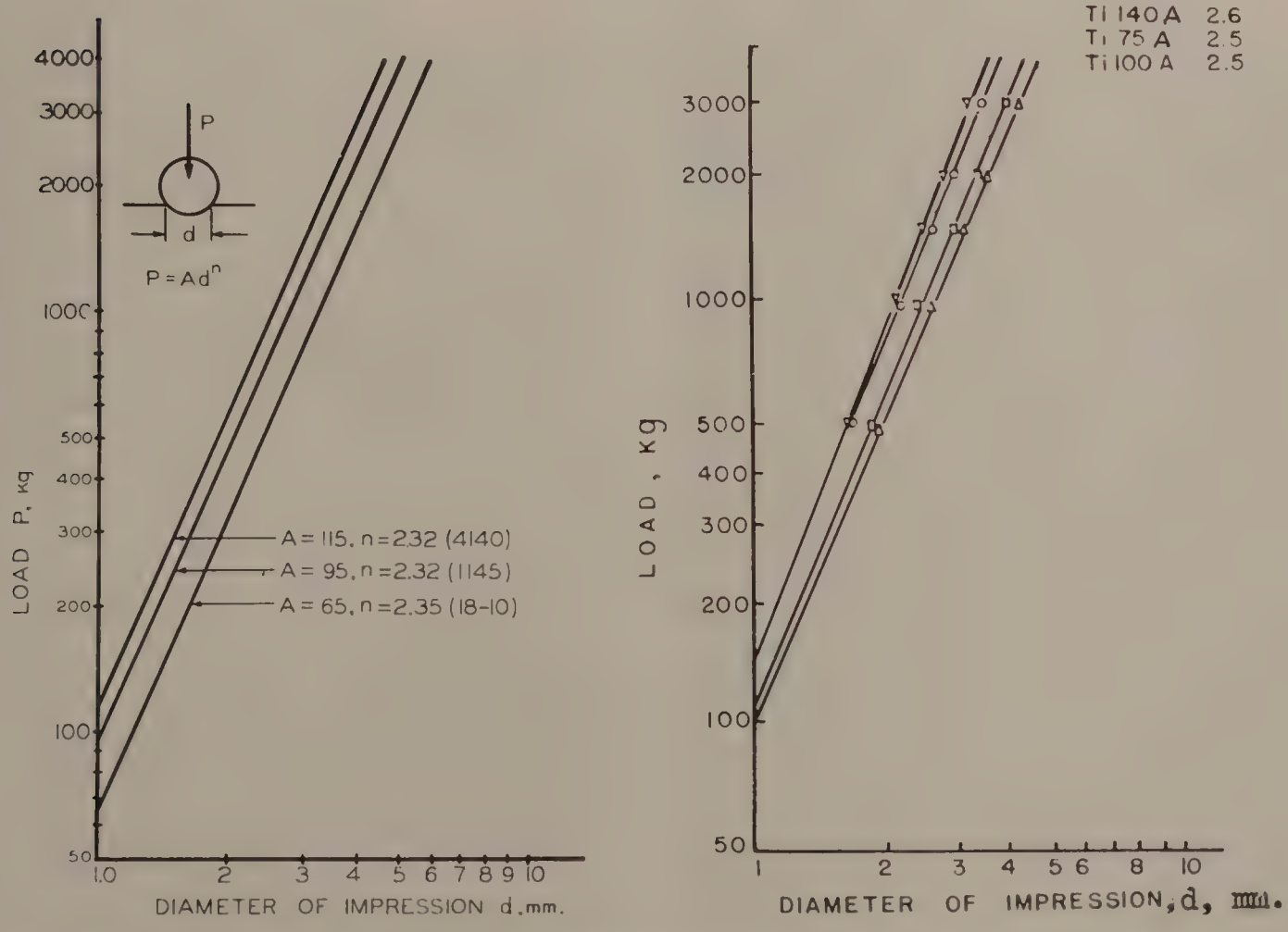

Fig. 7. Meyer hardness curves for titanium alloys and other metals.

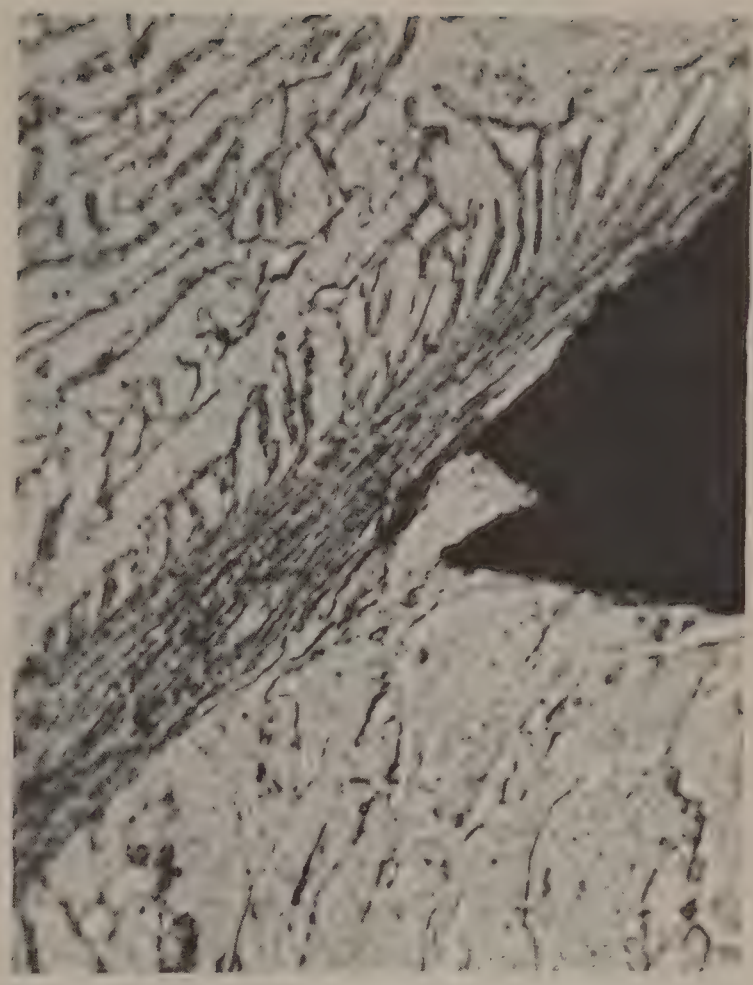

Fig. 8. Inhomogeneous titanium chip. Work material RC130B cut at 175 fpm
a.) Magnification, 400x
b.) Magnification, 1500x

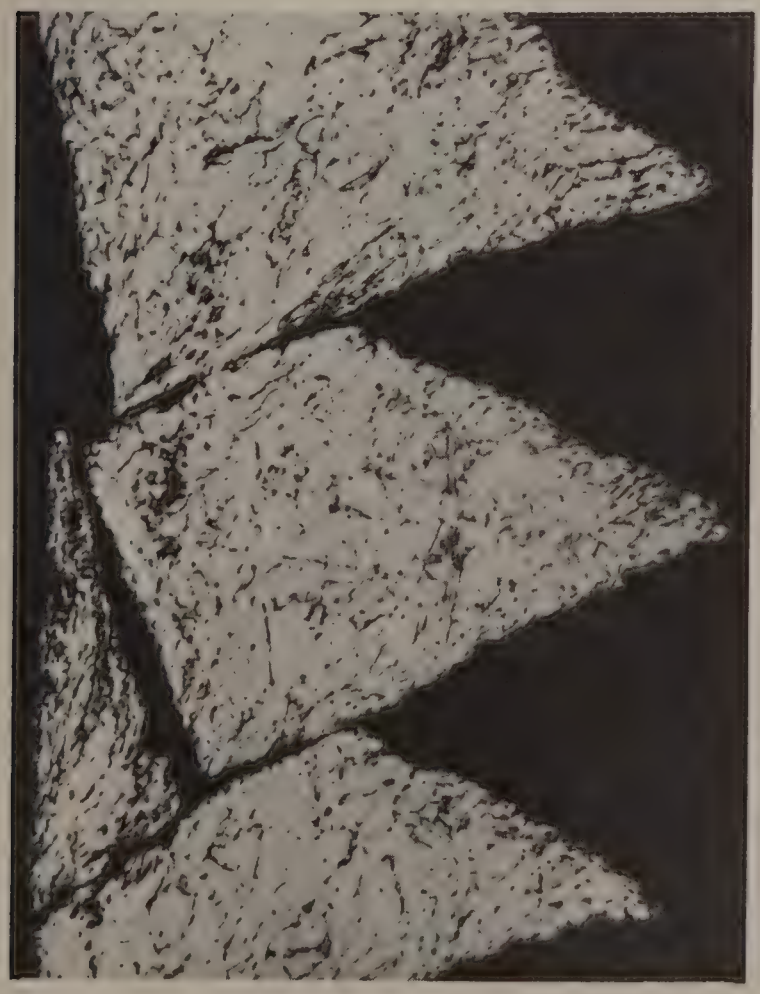

Fig. 9. Rewelded discontinuous titanium chip. Work material, Ti 75A cut at 1 in/min; 120x.

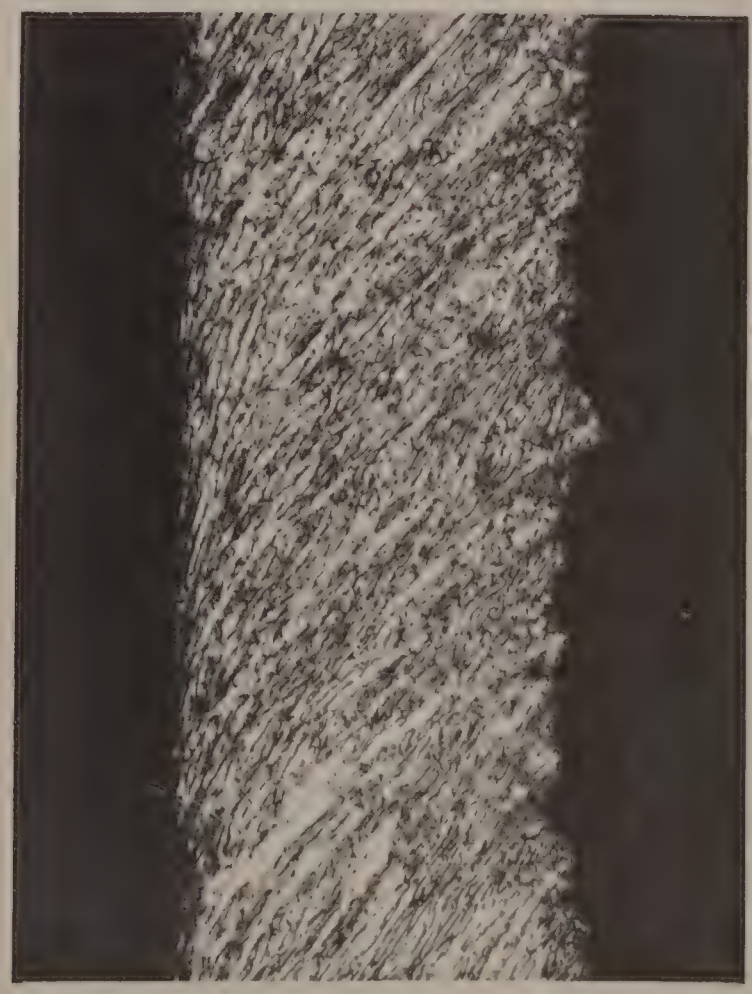

Fig. 10. Continuous titanium chip produced at 50 fpm. Tool face side of chip is on left.

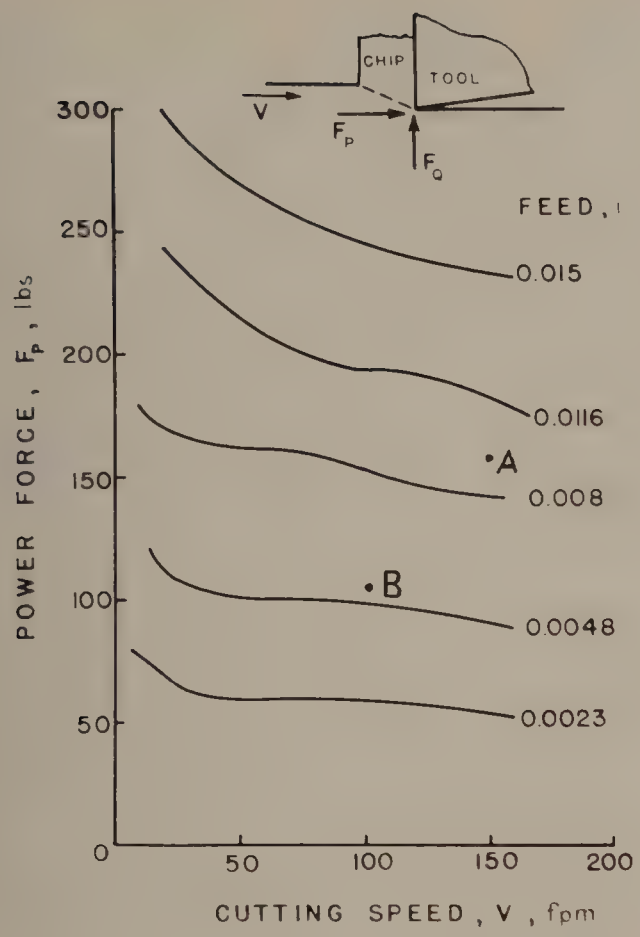

Fig. 11. Variation of power component of cutting force (F_p) with speed at constant feed rate. Work material, Ti 140A; depth of cut, 0.06 in; cutting fluid, none; tool material, K-6; tool geometry: 0, 0, 0, 6, 6, 6, .01.

Fig. 12. Lathe dynamometer for measuring components of force on tool.

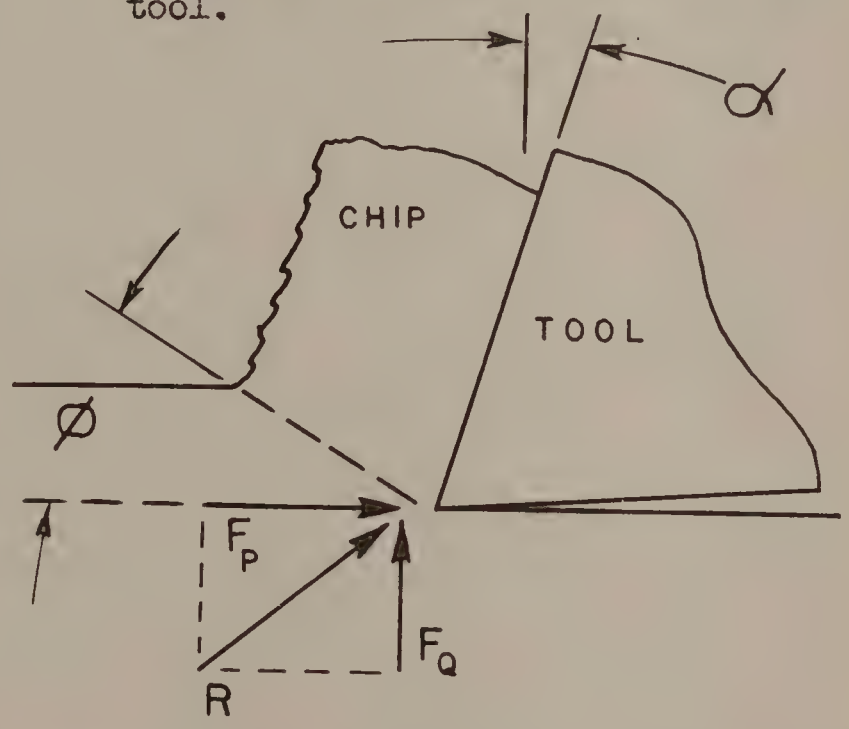

Fig. 13. Forces acting on tool point.

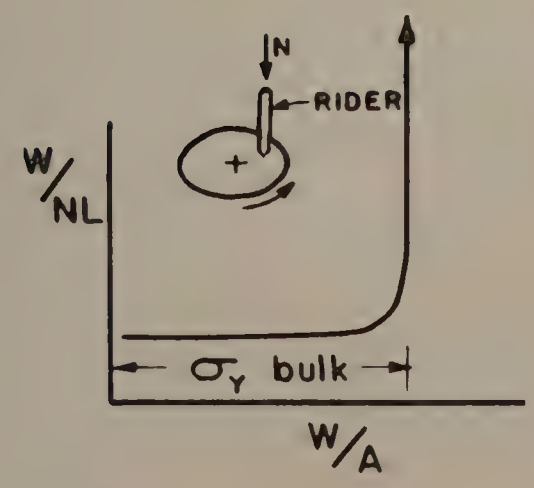

Fig. 14. Type of wear data obtained by Burwell and Strang(7) when two loaded surfaces were operated in sliding contact.

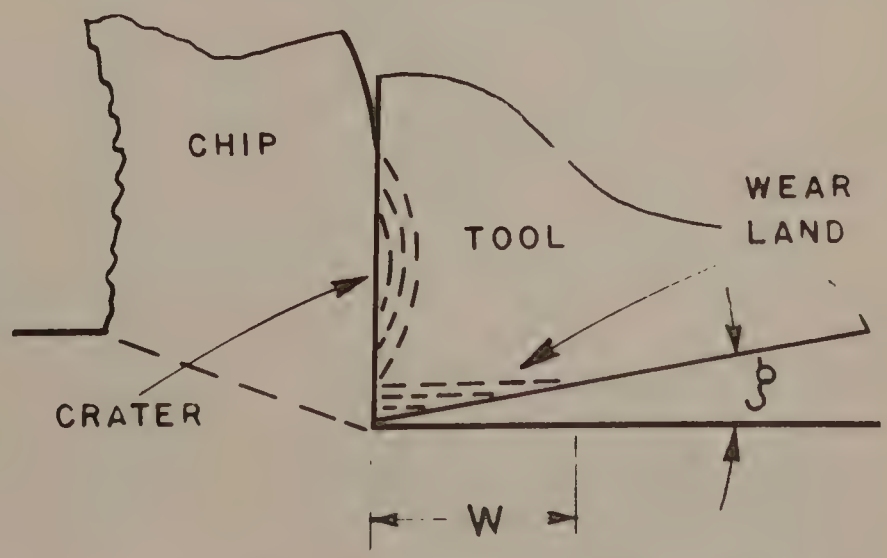

Fig. 15. Development of crater and wear land on chip and clearance faces of a tool respectively.

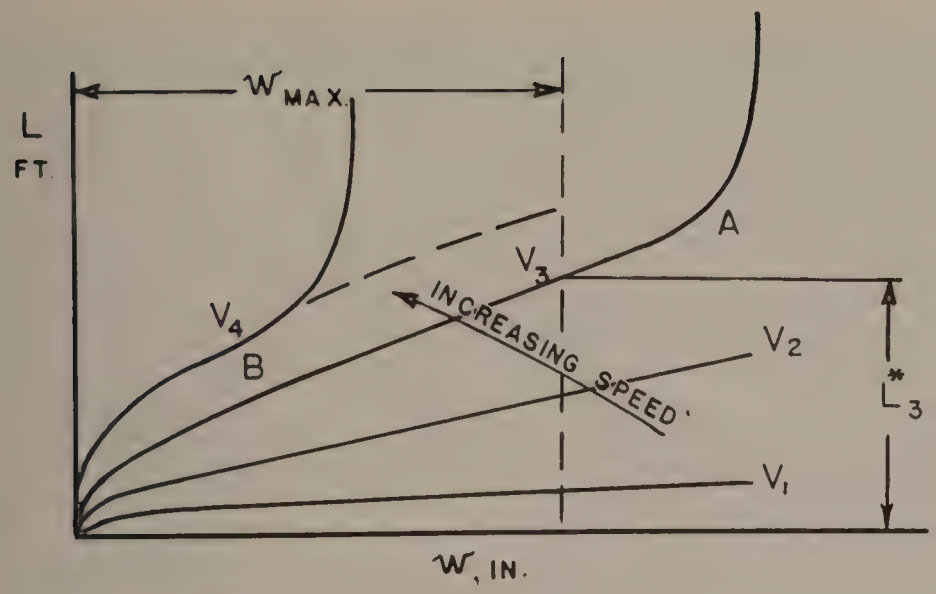

Fig. 16. Typical wear curves with distance of work traversing tool (L) plotted against size of wear land (w) for different constant values of cutting speed (V).

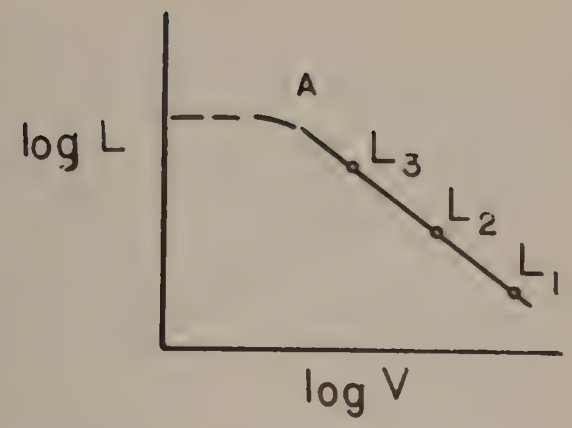

Fig. 17. Nature of curve obtained when length of work traversed for given wear land (L^*) is plotted against cutting speed (V) using log-log coordinates

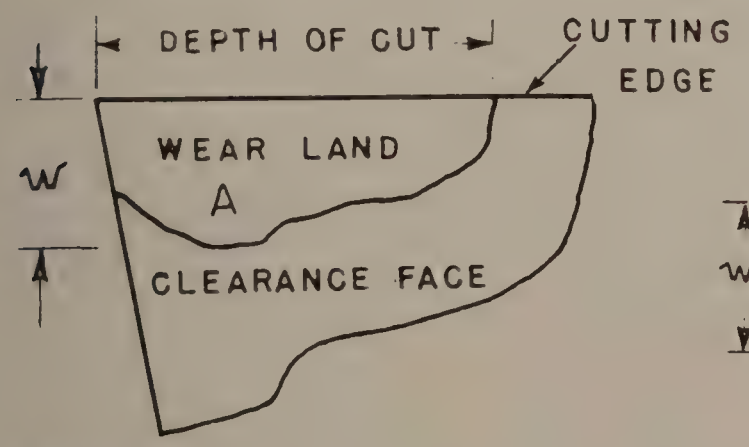

Fig. 18. Plan view of clearance face of worn tool showing representative variation of extent of wear land along cutting edge with maximum wear land w in the vicinity of point A.

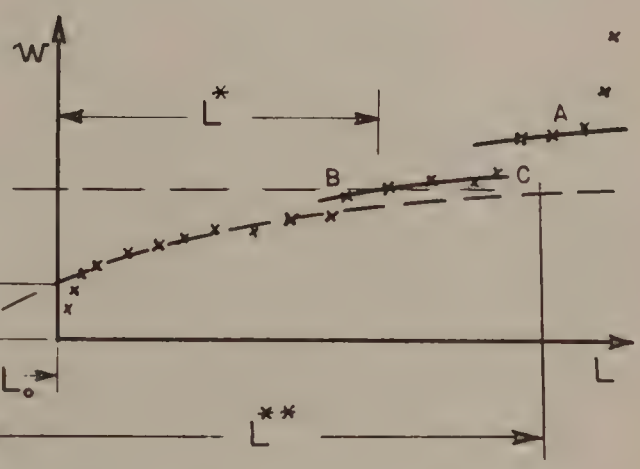

Fig. 19. Schematic wear curve for titanium cutting test where wear land (w) is plotted against distance (L).

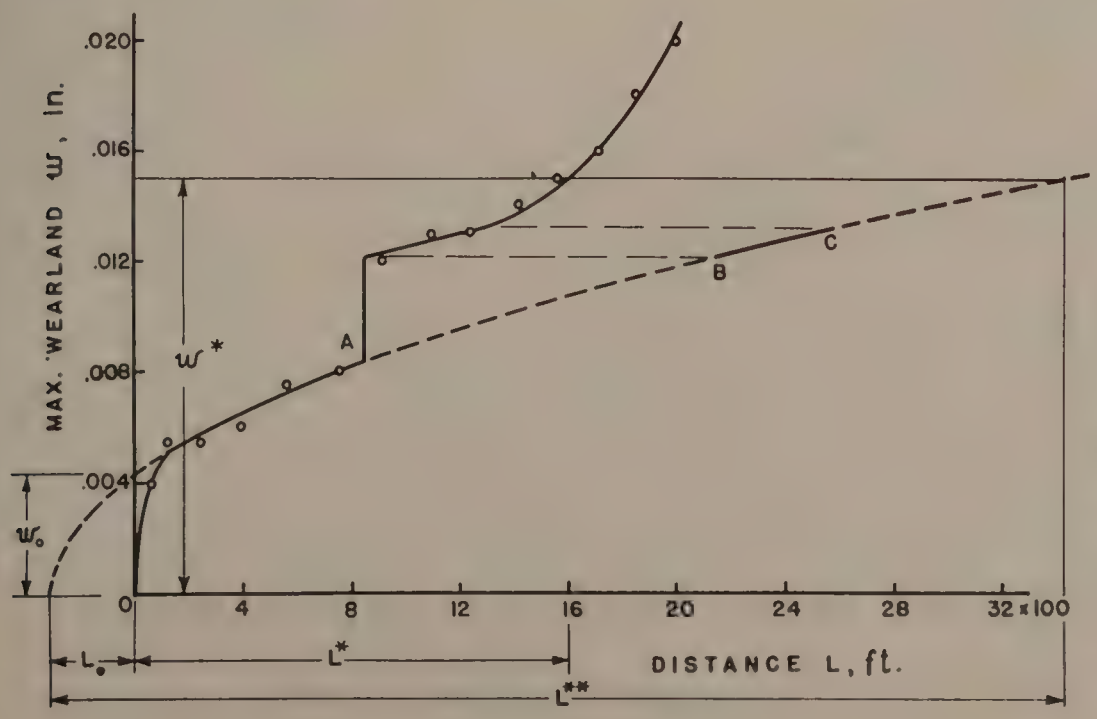

Fig. 20. Wear curve for Ti 140A cut at 150 fpm using K-6 carbide tool. Feed, 0.0104 ipr; depth of cut 0.06 in; cutting fluid, none; tool geometry: 0, 10, 5, 5, 5, 0, .015. Note excessive chipping at point A.

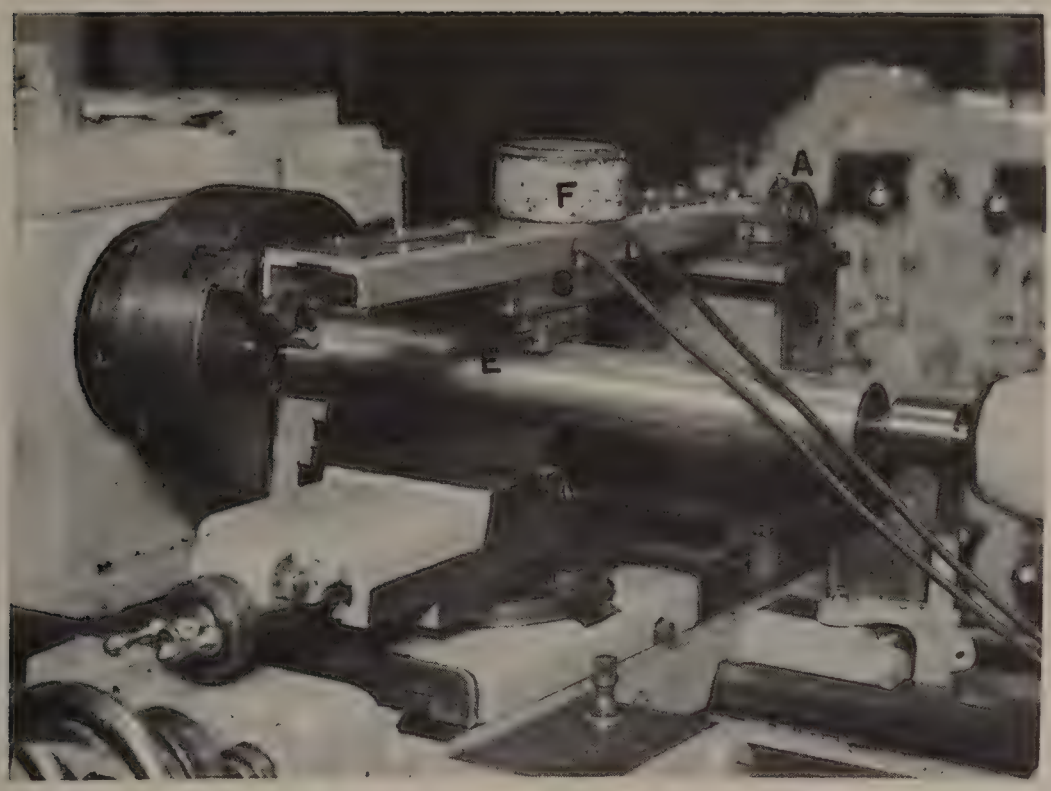

Fig. 21. Photograph of wear apparatus used to study the wear characteristics of titanium - tool material combinations.

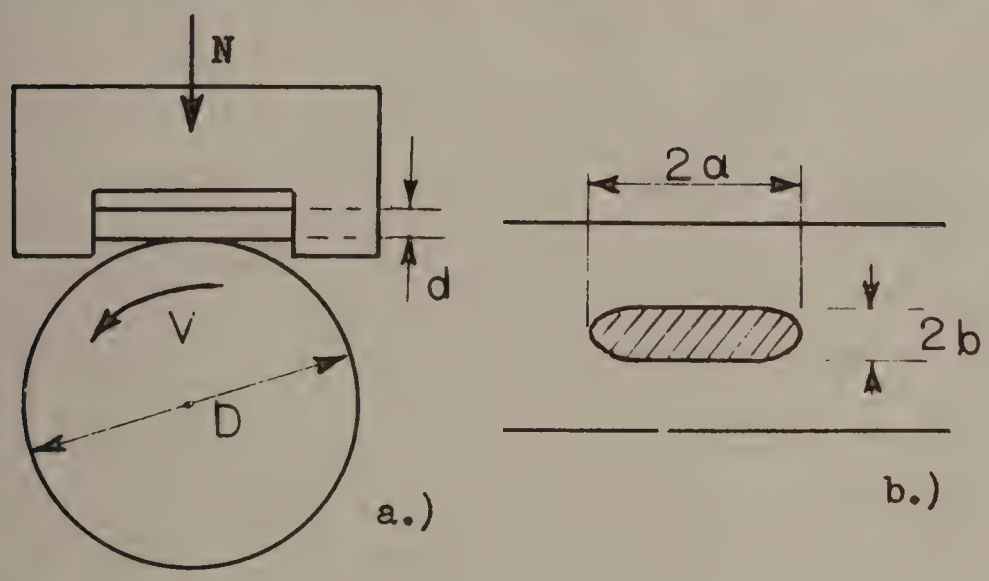

Fig. 22. Wear apparatus a.) Relative position of tool and work components, b.) Nature of wear scar left on tool specimen of diameter d.

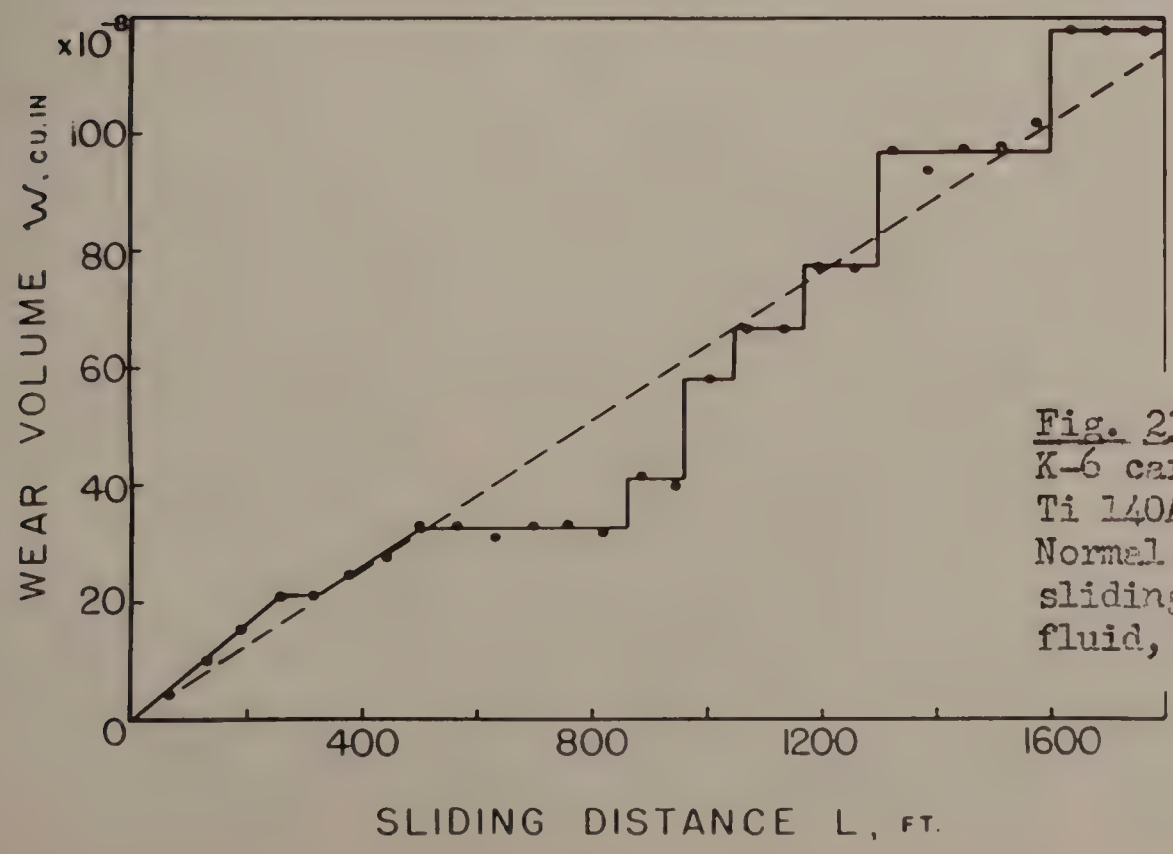

Fig. 23. Wear curve for K-6 carbide slider on Ti 140A specimen. Normal force (N) 7 lbs; sliding speed, 170 fpm; fluid, none.

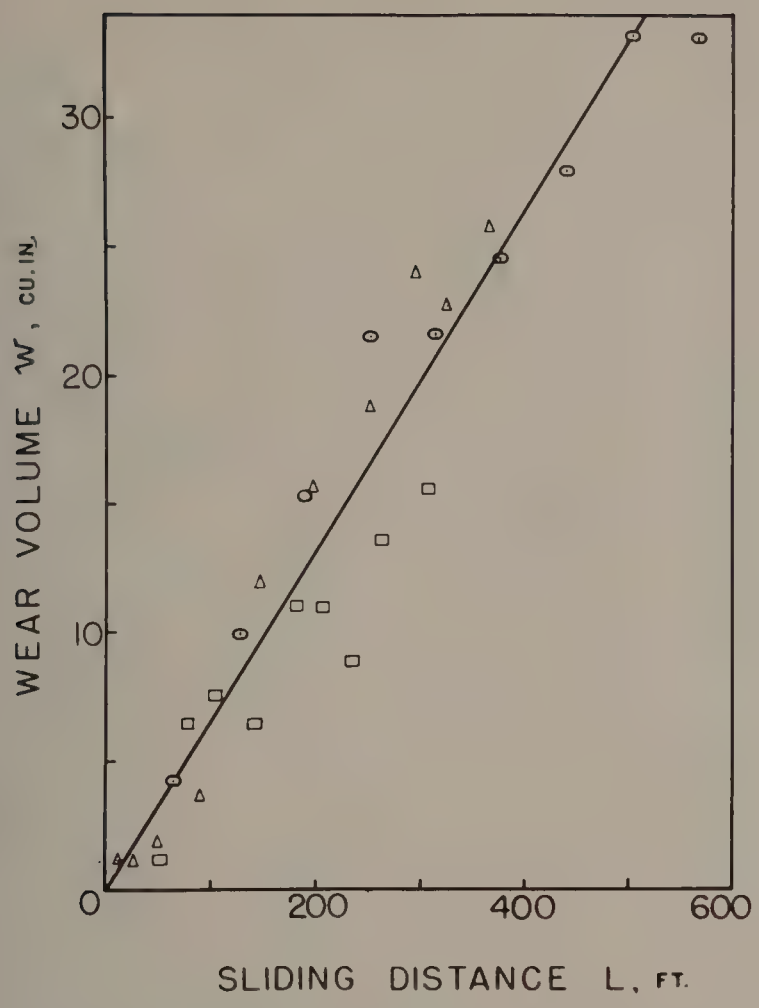

Fig. 24. Wear curve for K-6 carbide slider on Ti 140A specimen. Normal load (N), 7 lbs., slide speed: △ = 85 fpm, ⊡ = 140 fpm, ⊙ = 165 fpm., fluid, none.

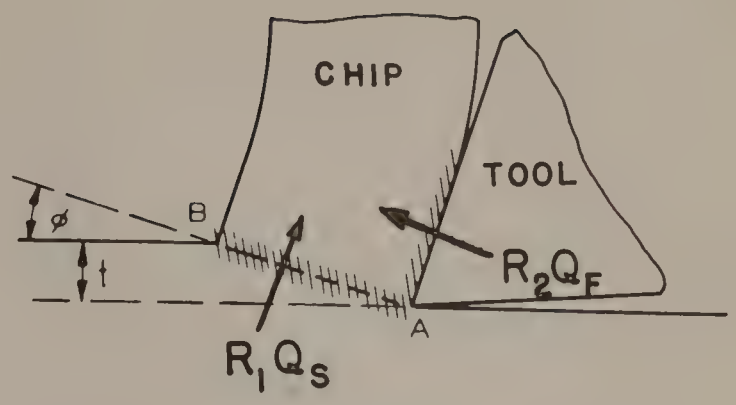

Fig. 27. Heat sources in the vicinity of the tool point.

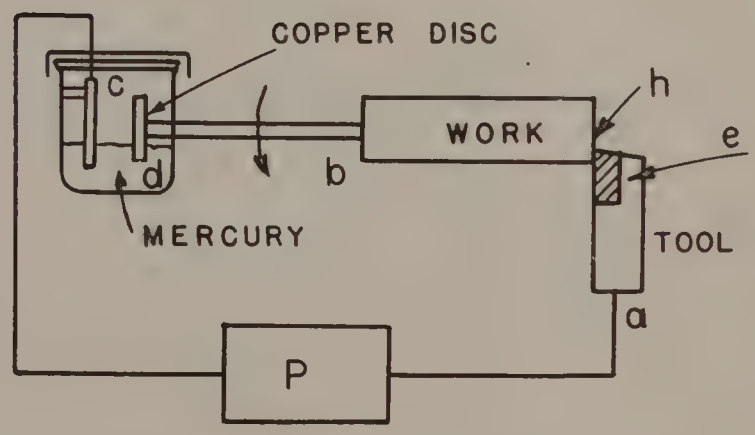

Fig. 28. Tool-chip thermocouple method of measuring mean cutting tool temperature.

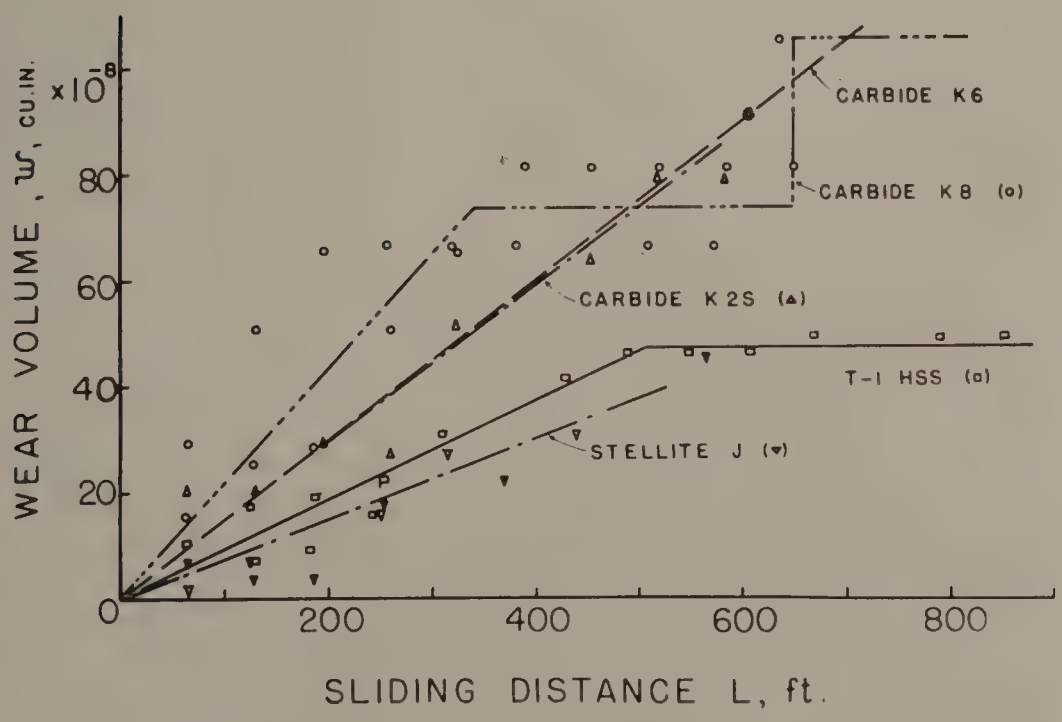

Fig. 25. Wear curve for different tool materials sliding on Ti 140A. Normal load (N), 9 lbs.; sliding speed, 150 fpm; fluid, none.

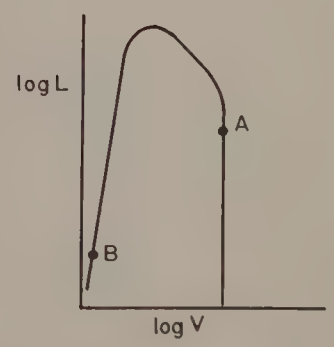

Fig. 26. Schematic representation of tool life - speed curve extending from very low to very high values of speed.

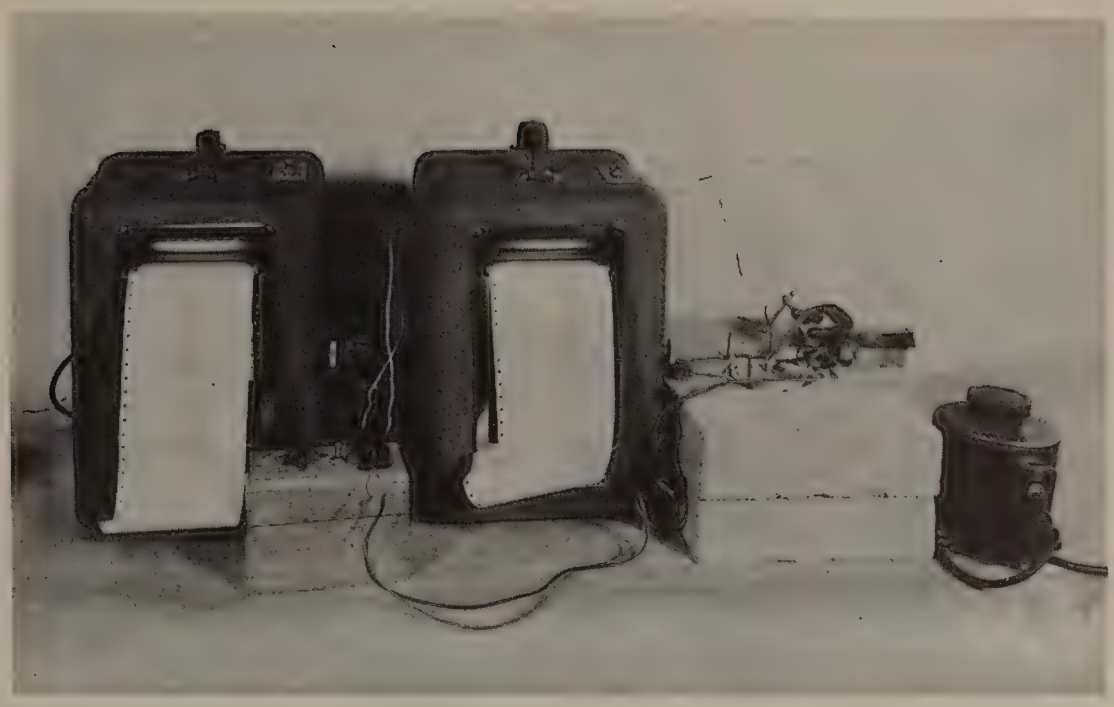

a.)

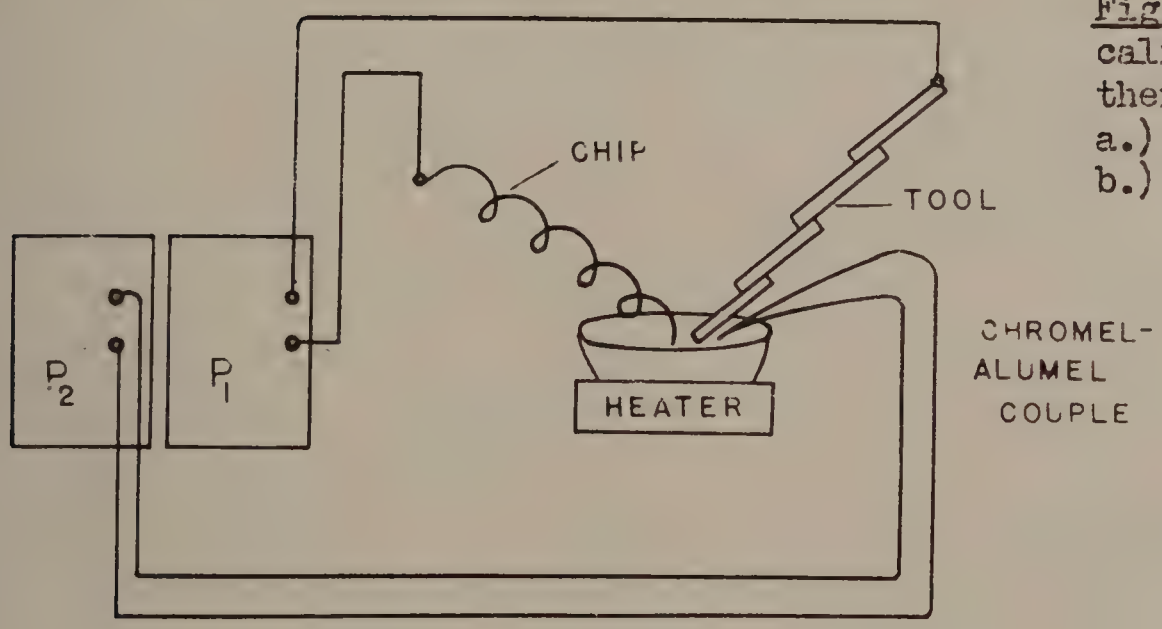

b.)

Fig. 29. Method of calibrating tool-work thermocouples.
a.) photograph
b.) schematic diagram

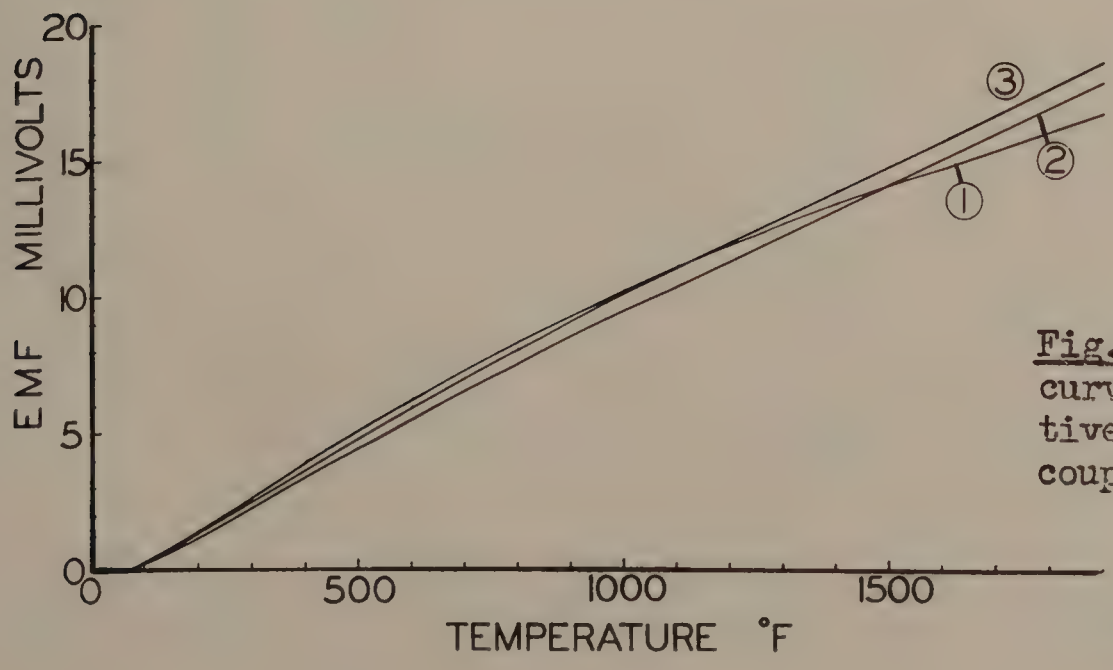

a.)

Fig. 30. Calibration curves for representative tool-work thermocouple combinations.

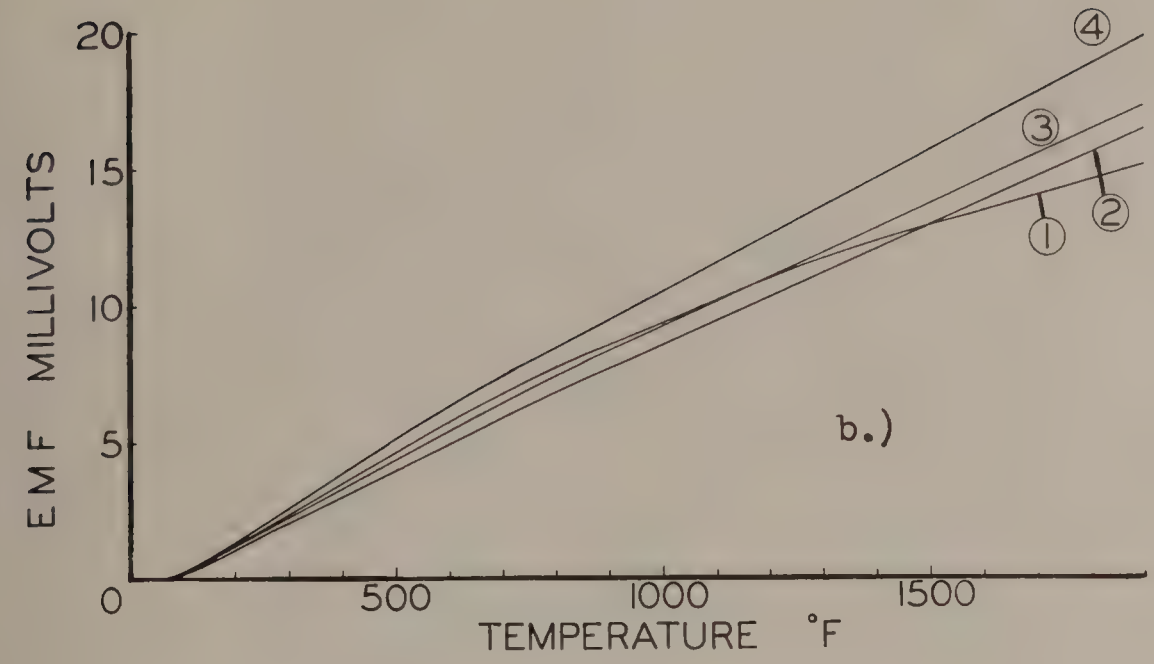

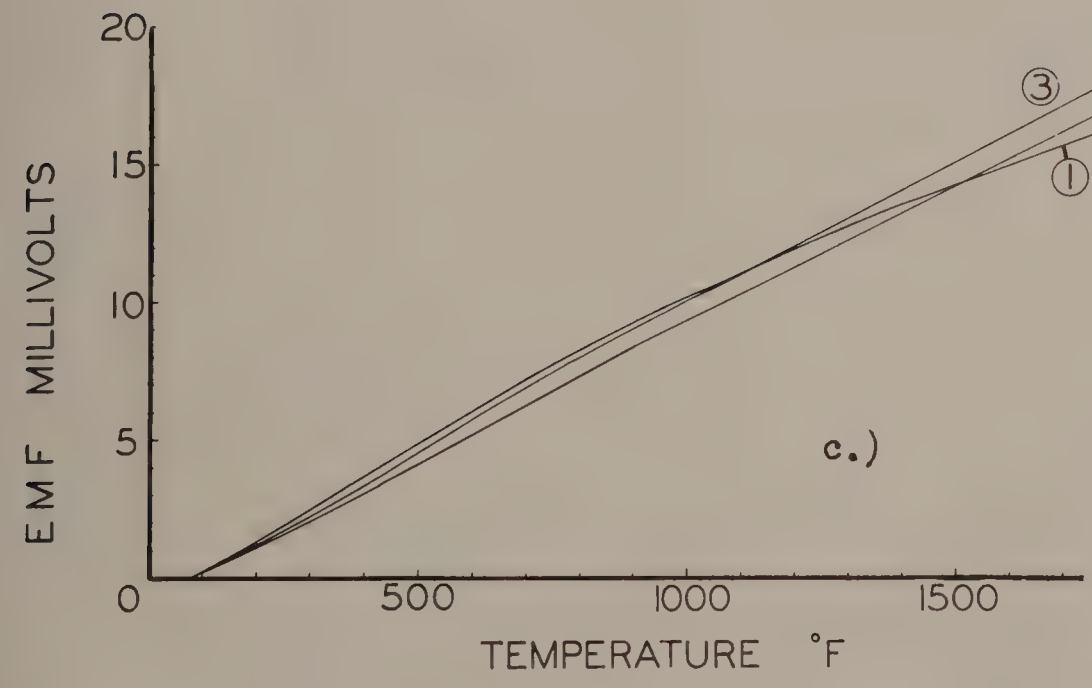

Fig. 30
(continued)

Work materials:

Curves (1) Ti-75A
" (2) Ti-100A
" (3) Ti-140A
" (4) SAE 1045 steel

Tool materials:
Plot (a) K-6 carbide
" (b) K-2S "
" (c) K-3 "
" (d) T-1 HSS
" (e) M-2 HSS

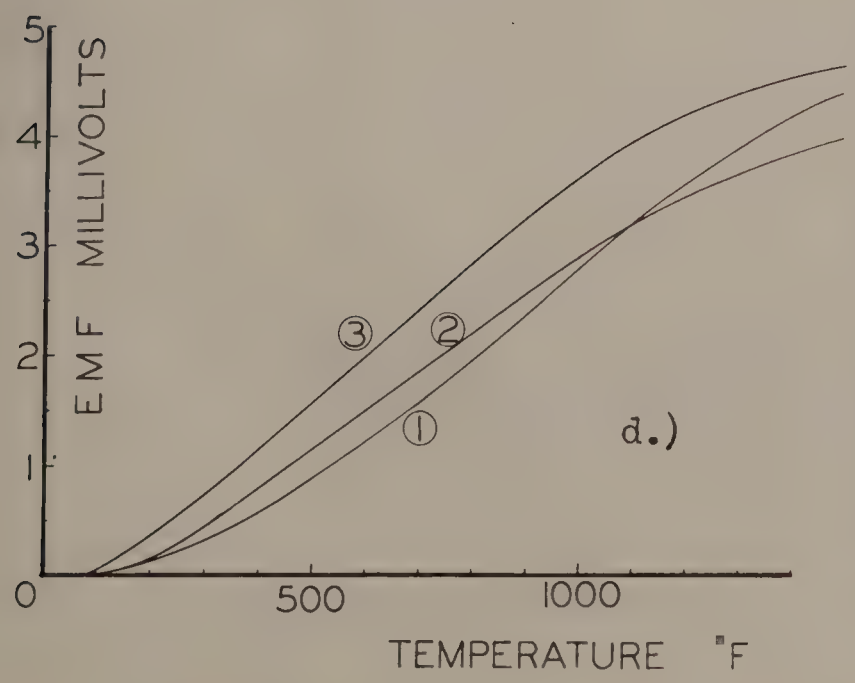

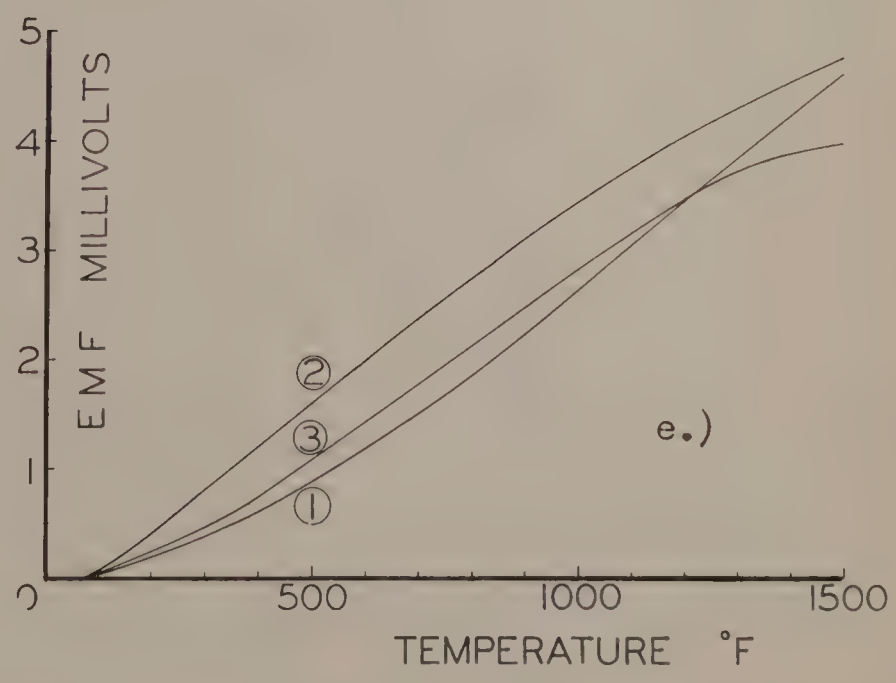

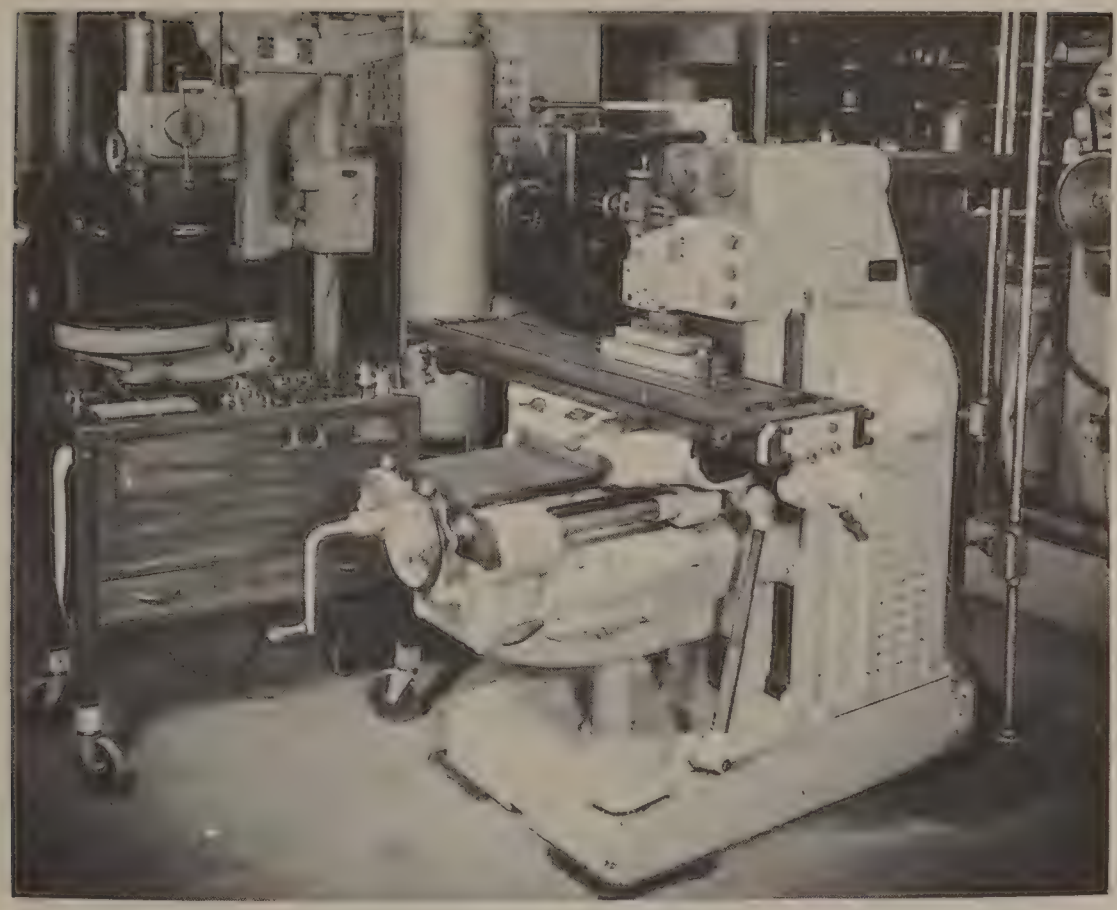

Fig. 31. General view of low speed cutting apparatus showing two channel strain recorder on left and milling machine in foreground.

Fig. 32. Close-up view of tool, workpiece, and dynamometer used in low speed cutting tests.

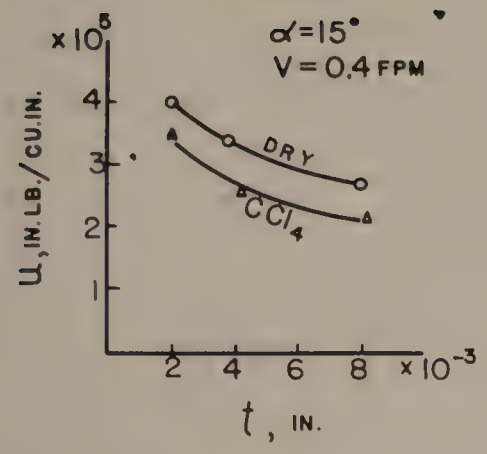

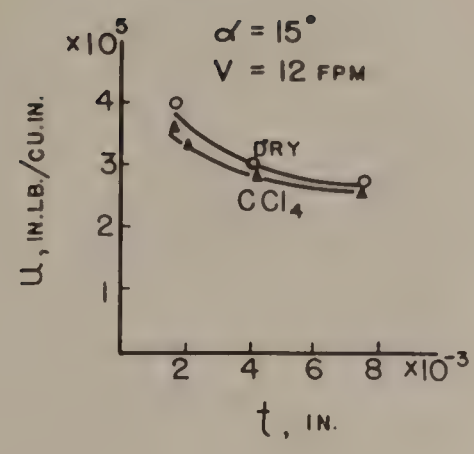

Fig. 33. Variation of energy per unit volume with depth of layer removed (t). Tool material, 18-4-1 HSS.
a.) For Ti 140 A.
b.) For C1112 steel

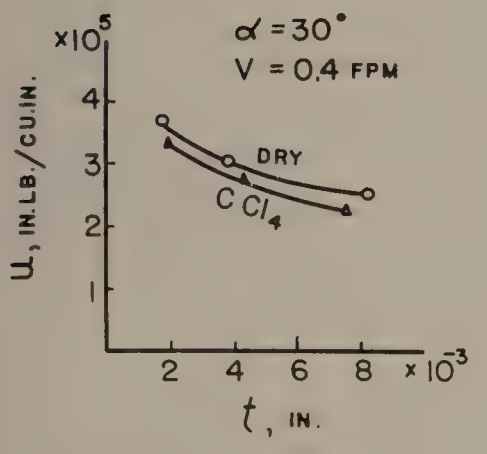

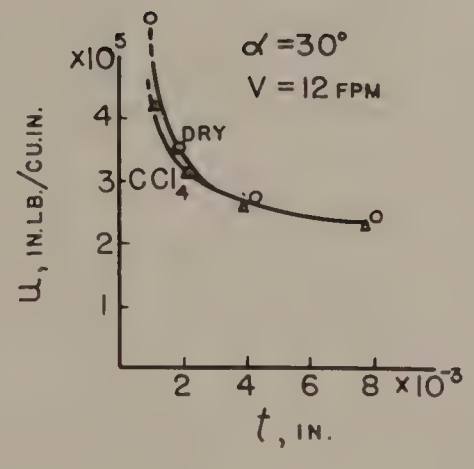

a.)

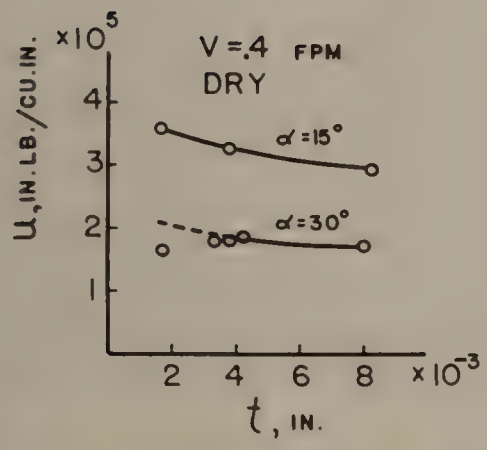

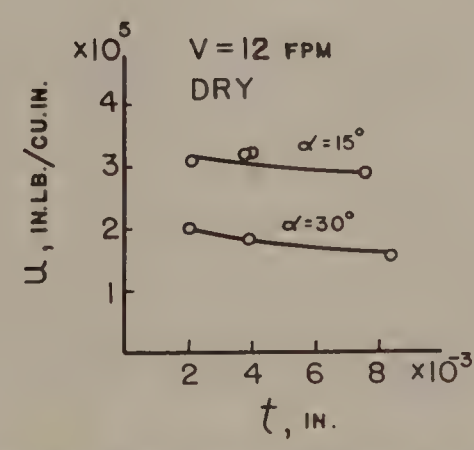

b.)

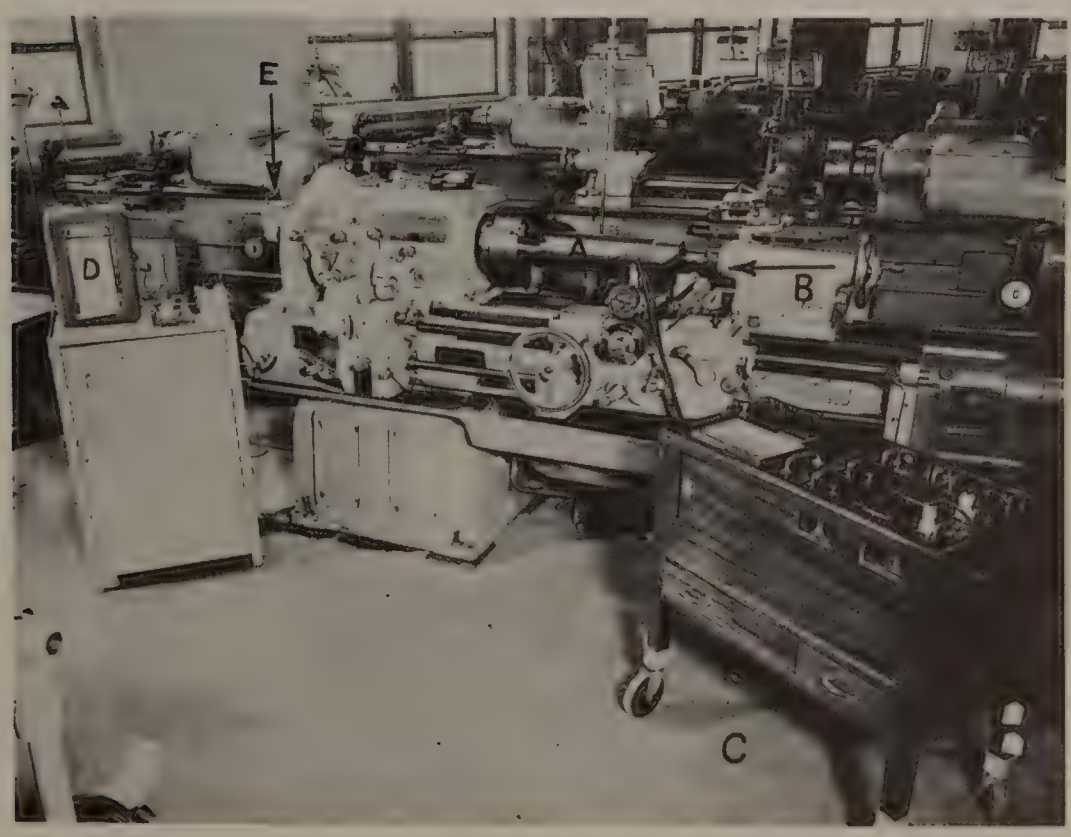

Fig. 34. General view of apparatus used in turning studies.

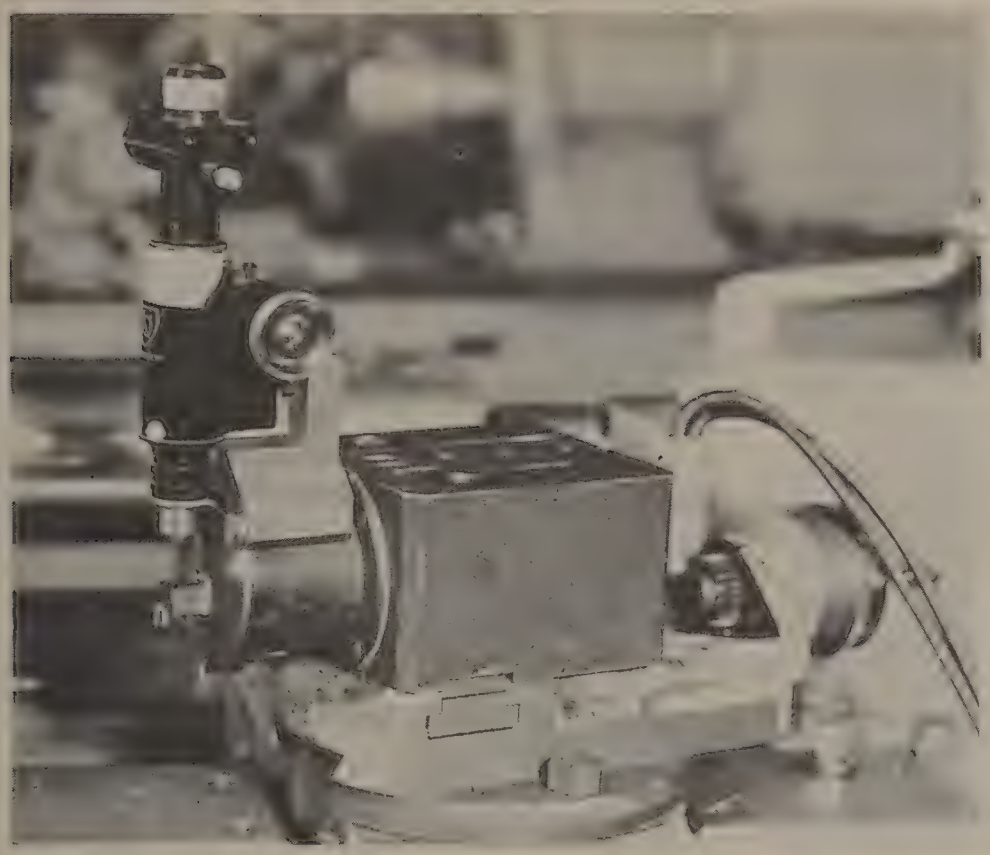

Fig. 35. Method used to examine tool faces in tool wear studies.

a.)

b.)

c.)

d.)

Fig. 36. Macroscopic chip pictures.

a.) Test 1 - Ti 140A cut at 150 fpm, 0.0104 ipr feed

b.) Test 2 - Ti 140A cut at 100 fpm, .0052 " "

c.) Test 3 - 1045 steel cut at 100 fpm, 0.0052 ipr feed

d.) Test 4 - 1045 " " " 150 fpm, .0104 " "

a.)

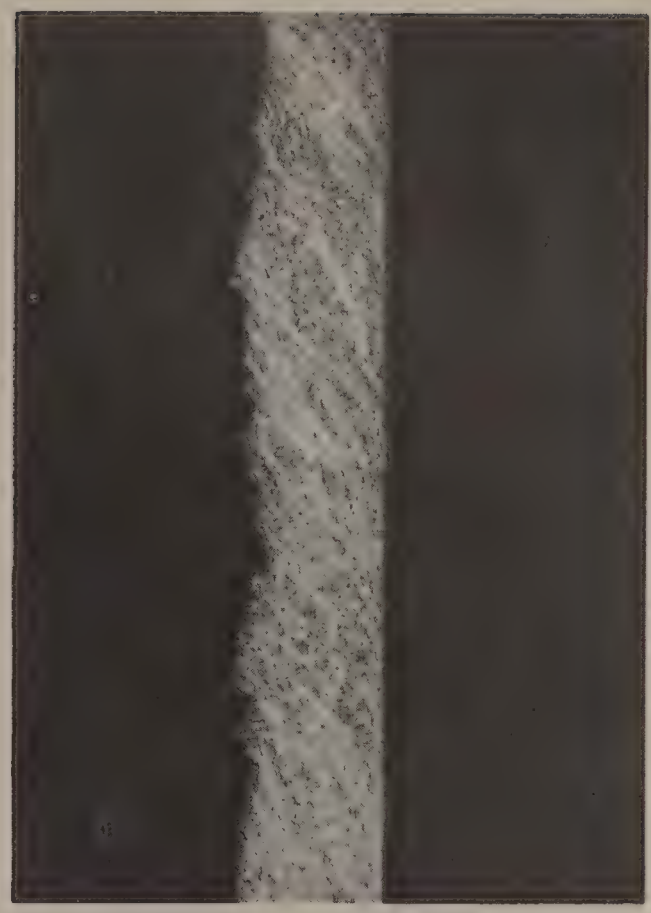

b.)

c.)

d.)

Fig. 37. Microscopic chip pictures

a.) Test 1 - Ti 140A cut at 150 fpm, 0.0104 ipr feed

b.) Test 2 - Ti 140A cut at 100 fpm, .0052 " "

c.) Test 3 - 1045 steel cut at 100 fpm, 0.0052 ipr feed

d.) Test 4 - 1045 " " " 150 fpm, .0104 " "

a.)

b.)

c.)

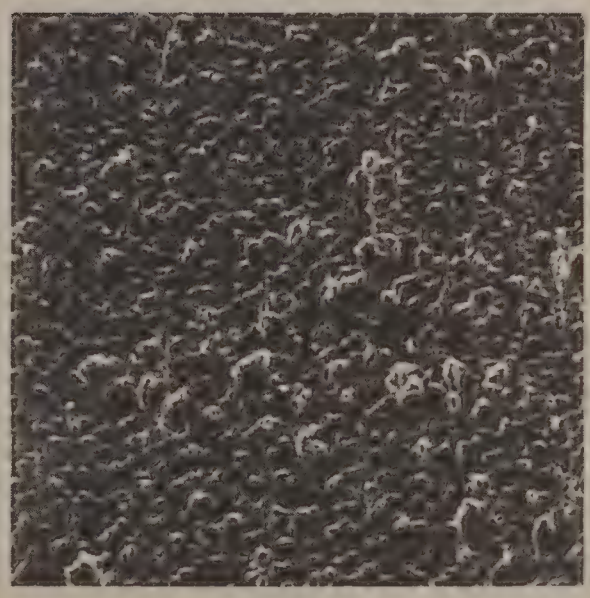

d.)

e.)

Fig. 38. Reproductions of plastic replicas of machined Ti 140A and 1045 steel surfaces. Magnification, 10x

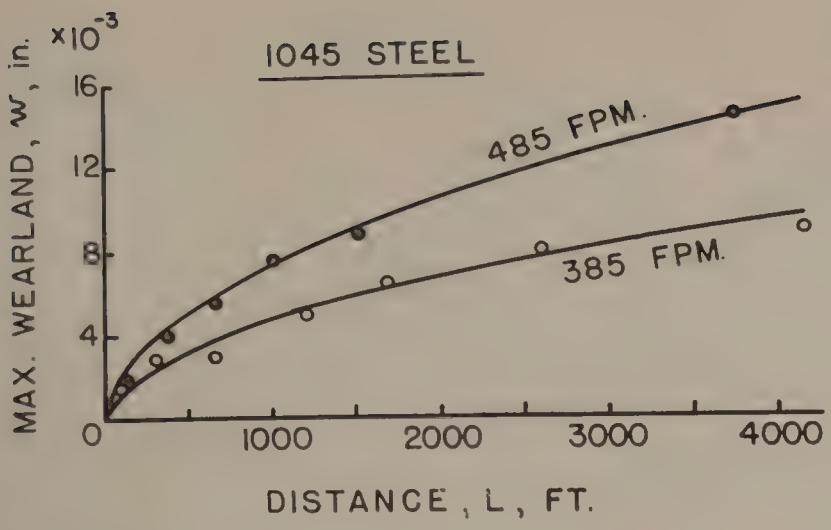

a.)

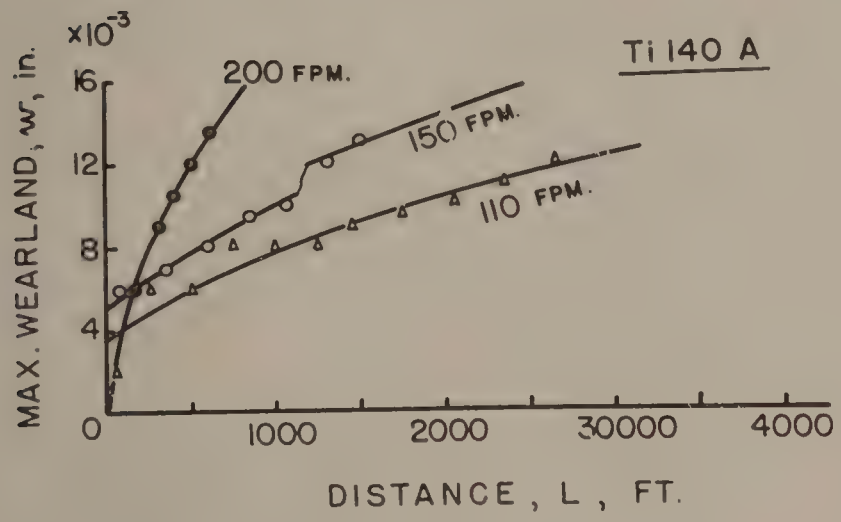

b.)

Fig. 39. Representative wear land curves for Ti 140A and 1045 steel.

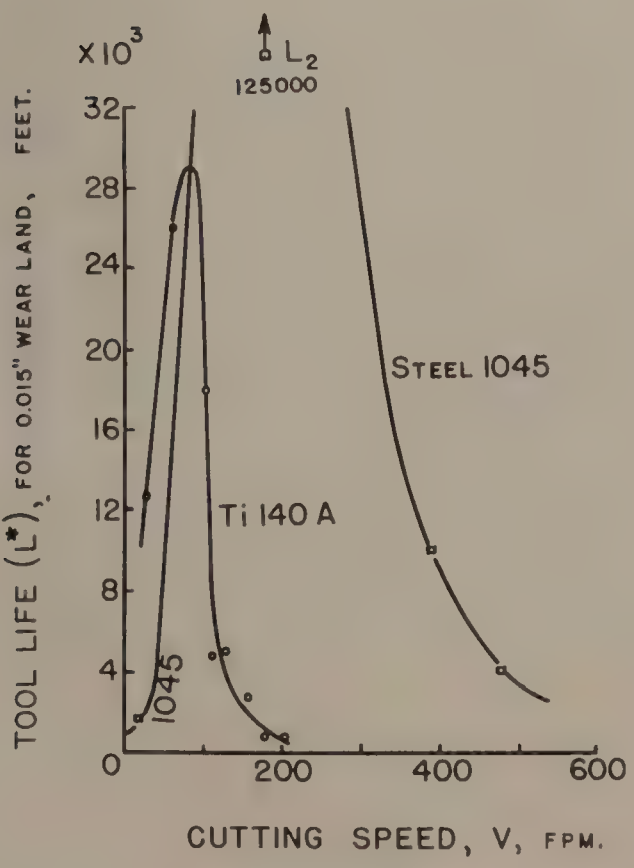

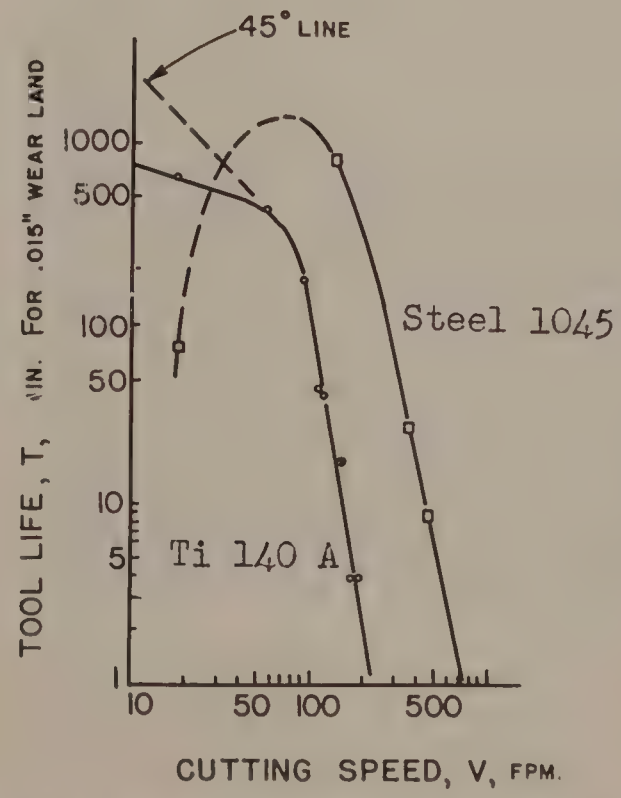

Fig. 40. Representative tool life data for Ti 140A and SAE 1045 steel. Tool material: K-6 carbide (Ti-140A) and K-2S carbide for SAE 1045 steel; feed, 0.0104 ipr.; depth of cut 0.060 in. Tool geometry: 0, 0, 5, 5, 0, 0.015; cutting fluid, none.
a.) L^* vs V plot b.) log T vs log V plot

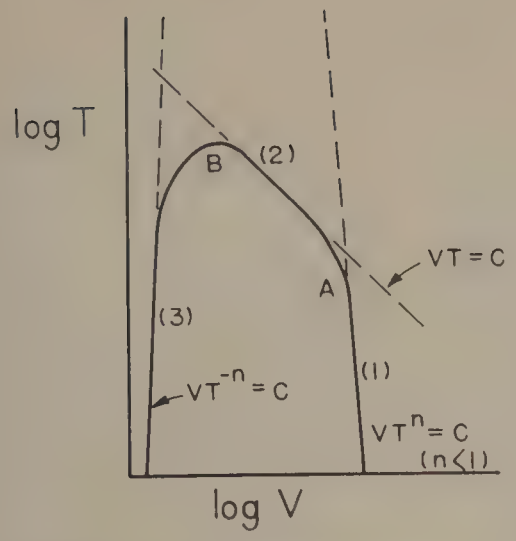

Fig. 41. Diagramatic representation of general tool life curve.

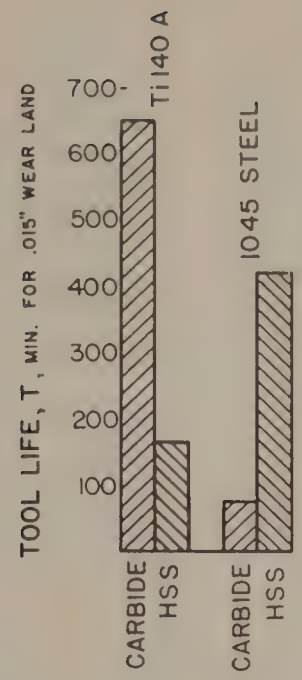

Fig. 42. Comparison of tool life results for Ti 140A and 1045 steel cut at 20 fpm using carbide and HSS tools. Tool material, HSS = 18-4-1, carbide = K-2S cutting fluid, none; feed, .0104 ipr; depth of cut 0.06 in. Tool geometry, 0^{o}, 0^{o}, 5^{o}, 5^{o}, 5^{o}, 0^{o}, .015 in.

a.)

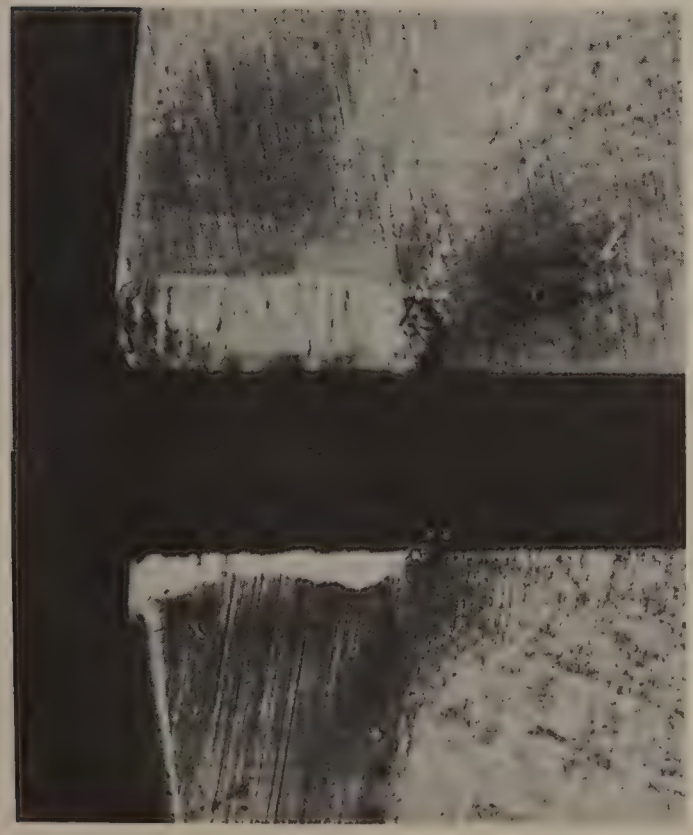

b.)

Fig. 43. Photographs of worn tools. Upper view shows chip face, lower view shows clearance face. Tool geometry: 0^{o}, 0^{o}, 5^{o}, 5^{o}, 5^{o}, 0^{o}, 0.015.
a.) K-6 carbide tool used to cut titanium alloy at 345 fpm; feed, 0.0104 ipr; depth of cut 0.06 in., wear land, 0.014 in., fluid, none.
b.) K-2S carbide tool used to cut 1045 steel at 485 fpm; feed, 0.0104 ipr; depth of cut, 060 in; wear land, 0145 in.; cutting fluid, none.

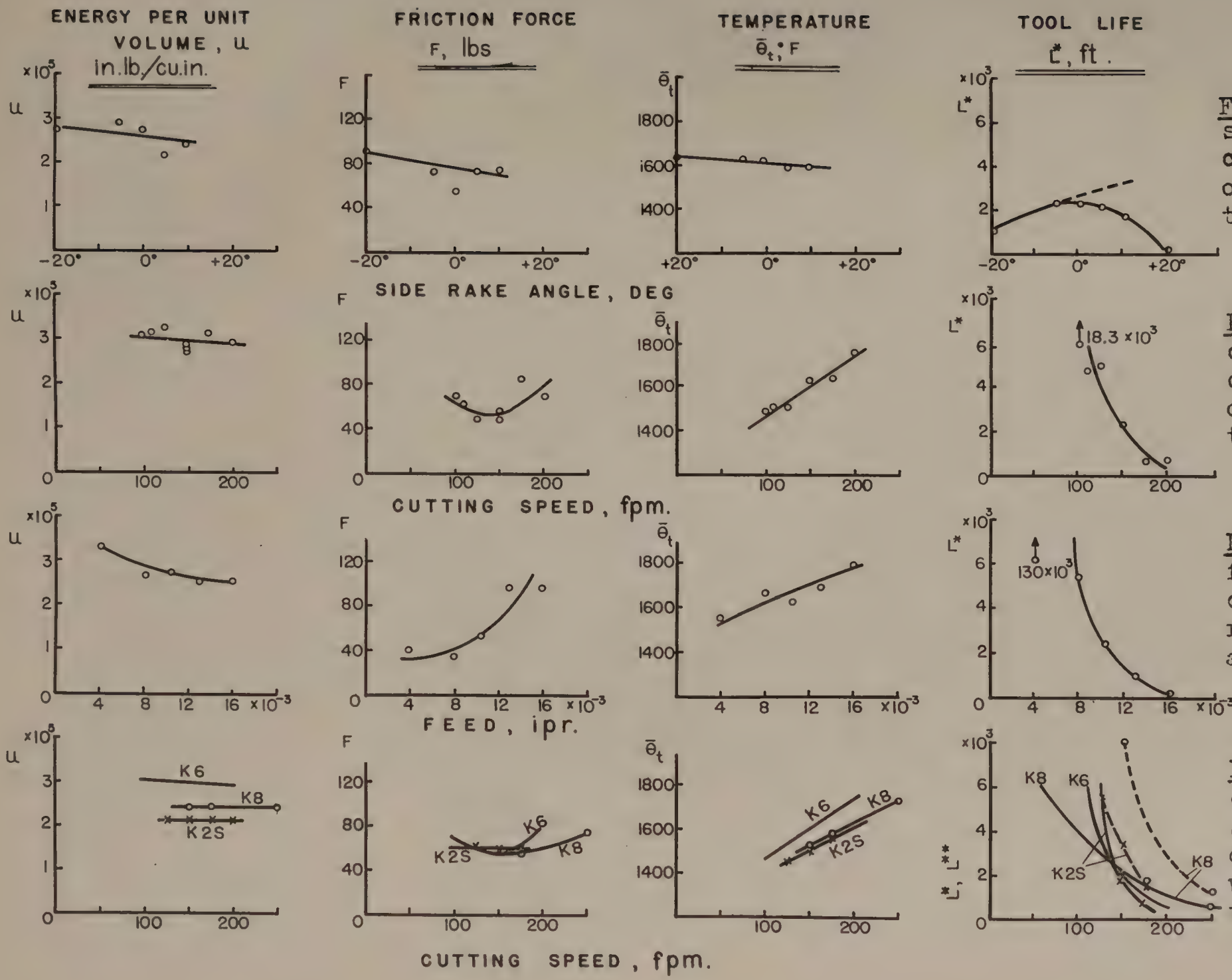

Fig. 44. Influence of side rake angle upon cutting characteristics of representative titanium alloy.

Fig. 45. Influence of cutting speed upon cutting characteristics of representative titanium alloy.

Fig. 46. Influence of feed upon cutting characteristics of representative titanium alloy.

Fig. 47. Performance characteristics of several carbide tools of different composition when machining representative titanium alloy

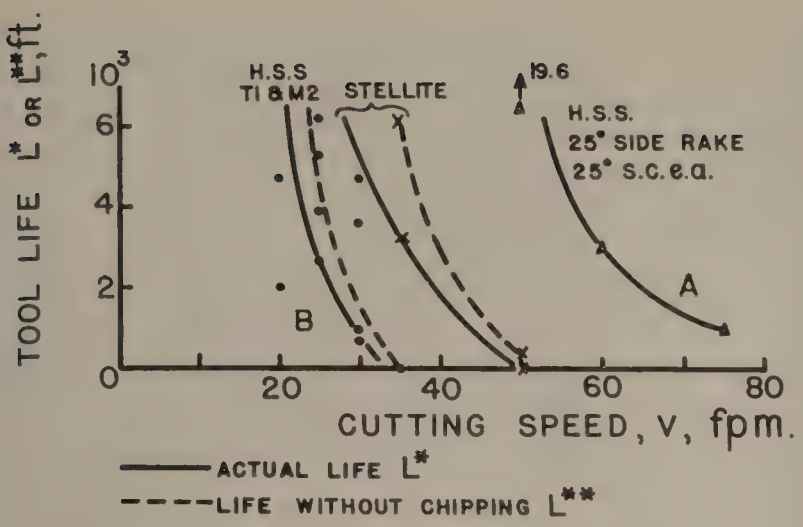

Fig. 48. Tool life curves for HSS and stellite tools.

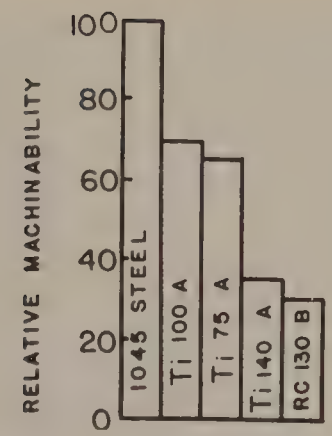

Fig. 50. Relative machinability of several titanium alloys compared with SAE 1045 steel. Basis for comparison is economic machining speeds.

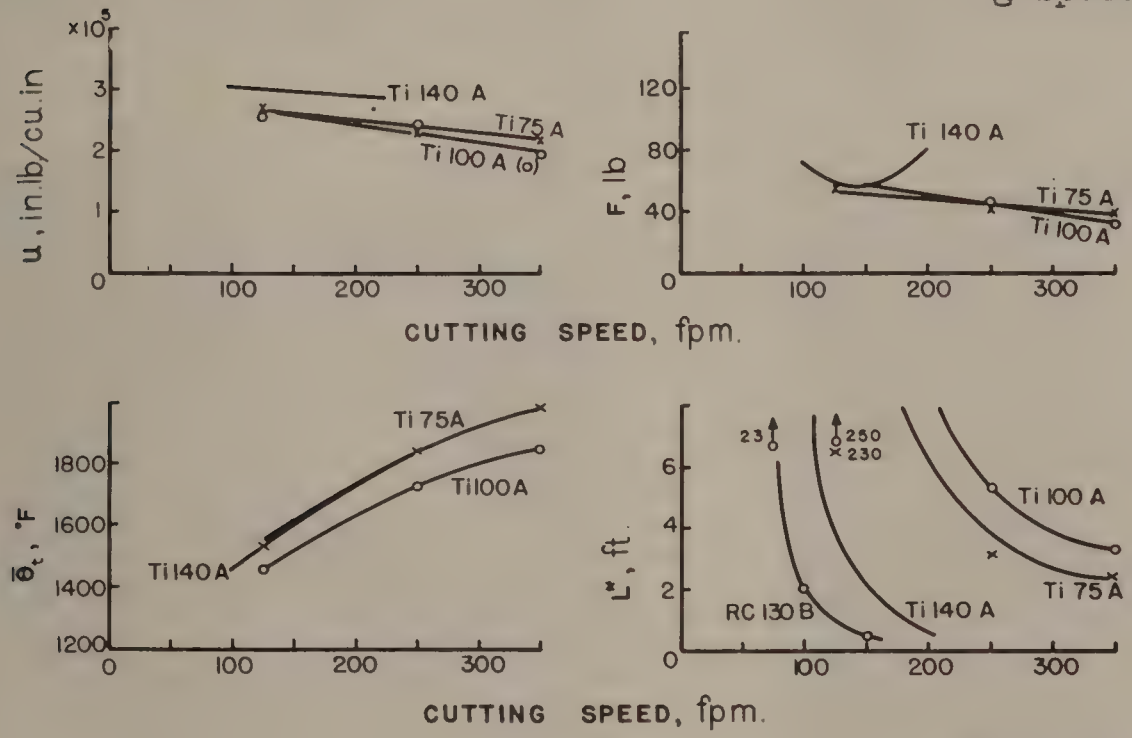

Fig. 49. Cutting characteristics of several titanium alloys.

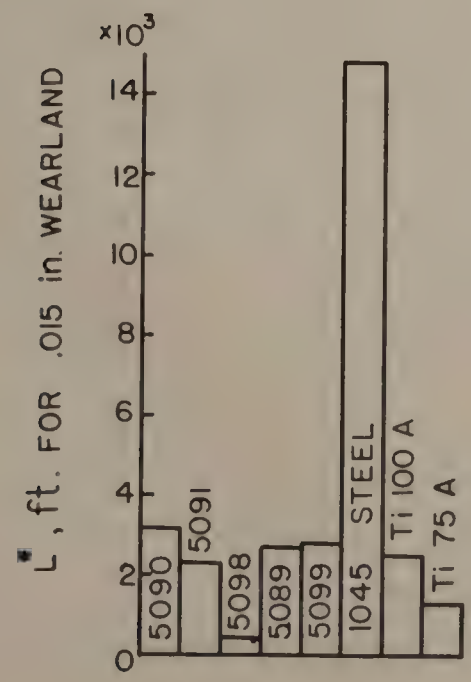

Fig. 51. Machinability characteristics of titanium alloys containing added oxygen and carbon at 345 fpm cutting speed.

a.)

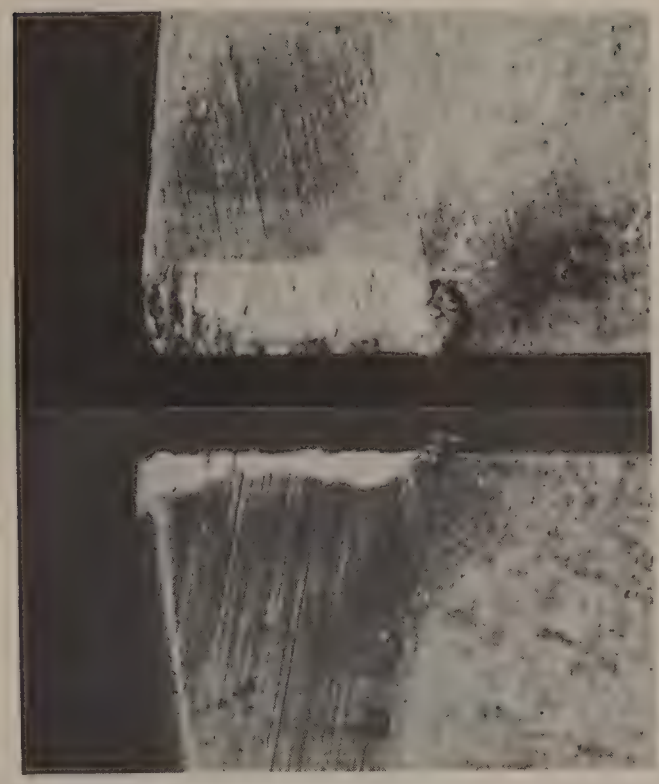

b.)

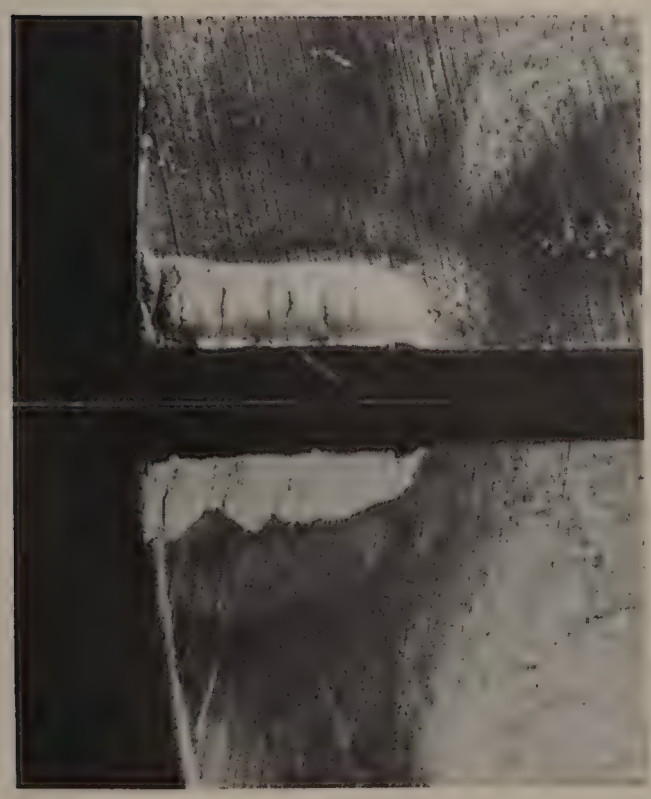

c.)

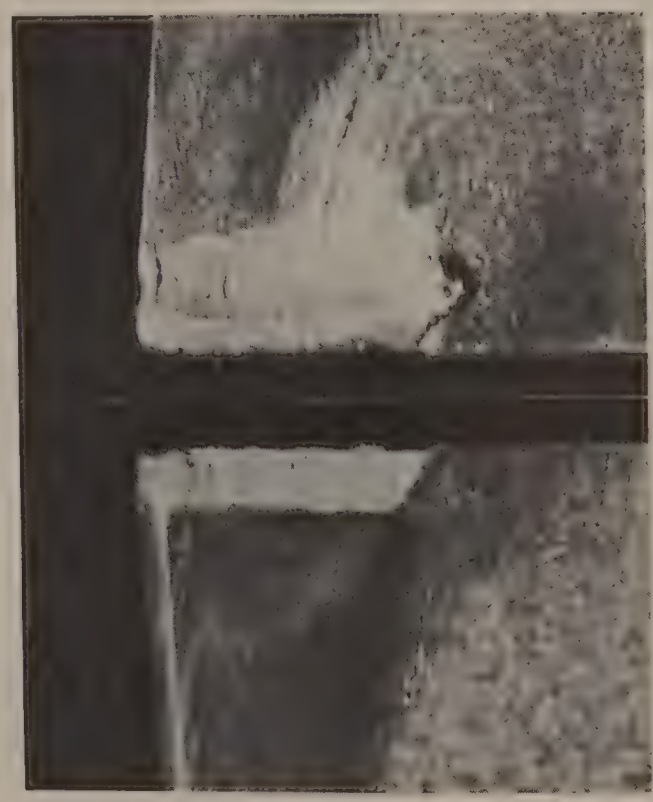

d.)

Fig. 52. Photographs of worn tools. Tool geometry: 0, 0, 5, 5, 5, 0.015.

a.) K-2S carbide tool used to cut 1045 steel at 485 fpm; feed, .0104 ipr; depth of cut, 0.06 in; wear land, .0145 in; cutting fluid, none.

b.) K-6 carbide tool used to cut heat number 5090 titanium alloy at 345 fpm; feed, .0104 ipr; depth of cut, .060 in; wear land, .014 in; cutting fluid, none.

c.) K-6 carbide tool used to cut heat number 5090 titanium alloy at 345 fpm; feed, .0104 ipr; depth of cut, .060 in; wear land .0195; cutting fluid, none.

d.) K-6 carbide tool as to cut heat number 5099 titanium alloy at 345 fpm; feed, .0104 ipr; depth of cut .060 in; wear land .015 in; cutting fluid, none.

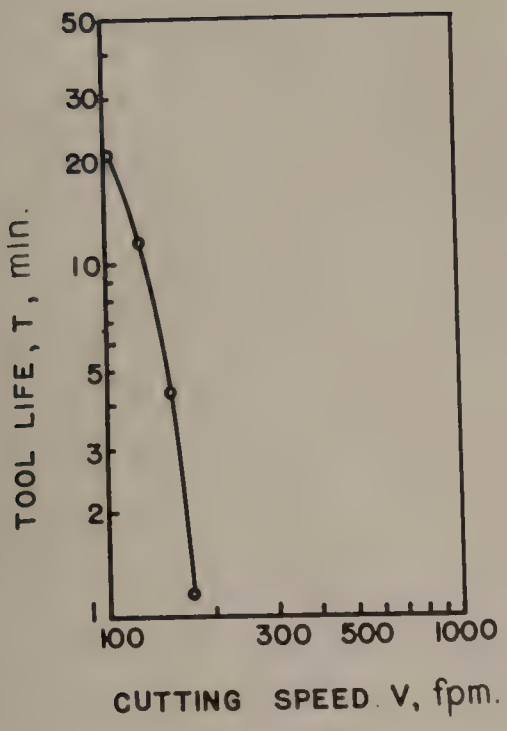

Fig. 53. Tool life curve for RC 130B. (382 BHN) cut with 78 carbide tool; 0, 6, 6, 6, 6, .040; feed, 0.009 ipr; depth of cut, 0.062 in; cutting fluid, none; wear land, 0.015 in. (From Air Force Report, reference 11).

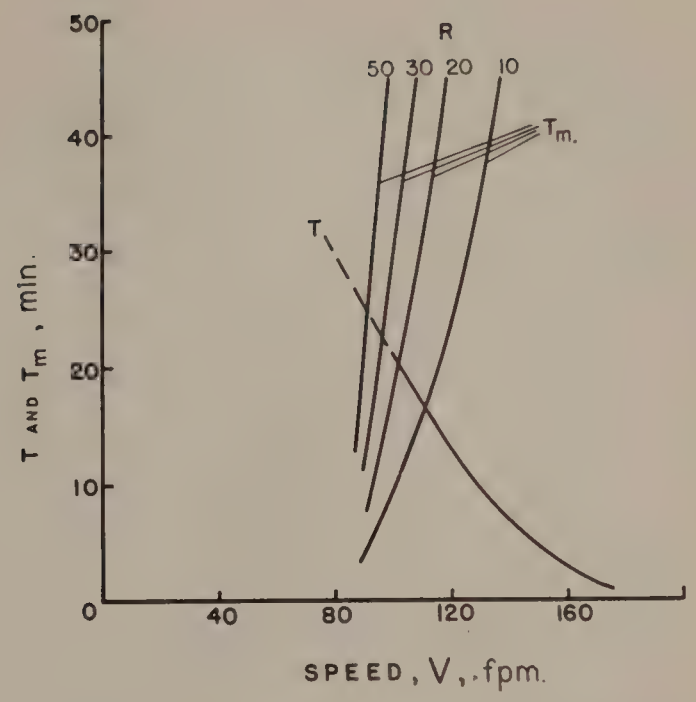

Fig. 54. Plot for determining economic speed corresponding to data of Fig. 52.

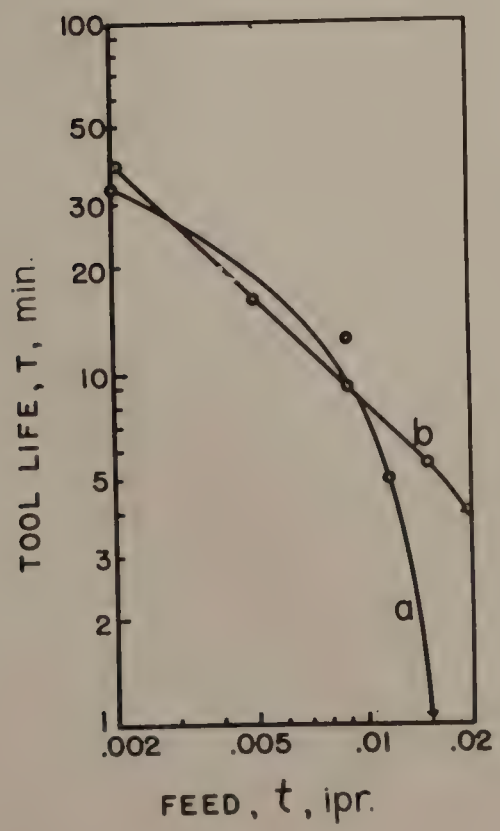

Fig. 55. Tool life curves from Air Force Report (reference 11).
a.) Work, Ti 140A; tool, T-1 HSS; geometry, 0, 15, 0, 5, 5, 0.005; cutting speed, 50 fpm; depth of cut, 0.062 in; cutting fluid, soluble oil, 1 to 25; wear land, 0.06 in.
b.) Work, Ti 150A; tool, K-6 carbide; geometry, 0, 6, 6, 6, 6, .040; cutting speed, 250 fpm; depth of cut, 0.062 in; cutting fluid, none; wear land, 0.015 in.

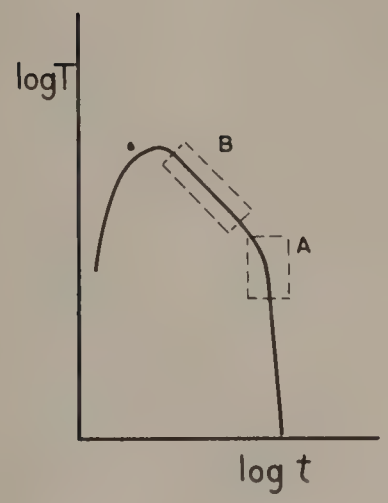

Fig. 56. Schematic representation of general variation of tool life with feed rate when cutting speed is held constant.

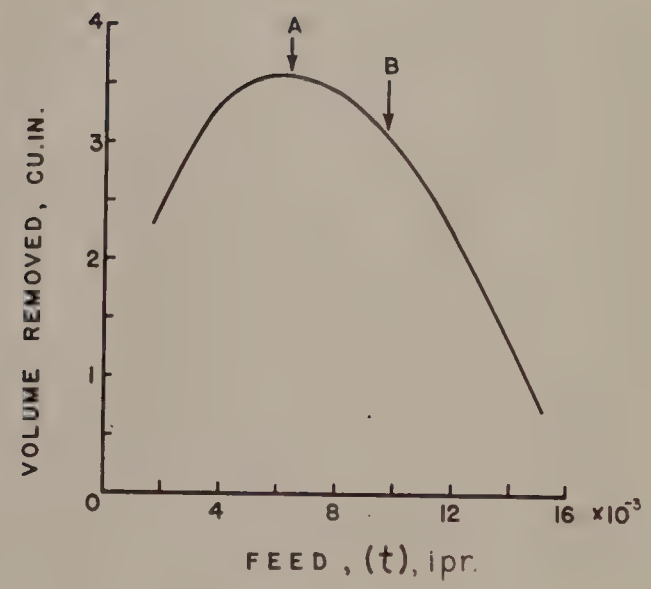

Fig. 57. Fig. (55a) replotted on rectangular coordinates with tool life expressed as volume of metal removed.

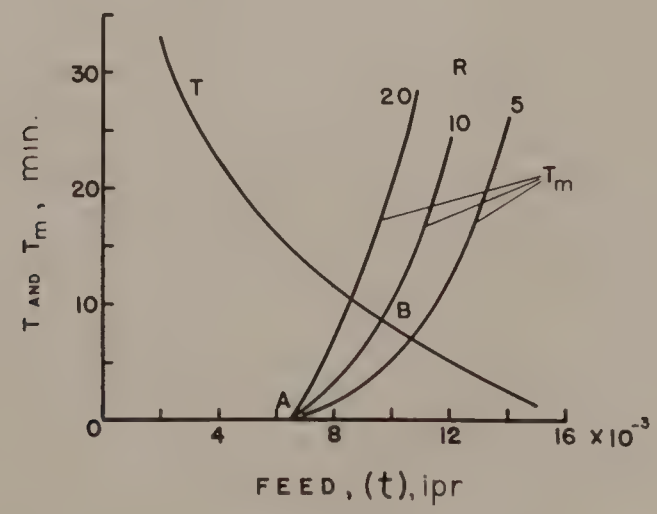

Fig. 58. Plot for determining economic feed corresponding to data of Fig. (55a).